University of Lisbon
Faculty of Science
DEPARTMENT OF CHEMISTRY AND BIOCHEMISTRY

THE PHYSIOLOGICAL ROLE OF PEROXIREDOXIN 2 IN HUMAN ERYTHROCYTES: A KINETIC ANALYSIS

Rui Manuel Vicente Benfeitas
Biochemistry Masters
2011

University of Lisbon
Faculty of Science
DEPARTMENT OF CHEMISTRY AND BIOCHEMISTRY

THE PHYSIOLOGICAL ROLE OF PEROXIREDOXIN 2 IN HUMAN ERYTHROCYTES: A KINETIC ANALYSIS

Advisors
Armindo Salvador, Ph.D. & Fernando Antunes Ph.D.

Rui Manuel Vicente Benfeitas
Biochemistry Masters
2011

To my advisors Dr. Armindo Salvador and Dr. Fernando Antunes, a big thank you for all your patience, efforts and very interesting discussions. Thanks for making this so fun!

To my family, friends, lab mates, thank you for pushing me forward.

Index

List of abbreviations

Latin alphabet

Abbreviation	Meaning
A_S	Erythrocyte surface area
C_P	Peroxidatic cysteine
C_R	Resolving cysteine
$Density_{RBC}$	Erythrocyte density
DeoxyHb	Hemoglobin (deoxyhemoglobin, Fe^{2+} oxidation state)
D_p	H_2O_2-induced intracellular damage during an H_2O_2 pulse
D_r	H_2O_2-induced intracellular damage between H_2O_2 pulses
DTNB	5,5'-dithiobis-(2-nitrobenzoic acid)
eH_2O_2	Extracellular hydrogen peroxide
f	Order of reaction of glutathione peroxidase 1 with respect to H_2O_2
g	Order of reaction of glutathione peroxidase 1 with respect to GSH
G6P	Glucose-6-phosphate
G6PD	Glucose-6-phosphate dehydrogenase
GPx1	Glutathione Peroxidase 1
$GPx1_{ox}$	Glutathione Peroxidase 1 (oxidized form)
$GPx1_{red}$	Glutathione Peroxidase 1 (reduced form)
GPx1-SG	Glutathione Peroxidase 1 (associated with glutathione)
GSH	Glutathione
GSR	Glutathione Reductase
GSSG	Glutathione (oxidized form)
GStot	Glutathione (total concentration in the erythrocyte)
H_2O_2	Hydrogen peroxide
Hb	Hemoglobin
i	Fraction of total body volume occupied by inflamed tissue
iH_2O_2	Intracellular hydrogen peroxide
k_c	Aggregated pseudo-first order rate constant for hydrogen peroxide consumption by catalase and glutathione peroxidase
$k_{catalase}$	Pseudo-first order rate constant for hydrogen peroxide consumption by catalase
$k_{CompoundI}$	Reactivity between Compound I and H_2O_2
$k_{CompoundII}$	Pseudo-first order rate constant for reduction of Compound II to Ferricatalase
k_D	Proportionality constant for the accumulation of iH_2O_2-induced damage to the cell
k_{efflux}	Pseudo-first order rate constant for hydrogen peroxide efflux
$k_{Ferricatalase}$	Reactivity between Ferricatalase and H_2O_2
k_{GPx1}	Pseudo-first order rate constant for hydrogen peroxide consumption by glutathione peroxidase 1

Abbreviation	Meaning
k_H	Henry's law constant for the solubility of O_2 in water
k_{IntN}	Reactivity between Intermediate and NADPH
k_{IntN}'	Pseudo-first order rate constant for reduction of Intermediate to Ferricatalase, with respect to Intermediate
k_{IntRed}	Pseudo-first order rate constant for reduction of Intermediate to Compound II
$K_m(Trx)$	Michaelis-Menten constant of thioredoxin reductase for thioredoxin
$K_m(NADPH)$	Michaelis-Menten constant of thioredoxin reductase for NADPH
k_{ox}	First-order rate constant for spontaneous glutathione oxidation
$k_{ox,in\ vivo}$	First-order rate constant for spontaneous glutathione oxidation *in vivo*, considering physiological pO_2
$k_{ox,exp}$	First-order rate constant for spontaneous glutathione oxidation experimentally determined under large pO_2
k_{spon}	First-order rate constant for oxidation of glutathione by oxygen
k_p	Pseudo-first order rate constant for H_2O_2 influx across the erythrocyte membrane
k_{Prx2}	Pseudo-first order rate constant for hydrogen peroxide reduction by peroxiredoxin 2
k_{PrxRed}	Reactivity between peroxiredoxin 2 and hydrogen peroxide
k_{PSO2H}	Second-order rate constant for the sulfinylation of Prx2
k_{PSOH}	First-order rate constant for the formation of disulfide form of Prx2
k_{PSSP}	Reactivity between disulfide peroxiredoxin 2 and reduced thioredoxin
k_R	Pseudo-first order rate constant for Prx2 reduction
k_{TrxR}	Pseudo-first order rate constant for thioredoxin reduction by thioredoxin reductase
MetHb	Hemoglobin (methemoglobin, Fe^{3+} oxidation state)
$MW_{catalase}$	Molecular weight of catalase monomer
MW_{GPx1}	Molecular weight of GPx1 monomer
MW_{Prx2}	Molecular weight of each monomer of peroxiredoxin 2
MW_{Trx}	Molecular weight of thioredoxin
MW_{TrxR}	Molecular weight of thioredoxin reductase
$NADP^+$	Nicotinamide adenine dinucleotide phosphate (oxidized form)
NADPH	Nicotinamide adenine dinucleotide phosphate (reduced form)
OxyHb	Hemoglobin (oxyhemoglobin, oxygen-bound state, Fe^{3+} oxidation state)
PPP	Pentose Phosphate Pathway
Prx_1	Peroxiredoxin 2 (singly-crosslinked monomers)
Prx2	Peroxiredoxin 2
Prxtot	Total concentration of monomeric peroxiredoxin 2 in human erythrocytes
PSO_2H	Peroxiredoxin 2 (sulfinic acid form)
PSSP	Peroxiredoxin 2 (disulfide form)
Q_{10}	Temperature coefficient
Srx	Sulfiredoxin
Srx_{Ox}	Sulfiredoxin (oxidized form)
Srx_{Red}	Sulfiredoxin (reduced form)
SOD	Superoxide Dismutase
T	Period of crossing an inflammation site
Trx	Thioredoxin

Abbreviation	Meaning
$Trx_{Holmgren}$	Concentration of thioredoxin in the erythrocyte
Trx_{Ox}	Thioredoxin (oxidized form)
TrxR	Thioredoxin reductase
Trx_{Red}	Thioredoxin (reduced form)
Trxtot	Total concentration of thioredoxin
TSA	Thiol-specific antioxidant
V_{bathed}	Volume of human body that is bathed with blood
$V_{blood\ cells}$	Total volume of human blood cells
$v_{CompoundI}$	Rate of Compound I-mediated H_2O_2 dismutation
v_{decay}	Rate of decay of Compound I to Intermediate
V_e	Erythrocyte cell volume
V_{ew}	Volume of erythrocyte water
v_{H2O2}	Total rate of H_2O_2 consumption by catalase, peroxiredoxin 2 and glutathione peroxidase 1
v_{influx}	Rate of H_2O_2 influx
$V_{interstitial}$	Volume of interstitial fluids
v_{IntRed}	Rate of reduction of Intermediate to Compound II
$V_{max}^{app}(Trx_{Ox})$	Apparent maximal rate of reduction of thioredoxin by thioredoxin reductase
V_{max}^{PPP}	Maximum rate of NADPH production by the pentose phosphate pathway
V_{max}^{Prx2}	Maximum rate of hydrogen peroxide consumption by peroxiredoxin 2
V_{max}^{Red}	Maximum rate of Prx2 reduction
V_{max}^{TrxR}	Maximum rate of activity of thioredoxin reductase
$v_{NADPHcons}$	Rate of NADPH-mediated reduction of Intermediate to Ferricatalase
V_o	Extracellular volume
$v_{catalase}$	Rate of H_2O_2 consumption by catalase
v_{Prx2}	Rate of H_2O_2 consumption by peroxiredoxin 2
v_{PSSP}	Rate of Prx2 reduction
$V_{skeleton}$	Average skeleton volume
V_{total}	Average total body volume
v_{TrxR}	Rate of activity of thioredoxin reductase
$WaterContent_{RBC}$	Average erythrocyte water volume

Greek alphabet

Abbreviation	Meaning
$\varepsilon_{catalase}$	Fold increase in catalase concentration in order to compensate for the absence of Prx2 or GPx1
ε_{GPx1}	Fold increase in GPx1 concentration in order to compensate for the absence of catalase or Prx2
ε_{Prx2}	Fold increase in Prx2 concentration in order to compensate for the absence of catalase or GPx1
κ	Hydrogen peroxide diffusion constant across the erythrocyte membrane
φ	Rate of H_2O_2 influx across the erythrocyte membrane
ϕ	Endogenous production of hydrogen peroxide
ϕ_1	Reciprocal rate constant for net forward reaction of Glutathione Peroxidase 1 with hydrogen peroxide
ϕ_2	Reciprocal rate constant for net forward reaction of Glutathione Peroxidase 1 with glutathione
Φ	Hydrogen peroxide production in the experiments of (Low et al., 2007)

List of values

Abbreviation	Value	Reference
A_S	1.35×10^{-5} dm^2	(Evans and Fung, 1972)
$Density_{RBC}$	1.094 Kg erythrocytes/L packed erythrocytes	(Raftos et al., 1999)
GPx1	0.97×10^{-6} M	Estimated, Section 5.1.1.1
GStot	3.2×10^{-3} M	(Thorburn and Kuchel, 1987)
Hb	340 g Hb/dm^3 packed erythrocytes	(Beutler, 1984)
	486 g Hb/dm^3 erythrocyte water	Estimated, considering V_{ew} by (Savitz et al., 1964)
k_c	258 s^{-1}	Estimated, Section 5.2.1.4
$k_{catalase}$	218 s^{-1}	(Mueller et al., 1997a)
$k_{CompoundI}$	1.6×10^{7} M^{-1} s^{-1}	(Chance et al., 1952)
$k_{CompoundII}$	8×10^{-6} s^{-1}	(Kirkman et al., 1999)
k_{efflux}	12 s^{-1}	Estimated, Section 5.2.1.4
$k_{Ferricatalase}$	0.6×10^{7} M^{-1} s^{-1}	(Chance et al., 1952)
k_{GPx1}	40 s^{-1}	Estimated, Section 5.1.1.1
k_H	1.3×10^{-3} M/atm	(Wilhelm et al., 1977)
$K_m(Trx)$	1.83×10^{-6} M	(Turanov et al., 2006)
$K_m(NADPH)$	6×10^{-6} M	(Urig et al., 2006)
k_{spon}	0.1 M^{-1}s^{-1}	(Scarpa et al., 1996)
k_p	8 s^{-1}	Estimated, Section 5.2.1.2
k_{Prx2}	3.7×10^{4} s^{-1}	Estimated, Section 5.1.1.3
k_{PrxRed}	10^{8} M^{-1} s^{-1}	(Manta et al., 2009)
k_{PSO2H}	0.23 M^{-1} s^{-1}	Estimated, Section 5.7
k_{PSOH}	0.26 s^{-1}	Estimated, Section 5.2.1.10
k_{PSSP}	2.1×10^{5} M^{-1}s^{-1}	(Manta et al., 2009)
k_R	1.7 s^{-1}	Estimated, Section 5.7
k_{TrxR}	0.5 s^{-1}	Estimated, Section 5.2.1.9
$MW_{catalase}$	25 600 Da	(Bonaventura et al., 1972)
MW_{GPx1}	23 000 Da	(Awasthi et al., 1975)
MW_{Prx2}	22 000 Da	(Moore and Shriver, 1994; Schroder et al., 2000)
MW_{Trx}	12 000 Da	(Cha and Kim, 1995)
MW_{TrxR}	116 000 Da	(Tsang and Weatherbee, 1981)
Prxtot	3.7×10^{-4} M	Estimated, Section 5.1.1.3
$Trx_{Holmgren}$	3.7×10^{-2} g/Kg erythrocyte	(Holmgren and Luthman, 1978)
TrxR	30×10^{-9} M	Estimated, Section 5.2.1.7
Trxtot	4.8×10^{-6} M	For bovine erythrocytes. Estimated, Section 5.2.1.6
V_{bathed}	48 dm^3	Estimated, Section 5.10.2
$V_{blood\ cells}$	2.3 dm^3	Estimated, Section 5.10.2
V_e	10^{-13} dm^3	(Evans and Fung, 1972)

Abbreviation	Value	Reference
V_{ew}	7×10^{-14} dm^3	Estimated, Section 5.2.1.4
$V_{interstitial}$	14 dm^3	Estimated, Section 5.10.2
V_{max}^{PPP}	1.9×10^{-6} M/s	(Albrecht et al., 1971; Gaetani et al., 1974)
V_{max}^{Red}	2.4×10^{-4} M/s	Estimated, Section 5.2.2
V_{max}^{TrxR}	0.77×10^{-6} M/s	Estimated, Section 5.2.1.9
$V_{skeleton}$	5.5 dm^3	Estimated, Section 5.10.2
V_{total}	70 dm^3	Section 5.10.2
$WaterContent_{RBC}$	0.7 dm^3 water/dm^3 erythrocytes	(Savitz et al., 1964)
κ	6×10^{-5} dm/s	(Nicholls, 1965)
ϕ_1	2.4×10^{-8} Ms	(Takebe et al., 2002)
ϕ_2	4.3×10^{-6} Ms	(Takebe et al., 2002)
Φ	0.69×10^{-9} M/s	Estimated, Section 5.2.1.6

List of figures

List of tables

1. Summary

Peroxiredoxin 2 (Prx2) is a hydrogen peroxide reducing protein abundant in human erythrocytes. Due to its large concentration (3.7×10^{-4} M) and high reactivity with hydrogen peroxide ($k\sim10^{8}$ $M^{-1}s^{-1}$) it is a potentially very relevant antioxidant for the defense of erythrocytes against hydrogen peroxide. However, its contribution for H_2O_2 defense is not clear. The antioxidant activity of Prx2 is affected by the limited capacity that erythrocytes have for reducing Prx2 to its active form after it is oxidized by hydrogen peroxide. Further, human erythrocytes also possess catalase, an H_2O_2 scavenger whose antioxidant activity entails minimal NADPH consumption. In contrast, Prx2-mediated H_2O_2 reduction is stoichiometrically coupled to NADPH oxidation. Why do then erythrocytes need Prx2? Why do they not rely only on catalase, the H_2O_2 scavenger whose activity requires less NADPH? Is Prx2 redundant for H_2O_2 defense in human erythrocytes?

We used kinetic analyses and mathematical modeling to clarify these issues. We considered the main processes protecting human erythrocytes against H_2O_2: glutathione peroxidase (GPx1), catalase and Prx2. The analysis of the dynamic behavior of the Prx2 system under various oxidative conditions indicates the following.

Basal oxidative conditions, assuming a sustained extracellular H_2O_2 (eH_2O_2) concentration $<10^{-7}$ M or intracellular H_2O_2 (iH_2O_2) concentration $<2\times10^{-11}$ M allow Prx2 to remain fully reduced. Prx2 then consumes more than 99% of the iH_2O_2. On the other hand, catalase becomes the main defense against H_2O_2 in erythrocytes facing sustained exposure to loads that fully oxidize Prx2 ($eH_2O_2> 1.4\times10^{-6}$ M). Catalase and GPx1 then contribute for 84% and 16% of the H_2O_2 consumption, respectively. Even when Prx2 is fully oxidized, eH_2O_2 consumption by erythrocytes is limited by membrane permeation. Thus, although erythrocytes are quite likely the main sink of plasma H_2O_2, Prx2 is dispensable for this role.

Despite the slow Prx2 regeneration under strong oxidative loads, our analyses also suggest that erythrocytes could not rely solely on catalase and Gpx1 for defense against H_2O_2. To fully replace Prx2, maintaining the same H_2O_2 concentration and response time as in normal erythrocytes, $\sim11\times10^{-12}$ g catalase (6×10^{-12} g GPx1) would be required. This would amount to 32% (18 %) of the hemoglobin in human erythrocytes. Such a solution could therefore impair

oxygen transport either by making erythrocytes bigger, and thus less able to cross capillaries, or by reducing the space available for hemoglobin. On the other hand, a <1 % increase in Prx2 concentration would suffice to compensate for the effect of catalase elimination on H_2O_2 concentration and response time at basal oxidative loads. These differences are due to the much higher specific activity of Prx2.

Our analyses also suggest that crossing of inflammation sites may lead to substantial but brief Prx2 oxidation. The residence time of a circulating erythrocyte in an inflammation site is determined by the time (~2 s) to cross the capillaries, where these cells are in most intimate contact with the vasculature walls and circulate most slowly. Full Prx2 oxidation occurs if those inflammation foci lead to > 25×10^{-6} M H_2O_2 in the plasma, which is in the scale of the strongest loads experimentally determined for inflammatory foci in other organisms.

Once all Prx2 is oxidized, erythrocytes can regenerate the reduced form in minutes if the oxidative load returns to basal values. However, a stepwise increase in Prx2 oxidation through repeated crossing of inflammation sites is very unlikely. This because such crossings are expected to occur many hours in between, time enough for Prx2 to be fully reduced.

Altogether, our results show that Prx2 is the main defense of human erythrocytes against H_2O_2 under most physiological circumstances. Extensive Prx2 oxidation may be attained in inflammation sites, affecting its contribution for H_2O_2 consumption. Yet, this does not impair the erythrocytes' ability to scavenge plasma H_2O_2 because they can still rely on catalase for the defense against H_2O_2. Our results have important implications for the study of antioxidant protection and reactive oxygen species-associated diseases in mammalian cells, where Prx2 and catalase are found.

Resumo

A Peroxirredoxina 2 (Prx2) é uma proteína que reduz peróxido de hidrogénio e uma das mais abundantes em eritrócitos humanos. Nestas células a Prx2 representa uma defesa potencialmente importante contra o peróxido dada a sua concentração (3.7×10^{-4} M) e reactividade com o peróxido de hidrogénio ($k\sim10^{8}$ $M^{-1}s^{-1}$). No entanto, a sua contribuição para a protecção contra H_2O_2 não é clara. A actividade antioxidante da Prx2 é condicionada pela capacidade limitada de redução da Prx2 à sua forma activa após ter reagido com o H_2O_2. Para além disso, os eritrócitos humanos possuem também catalase, um enzima cuja actividade antioxidante acarreta apenas um consumo mínimo de NADPH. Por outro lado, a redução de H_2O_2 pela Prx2 está estequiometricamente associada à oxidação de NADPH. Se assim é, porque é que os eritrócitos precisam de Prx2? Porque é que a defesa destas células contra o peróxido de hidrogénio não é constituída apenas pelo catalase, visto que a sua actividade requere menos NADPH? Será a Prx2 uma defesa contra o H_2O_2 redundante nos eritrócitos humanos?

Com o intuito de responder a estas questões utilizámos análises cinéticas e modelação matemática. Considerámos os principais mecanismos de protecção contra o H_2O_2 presentes nos eritrócitos humanos: peroxidase de glutationo 1 (GPx1), catalase e Prx2. A análise do comportamento do sistema da Prx2 sob várias condições oxidativas indica o seguinte.

Em condições oxidativas basais, assumindo exposição constante a peróxido extracelular (eH_2O_2) $<10^{-7}$ M ou intracelular (iH_2O_2) $<2\times10^{-11}$ M, a Prx2 permanece na forma reduzida. Isto permite que mais de 99% do iH_2O_2 seja consumido pela Prx2. Por outro lado, o catalase torna-se a principal defesa contra H_2O_2 quando a carga oxidativa a que os eritrócitos são sujeitos leva à oxidação completa da Prx2 ($eH_2O_2> 1.4\times10^{-6}$ M). Nessas condições, a catalase e a GPx1 contribuem respectivamente para 84% e 16% do consumo de H_2O_2. No entanto, o consumo de eH_2O_2 pelos eritrócitos é limitado pela permeação membranar mesmo quando a Prx2 está completamente oxidada. Portanto, ainda que os eritrócitos sejam provavelmente o principal sumidouro de H_2O_2 no plasma, a Prx2 não é necessária para tal.

A regeneração da Prx2 é lenta quando o eritrócito é exposto a elevadas cargas oxidativas. No entanto, os nossos resultados sugerem que esta célula não poderia utilizar catalase ou GPx1

como as suas únicas defesas contra o H_2O_2. Seriam necessário ~11×10^{-12} pg catalase (6×10^{-12} g GPx1) para substituir completamente a Prx2, mantendo o mesmo iH_2O_2 e tempo de resposta que num eritrócito normal. Isto totalizaria 32% (18%) da hemoglobina presente na célula. No entanto isto afectaria o transporte de oxigénio por esta célula pois ou seria necessário uma célula maior (impossibilitando portanto a sua capacidade para atravessar capilares), ou limitaria o espaço intracelular disponível para a hemoglobina. Por outro lado, um mero aumento de <1 % na concentração total de Prx2 seria suficiente para compensar a ausência de catalase, mantendo a mesma concentração de iH_2O_2 e tempo de resposta encontrados em cargas oxidativas basais. Estas diferenças são devidas à actividade específica da Prx2, muito maior do que as actividades específicas do catalase ou GPx1.

Os nossos resultados sugerem também que exposição a focos de inflamação poderá levar à oxidação substancial, ainda que transiente, da Prx2. A duração da exposição a um foco inflamatório é determinada pelo tempo (~2 s) que o eritrócito demora a atravessar um capilar, o local onde esta célula está em mais íntimo contacto com o endotélio e onde a velocidade do fluxo sanguíneo é menor. A oxidação completa da Prx2 dá-se nesses locais se o $eH_2O_2> 25\times10^{-6}$. Este eH_2O_2 está na escala das cargas oxidativas mais elevadas detectadas experimentalmente, em focos inflamatórios noutros organismos.

Quando completamente oxidada a Prx2 é regenerada em minutos se a carga oxidativa regressar a condições basais. No entanto, a oxidação cumulativa da Prx2 devido à exposição a focos inflamatórios sucessivos é muito pouco provável dado que são necessárias várias horas para um eritrócito ser exposto a dois focos sucessivos. Isto permite que haja tempo suficiente para a Prx2 ser completamente reduzida.

Estas evidências mostram que a Prx2 é a principal defesa dos eritrócitos humanos contra H_2O_2, na maioria das condições fisiológicas. A oxidação substancial da Prx2 pode dar-se em focos inflamatórios, afectando a capacidade deste antioxidante para consumir H_2O_2. No entanto não condiciona a capacidade dos eritrócitos para consumir H_2O_2 do plasma, dado que estas células possuem ainda catalase para se defenderem contra H_2O_2. Estes resultados têm implicações importantes para o estudo da protecção antioxidante e de doenças associadas a espécies reactivas de oxigénio em células de mamíferos onde a Prx2 e catalase estejam presentes.

2. Introduction

Erythrocytes are often exposed to hydrogen peroxide (H_2O_2), one type of Reactive Oxygen Species (ROS) that may have toxic effects in these cells. The role of antioxidant enzymes such as Glutathione Peroxidase or Catalase in the protection of human erythrocytes against H_2O_2 has been studied for long (Cohen and Hochstein, 1963; Flohé et al., 1972; Gaetani et al., 1989; Johnson et al., 2000; Johnson et al., 2010). More recently, (Peskin et al., 2007) found that these cells also contain very large quantities of Peroxiredoxin 2, a peroxidase. But despite the very high reactivity [10^8 M^{-1} s^{-1} (Manta et al., 2009)] of Prx2 with H_2O_2, (Low et al., 2007) observed that erythrocytes have a very limited capacity for regenerating Prx2 once it is oxidized to its disulfide form by H_2O_2. Therefore, the role and relevance of Prx2 for antioxidant protection in human erythrocytes is currently a matter of debate. The present work uses a set of mathematical models and kinetic analyses of H_2O_2 metabolism in human erythrocytes to analyze relevant aspects of Prx2 action *in vivo* and to clarify its physiological role.

2.1. Reactive Oxygen Species and biological sources of H_2O_2

Reactive Oxygen Species (ROS) are oxygen-containing molecules highly reactive in redox reactions. They regulate several processes such as cell growth and survival (Davies et al., 1995), transcription (Liu et al., 2005), and have important effects in wound healing (Broughton et al., 2006). However, these molecules also have toxic effects in the cell, such as oxidation of proteins and nucleic acids or lipid peroxidation (Sarsour et al., 2009; Watson and Jones, 2003). ROS were also related with the development of some diseases like cancer, diabetes, fibrosis, neurodegenerative diseases, cellular aging (Sarsour et al., 2009), atherosclerosis (Lusis, 2000; Rose and Afanasyeva, 2003), and Parkinson's disease (Lotharius and Brundin, 2002).

Hydrogen Peroxide (H_2O_2) is one of the most investigated ROS and was related with many of these processes. Like other ROS, it can be found in many different cell types in the human body (Halliwell et al., 2000). It permeates cellular membranes (Chance et al., 1979) and is produced endogenously in the mitochondrial respiratory chain, or *via* the dismutation of superoxide, among others (Chance et al., 1979; Gonzalez-Flecha and Demple, 1995; Messner and Imlay, 1999).

In the human erythrocyte (the target cell of our study), some of the endogenous sources of H_2O_2 are glutathione autoxidation, hemoglobin autoxidation, and dismutation of superoxide. However,

this cell is also exposed to exogenous H_2O_2 while in circulation. We will now discuss evidence that points out the oxidative stress caused by H_2O_2 to these cells. Except where otherwise stated, all the evidence here reported pertains to analyses done in human erythrocytes.

2.1.1. Glutathione autoxidation

Glutathione (GSH) autoxidation may have a significant contribution for the H_2O_2 produced endogenously as we now show. (Thorburn and Kuchel, 1985) assessed the rate of GSH autoxidation in human erythrocytes. The authors observed a first-order decay of GSH to its oxidized form (GSSG) with rate constant k_{ox} = 7.4×10^{-5} s^{-1} for the spontaneous oxidation of glutathione.

$$GSH \rightarrow 0.5\ GSSG \qquad \textbf{Reaction 2.1}$$

This rate constant was determined from erythrocytes from venous blood (hematocrit 60%), with no added glucose, incubated at 37ºC under a humidified stream of gas (O_2:CO_2 = 19:1, which corresponds to a $pO_2 \approx 720$ torr if we consider the total gas pressure of 760 torr). Under these conditions it corresponds to a continuous GSH oxidation of $\approx 2\times10^{-7}$ M GSH/s considering a GSH concentration[1] of 3.2×10^{-3} M in the erythrocyte (Thorburn and Kuchel, 1985).

However, these experiments were performed under an oxygen pressure much higher than what is found *in vivo*. Considering a pO_2 = 90 torr [as reported by (Scarpa et al., 1984) for venous blood], and assuming that O_2 freely diffuses across the erythrocyte membrane, we may find an upper estimate for the value of k_{ox}, and the corresponding rate of GSH oxidation. To adjust the value of k_{ox} for the O_2 partial pressure found *in vivo* consider Equation 2.1

$$k_{ox,in\ vivo} = k_{ox,exp} \cdot \frac{pO_{2,corrected}}{pO_{2,exp}} \qquad \textbf{Equation 2.1}$$

Where $k_{ox,in\ vivo}$ is the adjusted rate constant, $k_{ox,exp} = 7.4 \times 10^{-5}$ s^{-1} was the rate constant observed by (Thorburn and Kuchel, 1985), and $pO_{2,corrected}$ and $pO_{2,exp}$ are the *in vivo* (pO_2 = 90 torr) and experimental (pO_2 = 720 torr) partial oxygen pressures considered. Replacing these values into

[1] **From this point on, all concentrations are referred to as moles per liter of erythrocyte water.**

Equation 2.1 gives $k_{ox,in\ vivo} \approx 9.3 \times 10^{-6}$ s^{-1}. This would lead to a constant oxidation of GSH of $\approx 29 \times 10^{-9}$ M/s, again assuming a GSH concentration of 3.2×10^{-3} M in the erythrocyte (Thorburn and Kuchel, 1985).

Oxygen oxidizes GSH enzymatically (Winterbourn et al., 2002) and non-enzymatically (Scarpa et al., 1996), with overall reaction

$$2\ GSH + O_2 \rightarrow GSSG + H_2O_2$$ **Reaction 2.2**

(Scarpa et al., 1996) used the rate of GSH oxidation and determined the rate constant for the reaction above, finding $k_{spon} = 0.1\ M^{-1}s^{-1}$, as determined from the rate of GSH oxidation.

How does this rate constant compare with the experiments by (Thorburn and Kuchel, 1985)? Considering a $k_H = 1.3 \times 10^{-3}$ M O_2/atm $\approx 1.7 \times 10^{-6}$ M O_2/torr (Wilhelm et al., 1977) for Henry's law constant of O_2 dilution in water, and assuming that the experiments of (Thorburn and Kuchel, 1985) were done at $pO_2 = 720$ torr, this k_{spon} would correspond to an apparent $k_{ox} \approx 1.2 \times 10^{-4}$ s^{-1}. This value is not very far from what was obtained by (Thorburn and Kuchel, 1985), which further adds confidence to these estimates.

But how does this rate of GSH oxidation compare with k_{ox} found *in vivo*? And what would be the corresponding rate of H_2O_2 production due to GSH oxidation (Reaction 2.2)? Considering $k_{spon} = 0.1\ M^{-1}s^{-1}$, we obtain a $k_{ox} = 1.5 \times 10^{-5}$ s^{-1} for the O_2 partial pressure in venous blood ($pO_2 = 90$ torr, $k_H = 1.7 \times 10^{-6}$ M/torr). This value would thus correspond to a maximal rate of 48×10^{-9} M H_2O_2/s produced, considering that all of the glutathione contents in the cell [$GStot = 3.2 \times 10^{-3}$ M, (Thorburn and Kuchel, 1985)] is in reduced form. Because part of the GSH contents may be oxidized, this value represents an upper estimate for the rate of H_2O_2 produced due to GSH oxidation. Nevertheless, it shows that GSH autoxidation may potentially be a source of oxidative stress in the human erythrocyte.

2.1.2. Superoxide dismutation

Hydrogen peroxide may also be produced due to the dismutation of superoxide. Hemoglobin autoxidation produces superoxide that may then be dismutated to H_2O_2, in a reaction catalyzed by superoxide dismutase (SOD):

$$2\ O_2^- + 2H^+ \xrightarrow{SOD} H_2O_2 + O_2$$ **Reaction 2.3**

The rate of production of superoxide was determined by (Scarpa et al., 1984) in hemolysates, at various oxygen pressures. Considering the oxygen pressure in arterial blood (≈90 torr ≈ 0.12 atm) the authors obtained a rate of superoxide production of ≈ 15×10^{-9} M/s. If all of the superoxide produced is dismutated by superoxide dismutase this would correspond to 7.5×10^{-9} M H_2O_2/s, assuming that superoxide production limits the activity of SOD.

However, (Scarpa et al., 1996) refer that only a small fraction (≈1.6%) of the H_2O_2 produced due to glutathione autoxidation results from superoxide dismutation. Considering 48×10^{-9} M H_2O_2/s from the glutathione autoxidation by (Thorburn and Kuchel, 1985) at 90 torr, superoxide dismutation cannot account for more than ≈7.7×10^{-10} M superoxide/s. Therefore, another process must be contributing for the larger superoxide produced as determined by (Scarpa et al., 1996).

2.1.3. Hemoglobin autoxidation

Hemoglobin (Hb) autoxidation has been referred as one of the main sources of superoxide in the erythrocyte (Misra and Fridovich, 1972; Wever et al., 1973), which is then dismutated to H_2O_2. H_2O_2 dismutation occurs at a rate of 2-3% of the total hemoglobin contents per day (Bunn and Forget, 1986), which would correspond to ≈9.7×10^{-9} M/s considering 7×10^{-3} M Hb (Gerber et al., 1973) and that superoxide is produced per monomer of Hb. This rate of superoxide production is in the same order of magnitude as the 15×10^{-9} M superoxide/s reported by (Scarpa et al., 1984), and the differences may be explained by the hemolysate dilution in the latter work. However, because the dilution is not clearly referred by (Scarpa et al., 1984) we cannot estimate an approximate rate of superoxide production *in vivo* from those experiments.

If all of the superoxide is dismutated to H_2O_2, the 9.7×10^{-9} M superoxide/s corresponds to a rate of H_2O_2 production of ≈4.9×10^{-9} M/s. Yet, this value is also lower than the estimates of H_2O_2 produced from glutathione autoxidation or superoxide dismutation found above. Although this does not rule out the potentially relevant contribution of Hb autoxidation for endogenous H_2O_2 production, it does not support the claim that Hb autoxidation is the main source of ROS in the human erythrocyte (Giulivi et al., 1994; Johnson et al., 2005; Low et al., 2007).

2.1.4. H_2O_2 influx from plasma

Various processes may expose erythrocytes to extracellular H_2O_2. In localized infection foci there is recruitment of leukocytes that produce H_2O_2 at various rates (Iyer et al., 1961; Kazura et al., 1981; Nakagawara et al., 1981; Reiss and Roos, 1978). Leukocyte recruitment occurs in

wounds, tumors (Dvorak, 1986; Szatrowski and Nathan, 1991) and atherosclerotic lesions (Faggiotto et al., 1984; Gerrity et al., 1979; Watson et al., 1997), therefore increasing the H_2O_2 concentration near those locations.

Blood plasma possesses antioxidants to scavenge H_2O_2: glutathione peroxidase (Avissar et al., 1989; Maddipati and Marnett, 1987), peroxiredoxins (Schwertassek et al., 2007), low-molecular weight antioxidants (Jones et al., 1995; Jones et al., 2002), among others (Frei et al., 1988). This decreases the oxidative load that erythrocytes face[2]. Yet, erythrocytes may be exposed to strong oxidative stress while passing by inflammatory foci. These cells are actually regarded as the main H_2O_2 sinks in the human blood (Manta et al., 2009; Winterbourn and Stern, 1987). But does H_2O_2 permeation across the erythrocyte membrane allow a rapid diffusion of H_2O_2 across the cell membrane?

(Nicholls, 1965) determined the H_2O_2 diffusion constant across the membrane of horse erythrocytes. Using the catalase activity in hemolysates and intact cells, the authors determined an H_2O_2 diffusion constant $\kappa \approx 6\times10^{-4}$ cm/s. We may use this constant to estimate a pseudo-first order rate constant for H_2O_2 permeation across the membrane (k_p) from Equation 2.2.

$$k_p = \kappa \cdot \frac{A_S}{V_{ew}} \qquad \textbf{Equation 2.2}$$

where A_S is the erythrocyte surface area [$=1.35\times10^{-8}$ dm^2 (Evans and Fung, 1972)], and V_{ew} is the erythrocyte water volume [$=7\times10^{-14}$ dm^3/cell, obtained by considering 0.7 dm^3 water/dm^3 cells (Savitz et al., 1964) and erythrocyte volume of 10^{-13} dm^3 (Evans and Fung, 1972)]. Considering these values we obtain a $k_p \approx 8$ s^{-1}.

(Mueller et al., 1997b) also used the dismutase activity of catalase to determine the H_2O_2 influx rate constant. To do so they determined the breakdown of H_2O_2 using spectrophotometric methods. Prx2's contribution for H_2O_2 scavenging is very likely negligible given the very diluted hemolysate considered [0.086 g Hb/dm^3, corresponding to ≈0.2 % if 329 g Hb/dm^3 erythrocytes

---

[2] Oxidative load refers to the total iH_2O_2 production, both from endogenous processes and H_2O_2 influx. If the rate of endogenous production is small and fixed, the oxidative load is approximately proportional to eH_2O_2.

(Thorburn and Kuchel, 1985)] and high H_2O_2 concentrations (10^{-5} M) repetitively added to the mixture, which likely allows Prx2 to accumulate in oxidized form and become inactivated.

(Mueller et al., 1997b) obtained a pseudo-first order rate constant for the activity of catalase $k_{catalase}$ = 0.5 s^{-1}·g Hb^{-1}·dm^3 (expressed per dm^3 of solvent). This corresponds to $k_{catalase}$ = 235 s^{-1} considering 329 g Hb/dm^3 erythrocytes (Thorburn and Kuchel, 1985) and 0.7 dm^3 water/dm^3 erythrocytes. Assuming that catalase is the main H_2O_2 scavenger in the conditions of the experiment we may consider the reaction scheme

$$eH_2O_2 \underset{k_P}{\overset{k_P}{\rightleftharpoons}} iH_2O_2 \xrightarrow{k_{catalase}}$$

Where k_p is the pseudo-first order rate constant for H_2O_2 permeation across the erythrocyte membrane. One may describe mathematically the reactions above according to Model 2.1.

$$\frac{d\ eH_2O_2}{dt} = k_p \cdot \left(iH_2O_2 - eH_2O_2\right)$$
$$\frac{d\ iH_2O_2}{dt} = k_p \cdot eH_2O_2 - iH_2O_2 \cdot (k_p + k_{catalase})$$

Model 2.1

When iH_2O_2 is in steady state and taking Model 2.1 into consideration we get

$$\frac{d\ eH_2O_2}{dt} = -\frac{1}{\frac{1}{k_p} + \frac{1}{k_{catalase}}} eH_2O_2$$

Equation 2.3

Which, considering that hemolysates present only 5.8% of the catalase activity of intact cells as found by (Mueller et al., 1997b) gives

$$\frac{1}{\frac{1}{k_p} + \frac{1}{k_{catalase}}} = 0.058 \cdot k_{catalase}$$

Equation 2.4

Replacing $k_{catalase}$ = 235 s^{-1} as found by (Mueller et al., 1997b) into the equation above we obtain a $k_p \approx 13.6$ s^{-1}. This value is slightly higher than $k_p = 8s^{-1}$ obtained from the permeability constant of (Nicholls, 1965) but is still in agreement with the latter.

These two independent experiments determined the pseudo-first order rate constants for H_2O_2 permeation across the erythrocyte membrane. The values obtained (k_p = 8 – 14 s^{-1}) show that the kinetics of H_2O_2 diffusion across the erythrocyte membrane may occur at fast rates if the plasma

H_2O_2 is relatively high. Because erythrocytes may be exposed to H_2O_2 concentrations up to the micromolar range in pathological conditions (Lacy et al., 1998; Niethammer et al., 2009; Varma and Devamanoharan, 1991), extracellular H_2O_2 represents a potential source of oxidative stress for this cell.

2.2. Relevance of the main defenses against H_2O_2 in erythrocytes

The accumulation of H_2O_2 may have various deleterious effects for the erythrocyte. Exposure to high H_2O_2 loads leads to the formation of echinocytes, increases membrane rigidity, and leads to phagocytosis of erythrocytes by monocytes (Snyder et al., 1985). H_2O_2 leads to lipid peroxidation (Bunyan et al., 1960), oxidizes hemoglobin leading to larger ROS production (Fox et al., 1974; Giulivi and Davies, 1990; King and Winfield, 1963; Svistunenko et al., 1997; Winterbourn, 1985). H_2O_2 may also cause hemoglobin denaturation and induce hemolysis (Davies and Goldberg, 1987; Younkin et al., 1971), thus affecting oxygen transport. Because erythrocytes may be exposed to H_2O_2 from various sources (Sections 2.1.1 to 2.1.4) and H_2O_2 is potentially toxic for the cell, defenses against H_2O_2 are very important for these cells.

In this section we review relevant properties of the three main defenses against H_2O_2 in human erythrocytes: Glutathione Peroxidase 1 (GPx1), catalase, and Peroxiredoxin 2 (Prx2). Although we focus on human cells, some of the evidence that led to the current knowledge in H_2O_2 defense was obtained from studies done in other organisms. These studies will be referred to show how the current picture of H_2O_2 defense in human erythrocytes came to involve GPx1, catalase and Prx2.

2.2.1. The debate around the relative importance of catalase and GPx1

Catalase was discovered in the beginning of the twentieth century and was the first enzyme described with H_2O_2 scavenging ability (Loew, 1900). Due to its antioxidant properties it was since considered the intracellular defense against H_2O_2. In the erythrocyte, only fifty years later was another H_2O_2 defense found: (Mills, 1957) found in rat erythrocytes that this antioxidant, together with glutathione, was able to protect hemoglobin from oxidative breakdown. The authors had discovered GPx1. As we will see, GPx1 was then considered the main defense of human erythrocytes cells against H_2O_2. Further studies done later then set catalase as a more

relevant defense against H_2O_2. The peroxidase activity of Prx2 was only acknowledged in the 2000s.

The human erythrocyte GPx1 is responsible for reducing H_2O_2 and lipid peroxides. The experiments of (Mills, 1957, 1959) with rat erythrocytes put in question the role of catalase as the intracellular hydrogen peroxide scavenger. This issue was addressed by (Cohen and Hochstein, 1963) who demonstrated the presence of GPx1 in human erythrocytes.

GPx1-catalized H_2O_2 reduction is coupled with the oxidation of glutathione (GSH). Oxidized glutathione (GSSG) is then regenerated back to GSH by glutathione reductase (GSR) at the expense of NADPH (Figure 2.1). The pentose phosphate pathway (PPP) is the main source of NADPH in the human erythrocyte (Kirkman et al., 1986).

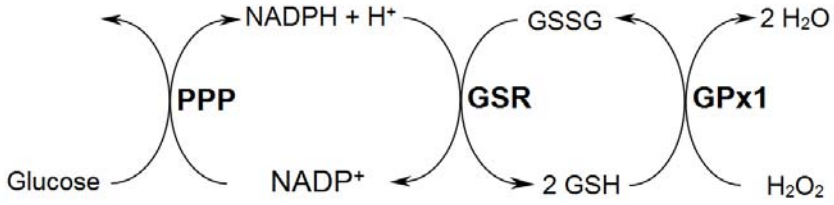

Figure 2.1 – H_2O_2 reduction by GPx1 and coupled oxidation of GSH. GSR reduces GSSG at the expense of NADPH, whose main source is the PPP. Adapted from (Cohen and Hochstein, 1963).

(Cohen and Hochstein, 1963) assessed the redox status of hemoglobin as a means to determine the intracellular H_2O_2 in the cytoplasm. They also quantified the amount of reduced glutathione (GSH) present in cells (GPx1 oxidizes GSH when reducing H_2O_2). They observed that erythrocytes subjected to H_2O_2 exhibited less GSH, accumulated methemoglobin (MetHb, an oxidized form of hemoglobin) and presented higher hemolysis than control (untreated) erythrocytes.

On the other hand, erythrocytes supplemented with glucose show practically no accumulation of MetHb, a low hemolysis and high GSH concentrations. These observations may be explained by a larger NADPH supply due to the glucose provided. Glucose-6-phosphate is used by the PPP as a substrate to produce NADPH. Reducing equivalents from NADPH are then used by GSR to regenerate glutathione (Worthington and Rosemeyer, 1976). If the NADPH supply is not limiting GSR's activity, GSH is regenerated and the H_2O_2 scavenging activity of GPx1 is not limited by GSH availability. Under those conditions, GPx1 is able to prevent the accumulation of H_2O_2 and MetHb. Further, even erythrocytes exposed to sozium azide (a catalase inhibitor), glucose and

H_2O_2 exhibited similar GSH levels to those found in untreated erythrocytes, showing that GPx1 is an efficient H_2O_2 scavenger under those conditions.

The evidence above led (Cohen and Hochstein, 1963) to conclude that GPx1 was the main line of defense against H_2O_2 in the human erythrocyte, only then followed by catalase. These conclusions were accepted for several years (Awasthi et al., 1975; Beutler, 1977; Little et al., 1970; Luzzatto and Testa, 1978). Further supporting them was the observation that a low NADPH supply leads to higher oxidative stress (Gaetani et al., 1974). If GPx1 was the main defense against H_2O_2, and because its activity is stoichiometrically coupled with NADPH oxidation, a deficient NADPH supply would affect the antioxidant activity of GPx1. This would explain why glucose-6-phosphate dehydrogenase (G6PD) deficient erythrocytes are particularly prone to suffer with oxidative stress, thus accumulating GSSG and presenting low NADPH/$NADP^+$ ratios (Gaetani et al., 1974; Kirkman et al., 1975).

The findings that catalase tightly binds NADPH (Kirkman and Gaetani, 1984) and that this NADPH prevents catalase inactivation (Kirkman et al., 1987) prompted a reassessment of the contribution of catalase and GPx1 for the defense of the human erythrocyte against H_2O_2.

The PPP is not only the main source of NADPH in the human erythrocyte (Kirkman and Gaetani, 1986), it is also the main source of CO_2 in this cell (Brin and Yonemoto, 1958). H_2O_2 reduction is stoichiometrically coupled to NADPH production by the PPP as 1Glucose-6-phosphate:2NADPH:1CO_2:4GSH:2H_2O_2. This means that oxidation of each glucose-6-phosphate (G6P) molecule to ribulose-5-phosphate by the PPP generates 2 NADPH and 1 CO_2 molecules. In turn, for every NADPH molecule used by GSR, 2 GSSG are regenerated to GSH. Because GPx1 consumes 2 GSH per H_2O_2 reduced, each G6P molecule consumed by the PPP allows the regeneration of two H_2O_2 molecules by GPx1. This verifies if GSR used all of the NADPH produced by the PPP.

(Gaetani et al., 1989) determined the rate of NADPH production by providing radioactively-labeled (^{14}C) glucose to erythrocytes and quantifying the amount of $^{14}CO_2$ as a proxy for the PPP activity. (Gaetani et al., 1989) compared the rate of $^{14}CO_2$ production to the rate of H_2O_2 consumed, by considering the stoichiometry of G6P oxidation/H_2O_2 consumed above.

According to (Gaetani et al., 1989), if GPx1/GSR was the main H_2O_2 defense, the rate of $^{14}CO_2$ formed would be about half of the rate of H_2O_2 added. The study of (Gaetani et al., 1989) further

differed from what had been previously done by (Cohen and Hochstein, 1963) because the authors were now able to expose erythrocytes to a constant and controlled rate of formation of H_2O_2 (through addition of glucose oxidase to the medium). This allowed the authors to directly compare the rates of NADPH produced (through $^{14}CO_2$ formed) with the rate of H_2O_2 formed in normal and acatalasemic human erythrocytes. According to the stoichiometry above, for every mole of H_2O_2 produced half a mole of $^{14}CO_2$ would be formed.

(Gaetani et al., 1989) observed that acatalasemic erythrocytes had larger rates of $^{14}CO_2$ formed than normal erythrocytes when exposed to H_2O_2. This suggested that those erythrocytes had to produce more NADPH for GPx1/GSR to scavenge H_2O_2, thus compensating for the absence of catalase. Based on the rate of $^{14}CO_2$ formed, the authors referred that about 90% of the H_2O_2 was consumed by GPx1 in acatalasemic erythrocytes. However, in normal erythrocytes GPx1 would only account for 20 – 40% of the H_2O_2 consumed. These results would go against what had been previously thought: catalase seemed to have a larger contribution for H_2O_2 scavenging than what was found from the studies of (Cohen and Hochstein, 1963).

The following later observations (Gaetani et al., 1994) further reinforced this conclusion. Instead of using acatalasemic erythrocytes, (Gaetani et al., 1994) now inhibited catalase (with 3-amino-l:2:4-triazole) to compare the relevance of GPx1 and catalase for defense of human erythrocytes against H_2O_2. Similarly to (Gaetani et al., 1989), they also determined the rate of NADPH formed by determining the rate of formation of $^{14}CO_2$. (Gaetani et al., 1994) found that erythrocytes exposed to aminotriazole supplemented with glucose did not exhibit accumulation of methemoglobin, depletion of GSH or extensive hemolysis, unlike what was observed by (Cohen and Hochstein, 1963) in catalase-inhibited erythrocytes. This suggested that a sufficient NADPH supply allows erythrocytes to remain protected against H_2O_2. (Gaetani et al., 1994) attributed this ability to GPx1/GSR. These results, in agreement with (Cohen and Hochstein, 1963), suggest that GPx1/GSR was able to protect human erythrocytes as long as the NADPH supply was sufficient to cope with the oxidative load.

With this in mind, the authors then aimed to determine the fraction of catalase inactivated under which the NADPH supply would increase, thus showing that GPx1 had the highest contribution for H_2O_2 consumption. This would allow them to find the fraction of catalase inactivation required for erythrocytes to rely mainly on GPx1/GSR for their H_2O_2 defense. They observed

that only >98% catalase inactivation would increase the rate of NADPH production, suggesting a very different contribution for the two antioxidants in defense against H_2O_2. These results support a more important role of catalase for H_2O_2 defense than previously thought.

Adding further support to this conclusion, (Gaetani et al., 1996) studied a cell-free system that consisted of a mixture of catalase and GPx1 and coupled cycles (GSH/GSR, NADPH production by G6PD). This allowed the concentration of individual components of the system to be changed, providing a better insight into the role of each defense in H_2O_2 removal than what could be gained using intact cells. The authors aimed to mimic the intracellular conditions found *in vivo*: catalase, GPx1 and Hb were purified and their concentrations were proportional to the ones found *in vivo*; oxidative conditions similar to the ones found in the cell (GSH and NADPH-wise). Excess G6PD and GSR were added to the reaction mixture, as well as a low and constant flow of $\approx 88 \times 10^{-9}$ M H_2O_2/s. (Gaetani et al., 1996) used the rate of formation of 6-phosphogluconate to determine the rate at which H_2O_2 was being removed by the GPx1/GSR system.

They found that in this cell-free system GPx1 consumes only ≈15% of the H_2O_2, the rest being consumed by catalase. These observations now imply that GPx1 contributes very little for defense against H_2O_2 comparatively to catalase. This conclusion was further supported by the experiments of (Mueller et al., 1997a) where the authors used both purified enzymes and hemolysates to determine catalase and GPx1 activity. The authors concluded that GPx1 consumes H_2O_2 at a rate that is at most 8% of that achieved by catalase. In agreement with these findings, (Johnson et al., 2000) addressed the contribution of GPx1 for the protection of mice erythrocytes. The authors disrupted the GPx1-encoding gene in mice and found that erythrocytes from GPx1-mutant mice did not exhibit larger accumulation of MetHb than wild type erythrocytes.

The observations of (Gaetani et al., 1996), (Mueller et al., 1997a) and (Johnson et al., 2000) showed that GPx1 has a small contribution for the defense of erythrocytes against H_2O_2. But if catalase is the main defense against H_2O_2 in human erythrocytes, why do these cells need GPx1? (Gaetani et al., 1996) hypothesized that GPx1 is required for defending these cells against organic peroxides. The importance of GPx1 for defense of erythrocytes from organic peroxides had been previously suggested by (Flohe, 1978). As showed by (Johnson et al., 2002), GPx1-

deficient mice erythrocytes exhibited larger concentrations of MetHb when exposed to cumene peroxide than wild type cells.

2.2.2. Evidence of an unknown antioxidant

The experiments of (Gaetani et al., 1996) went further to compare the rate of 6-phosphogluconate generated in their *in vitro* assay to that found in intact cells, relatively to catalase activity. They observe that the rate of generation of 6-phosphogluconate decreases with catalase activity, which is consistent with a decreasing relevance of GPx1/GSR for H_2O_2 decomposition with increasing catalase activity. Interestingly, they observed that the rate of 6-phosphogluconate generation decreases more steeply with increasing catalase activity in their cell-free experiments (no added Hb) than in the experiments done with whole cells (Gaetani et al., 1994). This difference suggests that another process besides GPx1/GSR is spending NADPH to consume H_2O_2.

While the NADPH-dependent prevention of catalase inactivation may account for part of the NADPH consumed, the rate at which catalase oxidizes NADPH is only ≈7% of its rate of H_2O_2 dismutation (Kirkman et al., 1987). Therefore, another process must account for the difference in rates of generation of 6-phosphogluconate between the experiments of (Gaetani et al., 1996) and (Gaetani et al., 1994). (Gaetani et al., 1996) hypothesize that the peroxidase activity of hemoglobin (Gunzler et al., 1974) may account for part of the differences found: when they added Hb to the reaction mixture there was a slight increase in the rate of 6-phosphogluconate produced. Yet, the peroxidase activity of Hb alone cannot account for the differences in 6-phosphogluconate produced between their experiments and the experiments of (Gaetani et al., 1994). This suggests that still another process may be oxidizing NADPH while consuming H_2O_2.

Further, as per studies done in mice, it was shown that certain acatalasemic tissues retain more than half of their H_2O_2-consumption activity comparatively to wild-type cells (Ho et al., 2004). Yet, this is unlikely due to GPx1 activity: the disruption of the GPx1-encoding gene does not change catalase activity or affect the survival in various mice tissues (Ho et al., 1997).

2.2.3. The relevance of peroxiredoxin

Thiol-specific antioxidant (TSA), a peroxidase that had recently been discovered in yeast was a plausible candidate for explaining such observations for the following three reasons. First, TSA homologues were found in human cells (Chae et al., 1994b), which prompted addressing whether

they would be contributing for H_2O_2 scavenging in human erythrocytes. Second, TSA had an important contribution for the defense against oxidative stress in various organisms (Chae et al., 1993; Kim et al., 1989). It could have a similar relevance for the defense of human erythrocytes against H_2O_2 if found in these cells. Third, its antioxidant activity was coupled with NADPH oxidation (Chae et al., 1994a). This could explain the differences in the rates of NADPH consumption observed in the experiments of (Ho et al., 1997) and (Ho et al., 2004).

TSA was first discovered by (Kim et al., 1985) in *Saccharomyces cerevisiae*. Although its importance for defense against H_2O_2 was not known at the time, its potential as an antioxidant was readily acknowledged. The authors observed that glutamine synthetase was inactivated in thiol-containing buffers but retained their activity in crude extracts containing the same thiols. This suggested the existence of a thiol protective protein.

The same group went on to study this enzyme (Kim et al., 1989; Kim et al., 1988). (Kim et al., 1989) compared the concentrations of TSA in *Saccharomyces cerevisiae* cultured in normal aerobic conditions (1atm, ≈21% O_2, ≈78% N_2), with those of cells either shifted to hyperaerobic conditions (1atm, 95% O_2, 5% CO_2) or anaerobic conditions (1atm, 95% N_2, 5% CO_2). The authors observed a ≈1.7 fold increase TSA concentration 4 hours after cells had been shifted to hyperaerobic conditions. On the other hand, cells shifted to anaerobic conditions exhibited a 65% decrease in TSA concentration. (Chae et al., 1993) then assessed the effects of TSA-deficiency on cell survival by constructing yeasts whose TSA-encoding gene had been knocked-out. The mutant cells exhibited similar growth rates to the wild-type cells when grown in anaerobic conditions but significant slower growth rates when cultured under aerobic conditions or when exposed to ROS (H_2O_2, superoxide or hydroxyl).

The studies of (Kim et al., 1989) and (Chae et al., 1993) suggested that TSA was an important antioxidant defense in yeast cells. TSA homologues were found in various organisms including humans, rodents, bacteria, fungi and plants (Chae et al., 1994b). This family of peroxidases was later renamed as peroxiredoxins. *Peroxi* comes from their ability to reduce peroxides and *redoxin* from the various types of electron donors they use. These donors may be thioredoxin [as found in *S. cerevisiae* (Chae et al., 1994a)], thioredoxin homologues [as found in *Salmonella typhimurium* (Jacobson et al., 1989)], or even glutaredoxin [as found in *Populus trichocarpa* (Rouhier et al., 2001)]. Their peroxide reducing activity relies in highly conserved cysteines (Chae et al., 1994a).

The discovery of peroxiredoxins in the human brain (Chae et al., 1994b; Lim et al., 1994a) prompted studies to determine if human erythrocytes also possessed such peroxidases. Indeed, a TSA homologue later called peroxiredoxin 2 was found to be the third most abundant protein in the human erythrocyte (Moore et al., 1991).

Initial studies of erythrocyte peroxiredoxin 2 showed that it was able to prevent peroxidation of the cell membrane (Lim et al., 1994b). This finding prompted further studies about its role as an antioxidant in this cell. (Lee et al., 2003) carried out one of the first studies to assess the relevance of Prx2 *in vivo*. They found that although the Prx2-knockout mice were healthy in appearance and fertile, exhibited hemolytic anemia and a series of pathologies in their erythrocytes: they formed Heinz bodies (accumulation of denatured Hb), accumulated ROS and MetHb, and were morphologically abnormal. The hematocrit of Prx2-deficient mice was also significantly decreased, although higher rates of erythropoiesis were found. This showed that although Prx2 was not essential for mice survival, it had an important role in redox physiology of the human erythrocyte.

(Johnson et al., 2005) went further to determine whether the H_2O_2 scavenging activity of Prx2 was indeed contributing for the protection of erythrocytes from H_2O_2. (Johnson et al., 2005) aimed to determine the rates of Hb autoxidation and endogenous generation of H_2O_2. They did so through experimental and modeling methods. First they quantified the amount of MetHb in mice erythrocytes and determined the rate of catalase inactivation. They used GPx1-deficient mice so that GPx1 would not compete with Prx2 for H_2O_2, thus assessing just the role of catalase and Prx2.

The rate of catalase inactivation was used for determining the H_2O_2 produced endogenously as we now explain. As ferricatalase reduces H_2O_2 there is accumulation of Compound I (a redox form of catalase), which may then be reduced back to ferricatalase through reaction with H_2O_2 again.

$$\text{Ferricatalase}(Fe^{3+}) + H_2O_2 \rightarrow \text{Compound I}(Fe^{4}{=}O) + H_2O \qquad \textbf{Reaction 2.4}$$

$$\text{Compound I}(Fe^{4}{=}O) + H_2O_2 \rightarrow \text{Ferricatalase}(Fe^{3+}) + H_2O + O_2 \qquad \textbf{Reaction 2.5}$$

The catalase inhibitor 3-Amino-1,2,4-Triazole competes with H_2O_2 for Compound I, irreversibly forming a product that cannot be converted to Ferricatalase:

Compound I + 3-Amino-1,2,4-Triazole → Inactive Compound **Reaction 2.6**

Thus, for 3-Amino-1,2,4-Triazole concentrations that are high enough to strongly outcompete H_2O_2 for Compound I the rate of catalase inactivation is proportional to H_2O_2 concentration. Using this approach, (Johnson et al., 2005) observed that catalase inactivation is very slow (≈3.5% catalase inhibition/hour), which indicates a low intracellular concentration of H_2O_2. This was observed both in GPx1-deficient and wild type erythrocytes, not exposed to exogenous H_2O_2.

With the aim of understanding if Prx2 was contributing for the defense against H_2O_2 in GPx1 deficient cells (Johnson et al., 2005) built a kinetic model. This model considered the H_2O_2-scavenging activity of Prx2 and catalase; interaction between superoxide and Hb; dismutation of superoxide by superoxide dismutase; and hemoglobin autoxidation and reduction. Using this model they observed that only the inclusion of Prx2 would permit fitting the predicted inactivation of catalase to the experimental data. With this model they also obtained similar MetHb levels as those found experimentally. This shows that the H_2O_2 scavenging activity of Prx2 is indeed necessary for explaining the low intracellular H_2O_2 found experimentally in erythrocytes.

The role of Prx2 in protecting human erythrocytes from endogenously generated H_2O_2 was further supported by the studies of (Low et al., 2007). The authors assessed the redox status of Prx2 when human erythrocytes (≈0.05% hematocrit) were exposed to 0 - 2×10^{-4} M H_2O_2 boluses. They observed that Prx2 was very sensitive to H_2O_2 oxidation: more than 60% of the Prx2 contents were oxidized when cells were exposed to 5×10^{-7} M H_2O_2. These results are further supported by the high reactivity of Prx2 with H_2O_2, of 10^7 M^{-1} s^{-1} (Peskin et al., 2007). However, because oxidized Prx2 does not reduce H_2O_2, accumulation of oxidized Prx2 affects the contribution of Prx2 for H_2O_2 scavenging. (Low et al., 2007) thus refer that Prx2 contributes for the protection of the human erythrocyte only against low H_2O_2 loads.

The importance of Prx2 for H_2O_2 consumption was later addressed by (Johnson et al., 2010). The authors compared the contributions of these three antioxidants using four gene knockout mice: catalase knockouts; GPx1 knockouts; catalase and GPx1 double knockouts; and Prx2 knockouts. They then assessed the redox status of erythrocytes from those knockouts by determining MetHb accumulation and the rate of accumulation of intracellular H_2O_2 [using similar methods to the

ones used by (Johnson et al., 2005)]. This was addressed by exposing the erythrocytes (5% hematocrit) to $0 – 5\times10^{-4}$ M H_2O_2 boluses.

In agreement with previous studies, they found that catalase knockout or double knockout erythrocytes accumulated MetHb. This accumulation was more extensive when cells were faced with higher H_2O_2 loads. GPx1 knockouts did not show substantial MetHb accumulation. On the other hand, Prx2 knockouts accumulate intracellular H_2O_2 when no exogenous H_2O_2 is added. Given that GPx1 contributes little for the defense against H_2O_2, this suggests that catalase is able to protect the erythrocyte under basal oxidative conditions. It also suggests that Prx2 activity is important for controlling the rate at which H_2O_2 accumulates due to endogenous production.

Using a model similar to the one built by (Johnson et al., 2005) the authors again assessed the rate of catalase inactivation in wild type and Prx2-deficient mice erythrocytes, obtaining a very good fitting to their experimental data. Using this model they estimate the intracellular H_2O_2 found in each of the knock-outs, under basal conditions. They estimate a ≈388% increase in intracellular H_2O_2 in the absence of Prx2, and only ≈23% and 4% in the absence of GPx1 and catalase, respectively.

These results suggest that Prx2 and catalase have very distinct roles in the defense of the human erythrocyte against H_2O_2. Catalase is the main defense against high H_2O_2 loads, thus protecting the cell from extracellular H_2O_2. On the other hand Prx2 plays an important role in the defense against low H_2O_2, thus being the main defense against endogenously generated H_2O_2.

However, if Prx2 is one of the most abundant proteins in the human erythrocyte and has a very high reactivity with H_2O_2 [$10^7 – 10^8$ $M^{-1}s^{-1}$, (Manta et al., 2009; Peskin et al., 2007)] what limits Prx2 activity? As previously suggested by (Chae et al., 1994a) in their studies from TSA in yeast, and later by the studies of (Low et al., 2007) in human erythrocytes, H_2O_2 consumption by Prx2 is affected by the regeneration of Prx2. Prx2 regeneration is in turn dependent on the ability of the Thioredoxin/Thioredoxin Reductase cycle to maintain a high rate of Prx2 reduction.

2.3. Peroxiredoxin 2: catalytic cycle and main features in human erythrocytes

As we will show in this section, Prx2 activity is highly dependent on the ability of the Thioredoxin/Thioredoxin Reductase to regenerate Prx2. Before further expanding this issue we will characterize several features of Prx2 in human erythrocytes.

Although human cells have various peroxiredoxins (Wood et al., 2003b), Prx2 is the most abundant peroxiredoxin in human erythrocytes. Other than its peroxidase activity, various reports showed that Prx2 is important for other processes: activates the Gardos channel for K^+ efflux (Moore et al., 1991; Moore et al., 1990), and acts as a chaperone against heat-shock (Jang et al., 2004; Moon et al., 2005). In human erythrocytes, Prx2 is the third most abundant protein after hemoglobin and carbonic anhydrase (Moore et al., 1991).

2.3.1. Prx2 structure

Prx2 is a pentamer of dimers (Figure 2.2) with a monomeric weight of 22 kDa (Moore and Shriver, 1994; Schroder et al., 2000).

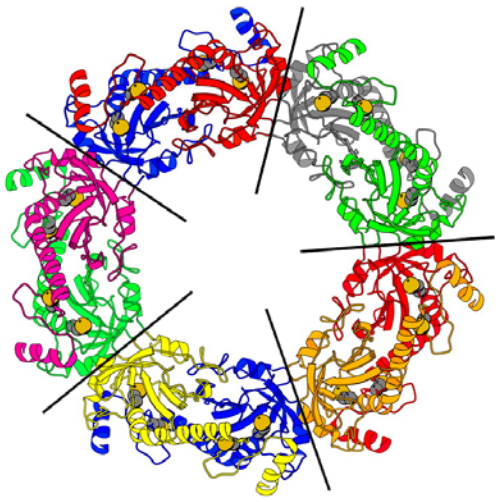

Figure 2.2– Quaternary structure of Prx2 adapted from (Schroder et al., 2000), deposited at the Protein Data Bank (Bernstein et al., 1977) with accession number 1QMV. The bars separate each dimer. Each monomer is marked with a different color.

There are various types of peroxiredoxins, classified based on their catalytic cycles. However, all of them rely on highly conserved cysteines to scavenge H_2O_2 (Chae et al., 1994b). Prx2 is a "typical 2-Cysteine" peroxiredoxin, meaning it relies on two cysteines per monomer to catalyze

H_2O_2 reduction: Cys_{51} and Cys_{172}. In each dimer, the two monomers are arranged in an anti-parallel way. Figure 2.3 shows this anti-parallel disposition and highlights the two cysteines.

Figure 2.3 – Antiparallel structure of two monomers (cyan and yellow) in each dimer of Prx2. A – Ribbon diagram of a dimer showing the location of Cys_{172} (red residues) and a Cys_{51} (black residues); taken from PDB (Bernstein et al., 1977) entry 1QMV. B – Representation of the antiparallel disposition of the two monomers, showing the peroxidatic (C_P) and resolving (C_R) cysteines in each monomer.

Cys_{51} and Cys_{172} are respectively called peroxidatic (C_P) and resolving (C_R) cysteine due to their role in the catalysis of H_2O_2 reduction. The antiparallel arrangement of the two monomers in a dimer permits that C_P of a monomer interacts with a C_R of the subsequent monomer during the catalytic cycle of Prx2 described below.

2.3.2. Catalytic cycle of Prx2

During the catalytic cycle of Prx2 (Figure 2.4), H_2O_2 oxidizes the peroxidatic cysteine (C_P-SH) to a sulfenic acid (C_P-SOH). This residue then condenses with the resolving cysteine from the other monomer (C_R-SH) to form a disulfide bond. (Cha and Kim, 1995) showed that these cysteines are then reduced to sulfidryl through the oxidation of thioredoxin (Trx). The oxidized Trx (Trx_{Ox}) is then reduced back (Trx_{Red}) by thioredoxin reductase (TrxR) at the expense of NADPH. The sulfenic acids may be further oxidized to sulfinic acid, inactivating the protein (Schroder et al., 2000). This reaction is often referred as “overoxidation” or “sulfinylation” of Prx2. (Biteau et al., 2003) showed that cysteines in sulfinic form may be reduced through sulfiredoxin (Srx) oxidation, coupled to ATP hydrolysis. *In vitro* experiments showed that Trx and GSH may both act as electron donors to regenerate Srx to its reduced form (Chang et al., 2004).

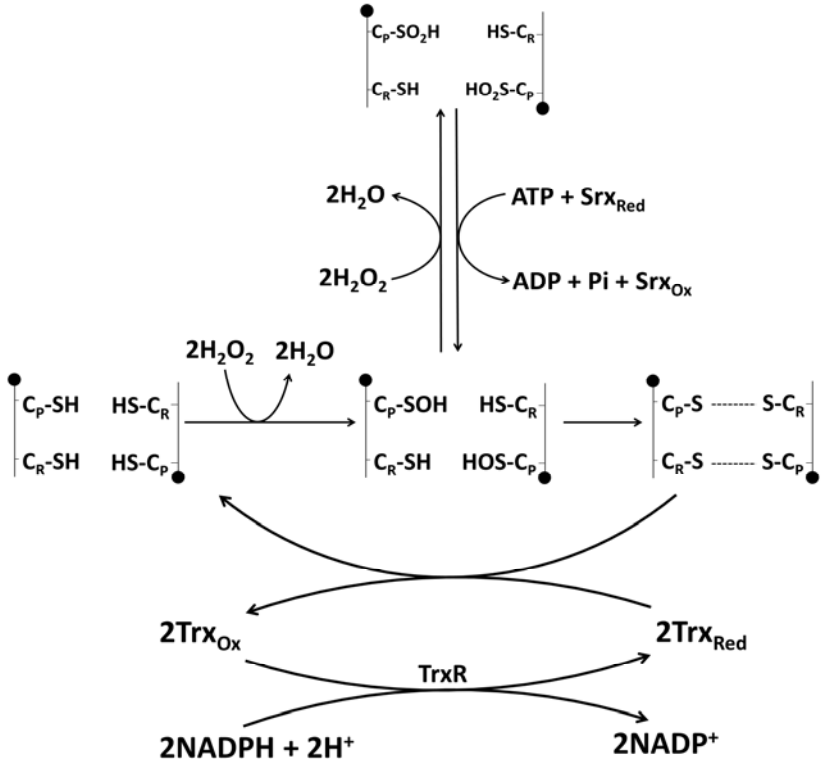

Figure 2.4 - Catalytic cycle of Prx2 showing the redox status of the peroxidatic (C_P) and resolving (C_R) cysteines. The dashed lines represent disulfide bonds. Trx_{Red} – Reduced thioredoxin; Trx_{Ox}– Oxidized thioredoxin; TrxR – Thioredoxin reductase; Srx_{Red} – Reduced sulfiredoxin; Srx_{Ox} – Oxidized sulfiredoxin.

Figure 2.4 represents a simplification of the catalytic cycle of Prx2, thought to involve unfolding of the active site and interaction with other conserved residues besides cysteines (Wood et al., 2003a). From this point on we will refer to the various redox forms of Prx2 as follows: reduced (Prx_{Red}), sulfenic-acid (PSOH), disulfide (PSSP), sulfinic-acid (PSO_2H).

2.3.3. Prx2 inactivation by H_2O_2

Prx2 may be inactivated by H_2O_2 if it accumulates either in PSO_2H or PSSP forms. The inactivation of Prx2 due to accumulation of PSSP was studied by (Low et al., 2007). The authors showed that Prx2 is very sensitive to oxidation: ≈60 % of the total Prx2 contents are in PSSP form when erythrocytes (hematocrit ≈ 0.05%) are exposed to 5×10^{-7} M H_2O_2 boluses. Higher oxidative loads lead to more extensive accumulation of PSSP.

Why does Prx2 accumulate in PSSP form? Various factors contribute to this. First, Prx2 has a very high reactivity with H_2O_2 [$k\approx 10^7 - 10^8$ $M^{-1}s^{-1}$ (Manta et al., 2009; Peskin et al., 2007)]. This allows Prx2 to be quickly oxidized by H_2O_2. Second, (Low et al., 2007) observed that Prx2 regeneration occurs slowly (takes about 20 minutes to fully reduce Prx2 that had accumulated in

PSSP form). (Low et al., 2007) found that TrxR has a slow rate of activity, as assessed by the rate of DTNB reduction, a TrxR substrate commonly used for assessment of TrxR activity. A slow TrxR activity leads to PSSP and Trx_{Ox} accumulation, hence limiting the Trx_{Red} available to reduce Prx2. However, it is not clear whether TrxR activity is limited by NADPH supply, total Trx, or low TrxR activity.

Prx2 may also be inactivated due to accumulation in PSO_2H form. This type of inactivation was found in peroxiredoxins from other human cells (Mitsumoto et al., 2001; Yang et al., 2002) and regeneration of PSO_2H occurs very slowly and consumes ATP (Biteau et al., 2003). It was proposed that this process allows Prx2 to act as a floodgate (Wood et al., 2003a). According to this hypothesis, Prx2 protects cells against low concentrations of H_2O_2. However, because Prx2 is inactivated by formation of PSO_2H when the oxidative load is too intense, the "floodgate opens" and H_2O_2 accumulates. This permits H_2O_2 to develop its signaling functions. The sulfinylation of Prx2 also allows this protein to aggregate into high molecular weight oligomers (such as decamers or dodecamers), switching *on* the chaperone activity of Prx2 (Jang et al., 2004; Moon et al., 2005). It also stimulates the association of Prx2 with membranes (Cha et al., 2000; Moore et al., 1991).

But the accumulation of PSO_2H affects the contribution of Prx2 for defense against H_2O_2. (Low et al., 2007) addressed whether Prx2 would accumulate in PSO_2H form in the human erythrocyte by exposing cells (≈0.05% hematocrit) to a 5×10^{-6} - 2×10^{-4} M H_2O_2 boluses for 10 minutes. The authors observed that PSO_2H accumulation does not occur in human erythrocytes, regardless of the H_2O_2 which the cells are exposed to. They explain the absence of PSO_2H with the slow rate of Prx2 regeneration: the accumulation of PSSP limits the formation of PSOH, thus affecting the accumulation of PSO_2H.

Another study also addressed the issue of PSO_2H accumulation (Cho et al., 2010). The authors detected PSO_2H in erythrocytes (50% hematocrit) 3 hours after exposed to a steady flux of 75×10^{-9} M H_2O_2/s. However, no PSO_2H was detected in absence of added H_2O_2 even when catalase had been inhibited by sozium azide or 3-Amino-1,2,4-Triazole. These results suggest that although the Srx activity is sufficient to keep PSO_2H below detection limits under basal H_2O_2 conditions, exposure to extracellular H_2O_2 leads to accumulation of PSO_2H. This may be attributable to the importance of Prx2 in scavenging low H_2O_2: because Prx2 is important for

protecting the erythrocyte from the endogenously generated H_2O_2, Srx activity must cope with the rate at which Prx2 is being sulfinylated under basal oxidative loads. For this reason, inhibiting catalase does not lead to accumulation of PSO_2H under basal oxidative loads.

The results of (Cho et al., 2010) seem in disagreement with what had been observed by (Low et al., 2007). However, as we now explain both results may be explained by the hypothesis raised by (Low et al., 2007) for absence of PSO_2H. Note that as per the conditions of their experiments, (Low et al., 2007) exposed erythrocytes to much larger oxidative stress than (Cho et al., 2010).

(Cho et al., 2010) addressed the redox status of Prx2 after having exposed erythrocytes to a constant flux of H_2O_2 that had generated 6×10^{-3} M extracellular H_2O_2 by the time of the assessment, as per experimental quantification. On the other hand (Low et al., 2007) exposed erythrocytes to a bolus of $<2\times10^{-4}$ M H_2O_2 and assessed the redox status of Prx2 only after 10 minutes of reaction. Yet, (Low et al., 2007) considered a very diluted hematocrit (≈1000-fold lower than the hematocrit considered by (Cho et al., 2010)). Therefore, the erythrocytes were subjected to much lower oxidative stress in the experiments of (Cho et al., 2010) than in the experiments of (Low et al., 2007).

A low oxidative stress may have allowed Prx2 regeneration to prevent accumulation of PSSP in the experiments of (Cho et al., 2010), thus allowing the accumulation of PSO_2H. Supporting this explanation is the observation that most of the Prx2 contents in the experiments of (Cho et al., 2010) are in reduced form at time of assessment, whereas most Prx2 is in PSSP form in the experiments of (Low et al., 2007). Altogether, these results suggest that Prx2 sulfinylation depends on the H_2O_2 load which erythrocytes are exposed to.

Nevertheless, we may hypothesize about the relative contribution of each defense in erythrocytes facing various H_2O_2 loads. Under basal oxidative conditions, Prx2 is the main scavenger of H_2O_2 due to its high abundance and reactivity with H_2O_2. On the other hand, H_2O_2 loads that lead to Prx2 inactivation may occur either if TrxR activity is insufficient to cope with the demand for Trx_{Red} or if Prx2 accumulates in sulfinylated form. Under such conditions, catalase becomes the main H_2O_2 scavenger.

3. Problem and objective

The observations above bring us to the objective of this work: to understand what is the physiological role of Prx2.

Prx2 is one of the most abundant proteins in the human erythrocyte, and has a very high reactivity with H_2O_2. For this reason, it is a potentially very relevant defense of human erythrocytes against H_2O_2. However, its role in the defense of this cell against peroxide is not clear. Prx2 regeneration is limited in erythrocytes facing strong oxidative stress, thus affecting the contribution of Prx2 for H_2O_2 scavenging. Furthermore, human erythrocytes also possess catalase, an H_2O_2 scavenger whose activity is sub-stoichiometrically coupled with NADPH oxidation. On the other hand, Prx2-mediated H_2O_2 consumption is stoichiometrically coupled with NADPH oxidation. Then why do human erythrocytes need Prx2? Why do they not rely only on catalase, the antioxidant whose activity requires much less NADPH? Is Prx2 a redundant antioxidant in the defense against H_2O_2? Why is such a high concentration of Prx2 needed?

With this work we aimed to address these questions, in order to clarify what is the relevance of Prx2 in the defense of human erythrocytes against H_2O_2. We analyzed these issues bearing in mind the physiological and pathological oxidative conditions that human erythrocytes face while in circulation.

4. Methods and Technical notes

The study of the redox behavior of the Prx2/Trx/TrxR system was fully done *in silico* with the help of *Wolfram Mathematica*™ 7 (Wolfram Research, 2008). This was a step-by-step study where we addressed various questions related with the redox behavior of the Prx2/Trx/TrxR system. We started with very simplified models and considerations to gain cleared understanding of the behavior of the system. As we would gain more insight, the complexity of the models was increased as required.

We tried to obtain analytical expressions whenever possible. Numerical analyses were used when the expressions obtained were too complex to be interpreted intuitively or when numerical results were relevant. For every computation, the results obtained were rounded by considering the significant figures and round-to-even rules. All the equations are presented in the most simplified form obtained through arithmetic simplification.

The following table is a list of some of the functions we used the most in Mathematica.

Table 4.1 – List of some of the most used Mathematica functions.

Function	Meaning
DSolve	Solves the differential equations
FindFit	Finds numerical values for parameters in order to give the best fit to a list of data
FindRoot	Searches for a numerical root of an expression
Fit	Finds a least-squares fit to a list of data
FullSimplify	Simplifies an expression to the simplest form it finds
Integrate	Finds the integral of an expression
Limit	Finds the limiting value of an expression
ListPlot	Plots a list of values
NDSolve	Find a numerical solution for the list of ordinary differential equations
Plot	Plots a graph
ReplaceAll	Applies a rule or list of rules in order to transform each subpart of an expression
Solve	Solve the system of equations for the specified variables

In the next sections all of the italic abbreviations represent the value of the respective parameter or variable. For instance, *Prxtot* represents the value of the total concentration of Prx2. A description of the values or abbreviations is present at the beginning of this report. All the intracellular concentrations are expressed with respect to volume of erythrocyte water.

In our results we have numbered every equation, figure, model, reaction and table according to the section of the results where it was first introduced.

5. Results - Part I

Study of defenses against H_2O_2 under steady state conditions

We start by addressing the kinetics of H_2O_2 consumption by the various defenses against H_2O_2 when erythrocytes are subjected to sustained exposure to H_2O_2. This analysis is relevant for sepsis, anaphylactic shock or diabetes, pathological conditions characterized by systemic inflammation. With this in mind, we analyzed the response of Prx2, catalase and GPx1 to different H_2O_2 loads, under steady state conditions

These three antioxidants were the only defenses against H_2O_2 considered in this work because they are currently thought to be the main defenses of human erythrocytes against H_2O_2. Because the Prx2 cycle is coupled with the oxidation of Trx, we also examine the kinetics of the Trx redox cycle and how it affects the antioxidant properties of Prx2, the antioxidant in focus.

In these analyses we considered a wide range of oxidative conditions because oxidative loads depend on organism, its immune response, infection state and other conditions. The highest oxidative loads correspond to hydrogen peroxide concentrations in blood plasma characteristic of systemic inflammation of the organism. On the other hand, basal oxidative loads correspond to hydrogen peroxide concentrations in blood plasma in absence of inflammation or other pathological sources of oxidative stress.

5.1. What is the relative contribution of Peroxiredoxin 2 for hydrogen peroxide consumption?

Seeking to find the process that potentially contributes the most for H_2O_2 consumption, we compared the pseudo-first order rate constants of Prx2, GPx1 and catalase, with respect to H_2O_2. Coupled reactions to each of these antioxidant enzymes are therefore not considered as limiting steps, a plausible assumption under basal oxidative loads. Before presenting and discussing the main results we will explain how the estimates of these rate constants were done.

5.1.1. Rate constant estimates

5.1.1.1. Pseudo-first order rate constant of GPx1 with respect to H_2O_2

Glutathione Peroxidase 1 has ping-pong kinetics (Flohé et al., 1972): its reaction cycle includes successive steps of oxidation and reduction, and a stepwise association with its two substrates,

H_2O_2 and glutathione (Reaction 5.1 to Reaction 5.3). In order to decompose H_2O_2, this enzyme is first oxidized by H_2O_2 and then reduced by GSH (Flohé et al., 1972):

$$GPx1_{red} + H_2O_2 \underset{k_{-1}^{GPx1}}{\overset{k_1^{GPx1}}{\rightleftharpoons}} GPx1_{ox} + H_2O \qquad \textbf{Reaction 5.1}$$

$$GPx1_{ox} + GSH \underset{k_{-2}^{GPx1}}{\overset{k_2^{GPx1}}{\rightleftharpoons}} GPx1\text{-}SG + H_2O \qquad \textbf{Reaction 5.2}$$

$$GPx1\text{-}SG + GSH \underset{k_{-3}^{GPx1}}{\overset{k_3^{GPx1}}{\rightleftharpoons}} GPx1_{red} + GSSG \qquad \textbf{Reaction 5.3}$$

We use the rate equation that describes H_2O_2 reduction through the three reactions above [Equation 5.1, (Flohé et al., 1972)] to compute the pseudo-first order rate constant for GPx1 catalysis.

$$v_{GPx1} = \frac{GPx1}{\frac{\phi_1}{H_2O_2} + \frac{\phi_2}{GSH}} \qquad \textbf{Equation 5.1}$$

In the above equation, ϕ_1 is the reciprocal rate constant for the net forward Reaction 5.1 ($\phi_1 = \frac{1}{k_1^{GPx1}}$); ϕ_2 is the reciprocal rate for the net reactions of GPx1 with glutathione in Reaction 5.2 and Reaction 5.3 (giving $\phi_2 = \frac{1}{k_2^{GPx1}} + \frac{1}{k_3^{GPx1}}$). For the human erythrocyte enzyme, ϕ_1 and ϕ_2 have values of 2.4×10^{-8} Ms and 4.3×10^{-6} Ms (Takebe et al., 2002) respectively.

We determined the pseudo-first order rate constant for H_2O_2 reduction by GPx1, with respect to H_2O_2, through Equation 5.1. Because we want to know if GPx1 is the main defense of the human erythrocyte against H_2O_2, we seek to find the highest possible value of this rate constant, irrespective of GSH reduction. Thus we assumed that all the glutathione is kept reduced. A constant value of 3.2×10^{-3} M *GSH* was used, corresponding to the total glutathione concentration (*GStot*) determined by (Thorburn and Kuchel, 1987). This high value of *GSH* only pertains to conditions in which glutathione reduction does not limit GPx1-mediated H_2O_2 reduction (i.e. low oxidative conditions), allowing glutathione to remain mostly reduced (Thornalley et al., 1996).

Therefore, the pseudo-first order rate constant obtained represents an upper limit and is smaller at higher H_2O_2.

To find the value of this pseudo-first order rate constant order we had to find the concentration of GPx1 in the cell. We estimate a value of 9.7×10^{-7} M *GPx1* from the experiments of (Mueller et al., 1997a) as follows. (Mueller et al., 1997a) determined the GPx1 activity in human hemolysates [0.094 g Hb/dm^3 erythrocytes, which corresponds to ≈ 0.03% hematocrit, if we consider 340 g Hb per liter of packed cells (Beutler, 1984)]. Using 1×10^{-4} M H_2O_2 and 2×10^{-3} M *GSH* as initial values, the authors obtained the following figure.

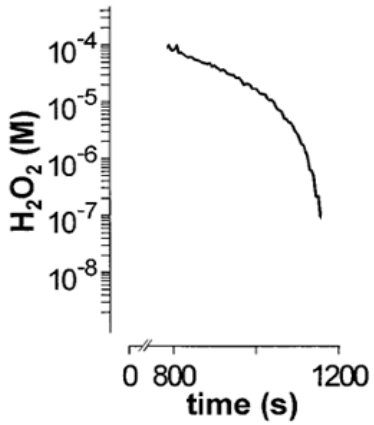

Figure 5.1 – H_2O_2 consumption by Glutathione Peroxidase (0.094 g Hb/dm^3, 2 mM *GSH*), from Figure 5 of (Mueller et al., 1997a). Initial concentration of H_2O_2 was 1×10^{-4} M. Catalase was inhibited with 1×10^{-3} M NaN_3.

We aimed to obtain values of ϕ_1, ϕ_2 and *GPx1* for Equation 5.1 that could reproduce the time course of H_2O_2 consumption by GPx1 from the figure above. Using Equation 5.1 and considering that 2 molecules of GSH are consumed per molecule of H_2O_2 reduced (as Reaction 5.1 to Reaction 5.3 show) we obtain Model 5.1.

$$\frac{d\ H_2O_2}{dt} = -\frac{GPx1}{\frac{\phi_1}{H_2O_2} + \frac{\phi_2}{GSH}}$$

$$\frac{d\ GSH}{dt} = -2\cdot\frac{GPx1}{\frac{\phi_1}{H_2O_2} + \frac{\phi_2}{GSH}}$$

Model 5.1

Using the above model and considering the initial values of H_2O_2 (1×10^{-4} M) and *GSH* (2×10^{-3} M) used in the experiment of (Mueller et al., 1997a) we computed the set of values of ϕ_1, ϕ_2 and *GPx1* that minimize the error function

$$\varepsilon(GPx1,\phi_1,\phi_2)=\sum_{i=1}^{N}\left(1-\frac{y_{comp}(GPx1,\phi_1,\phi_2,t_i)}{y_{exp}(t_i)}\right)^2 \qquad \textbf{Equation 5.2}$$

where $y_{comp}(GPx1,\phi_1,\phi_2,t_i)$ stands for the computed value of iH_2O_2 at time t_i as per Equation 5.1, $y_{\exp}(t_i)$ stands for the experimental value of iH_2O_2 at time t_i from Figure 5.1, and *N* stands for the number of points. Time points were sampled as shown in Figure 5.2. The best-fit values for ϕ_1, ϕ_2 and *GPx1* were 2.0×10^{-8} Ms, 4.7×10^{-8} Ms and 9.7×10^{-7} M, respectively. The values for ϕ_1 and ϕ_2 are close to those obtained in dedicated experiments by (Takebe et al., 2002), at different experimental conditions, which adds confidence on the estimated value of *GPx1*.

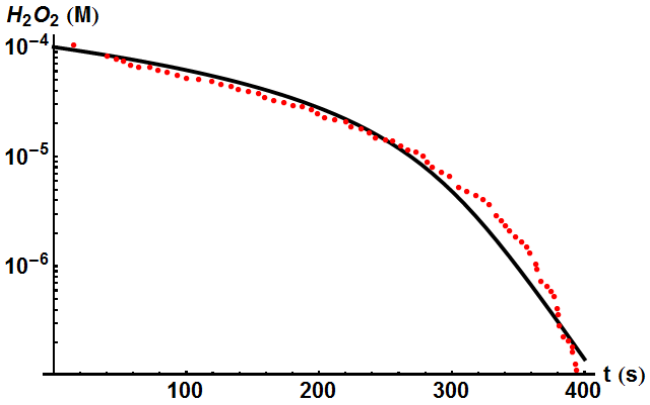

Figure 5.2 - Best-fit time course of H_2O_2 consumption to the data sampled (dots) from Figure 5 of (Mueller et al., 1997a).

The above estimate allowed us to obtain the parameters of Equation 5.1 expressed in Table 5.1.

Table 5.1 - Parameters used to compute the pseudo-first order rate constant for H_2O_2 consumption through GPx1.

Parameter	Value	Reference
GPx1	9.7×10^{-7} M	Estimated. See main text
GStot	3.2×10^{-3} M	(Thorburn and Kuchel, 1987)
ϕ_1	2.4×10^{-8} Ms	(Takebe et al., 2002)
ϕ_2	4.3×10^{-6} Ms	(Takebe et al., 2002)

Replacing these parameters into Equation 5.1 and considering *GSH* = *GStot* we get

$$v_{GPx1}=\frac{V_{max}^{app}H_2O_2}{K_m^{app}(H_2O_2)+H_2O_2} \qquad \textbf{Equation 5.3}$$

With $K_m^{app}(H_2O_2)$ = 18×10^{-6} M and V_{max}^{app} =7.1×10^{-4} M/s, which led to a pseudo-first order rate constant of $k_{GPx1} = \frac{V_{max}^{app}}{K_m^{app}(H_2O_2)} = 40$ s^{-1}. The value obtained for K_m^{app} (H_2O_2) indicates that H_2O_2 consumption by GPx1 is well approximated by a pseudo-first-order kinetics up to $iH_2O_2 \approx 2\times10^{-6}$ M, provided that nearly all the GSH remains in reduced form. Because physiological values of iH_2O_2 under basal to moderate oxidative loads are expected to be much lower [as per observations of (Giulivi et al., 1994)], we can confidently assume that under these conditions the kinetics of H_2O_2 consumption by GPx1 is well approximated by a pseudo-first-order rate expression.

5.1.1.2.Pseudo-first order rate constant of catalase with respect to H_2O_2

We considered the value of 218 s^{-1} for this pseudo-first order rate constant, as determined by (Mueller et al., 1997a). In their experiments the authors did not account for the contribution of Prx2 for H_2O_2 consumption. However, the following three reasons indicate that this omission did not substantially influence the estimate. First, given its reactivity with H_2O_2 [10^8 M^{-1}s^{-1}, (Manta et al., 2009)], Prx2 should be quickly and quantitatively converted to the inactive PSSP form under the conditions of the experiment. Namely, an initial 10^{-5} M H_2O_2 and a very dilute hemolyzate. Second, the progression curve for H_2O_2 consumption in these hemolysates in absence of added GSH is very well fitted by a single exponential. Third, addition of the catalase inhibitor NaN_3 under these conditions fully abolished H_2O_2 consumption.

5.1.1.3.Pseudo-first order rate constant of Prx2 with respect to H_2O_2

We estimated the concentration of monomeric Prx2 (*Prxtot* = 3.7×10^{-4} M) from Equation 5.4:

$$Prxtot = \frac{Prx2_{Moore}}{WaterContent_{RBC} \times MW_{Monomer}} \qquad \textbf{Equation 5.4}$$

In which $Prx2_{Moore}$ represents the concentration of Prx2 found by (Moore et al., 1991) (5.6g Prx2/L Packed Erythrocytes), $WaterContent_{RBC}$ is the average erythrocyte water volume [0.7 L water/L erythrocytes (Savitz et al., 1964)] and MW_{Prx2} is the molecular weight of Prx2 monomers [≈22 000 Da (Moore and Shriver, 1994; Schroder et al., 2000)]. Replacing these values into Equation 5.4 yields a concentration of 3.7×10^{-4} M Prx2 monomer. Because in each monomer

only one cysteine reacts with H_2O_2 this monomeric concentration also corresponds to the concentration of reactive cysteines.

Using the concentration estimated above and 10^8 $M^{-1}s^{-1}$ for the reactivity of reduced Prx2 with H_2O_2 (Manta et al., 2009) we obtain a value of 3.7×10^4 s^{-1} for the pseudo-first order rate constant of H_2O_2 reduction by Prx2.

5.1.2. Relative contribution of the three enzymes under low and high oxidative loads

Through the estimates above we obtain the following pseudo-first order rate constants for H_2O_2 consumption.

Table 5.2 - Pseudo-first order rate constants for H_2O_2 scavenging by GPx1 (k_{GPx1}), catalase ($k_{catalase}$) and Prx2 (k_{Prx2}).

Pseudo-first order rate constant	Value (s^{-1})
k_{GPx1}	40
$k_{catalase}$	218
k_{Prx2}	37 000

The rate constants of GPx1 and Prx2 represent upper limits because glutathione and Prx2 were considered fully reduced. Yet, these constants serve as a comparison for the potential of H_2O_2 consumption by each of the proteins, and should be representative of the *in vivo* situation under basal oxidative loads. The rate constant for Prx2 is approximately 1000 fold higher than the rate constant of GPx1. Likewise, the rate constant estimated in here for the activity of catalase is about 180-fold smaller than the rate constant for Prx2.

Knowledge of these rate constants allows us to analyze the contribution of each protein under various oxidative loads as follows. The relative contribution of Prx2 for H_2O_2 reduction may be computed from the values of the rate constants obtained in Table 5.2:

$$\frac{k_{Prx2}}{k_{Prx2}+k_{catalase}+k_{GPx1}} \approx 0.99 \qquad \textbf{Equation 5.5}$$

The above equation shows that when the oxidative load is low (i.e. loads that allow Trx and Prx2 to remain mostly reduced), Prx2 contributes to practically all of the H_2O_2 reduction (≈99%). Conversely, the relative contributions of GPx1 and catalase for H_2O_2 scavenging are respectively ≈0.1% and ≈0.6% under those conditions. Where the oxidative load is high enough for Prx2 to accumulate in the PSSP form, k_{Prx2} is practically null, giving

$$\frac{k_{catalase}}{k_{Prx2}+k_{catalase}+k_{GPx1}}=\frac{k_{catalase}}{k_{catalase}+k_{GPx1}}\approx 0.84 \qquad \textbf{Equation 5.6}$$

This means that when the concentration of cytoplasmic H_2O_2 leads to accumulation of oxidized Trx and Prx2, catalase is responsible for about 84% of the H_2O_2 consumption, and GPx1 is responsible for about 16% of H_2O_2 consumption. In the next section, we will discuss the basis for claiming that k_{Prx2} is practically null in conditions in which there is accumulation of oxidized Trx and Prx2.

Altogether, this further supports the notion that catalase, GPx1 and Prx2 have different relevance for H_2O_2 scavenging in the human erythrocyte. Prx2 is potentially the antioxidant that contributes the most for H_2O_2 reduction, under H_2O_2 loads that allow Prx2 to remain active. If the contribution of Prx2 for H_2O_2 scavenging is disregarded, catalase becomes the main H_2O_2 scavenger in the human erythrocyte.

5.2. What is the maximum rate of H_2O_2 decomposition by Prx2?

The rate at which Prx2 decomposes H_2O_2 (v_{Prx2}) depends on the oxidative load. If the latter is large, there is accumulation of PSSP and Trx_{Ox} (i.e. *PSSP=Prxtot* and Trx_{Ox}=*Trxtot*, with *Prxtot* and *Trxtot* as the total concentration of Prx2 and Trx in the erythrocyte, respectively). This allows the rate of Trx_{Ox} reduction to approach its maximum (V_{max}^{TrxR}), hence limiting the maximum rate of H_2O_2 decomposition by Prx2 (V_{max}^{Prx2}). In order to estimate V_{max}^{Prx2} at steady state we had to estimate several parameters. We discuss these estimates in the subsequent subsections.

5.2.1. Parameter estimates and considerations

5.2.1.1. Dismutase activity of catalase

We considered that catalase exhibits pseudo-first order kinetics with respect to H_2O_2 [218 s^{-1}, (Mueller et al., 1997b)]. This assumes that catalase is not inactivated. We now discuss the conditions in which catalase may be inactivated.

Four catalase forms are considered in its catalytic cycle, based on observations by (Chance et al., 1952),(Gaetani et al., 1989) and (Kirkman et al., 1999): Ferricatalase, Compound I, Compound II

and an Intermediate state. The Intermediate is an unstable state between Compound I and II, and may either be reduced to Ferricatalase at the expense of NADPH or to Compound II due to the presence of other electron donor (Hillar et al., 1994; Kirkman et al., 1999). NADPH is used to prevent accumulation of Compound II, an inactivate form of catalase (Kirkman et al., 1999; Kirkman et al., 1987). The formation and consumption of Compound II occurs by reduction, hence requiring the presence of electron donors. These donors may either be small molecules (e.g. ferrocyanide) or a poorly known endogenous donor found in catalase itself (Hillar and Nicholls, 1992; Hillar et al., 1994). The following figure is a simplified catalytic cycle of catalase that includes the four states and shows the reactions in which intracellular H_2O_2 and NADPH participate.

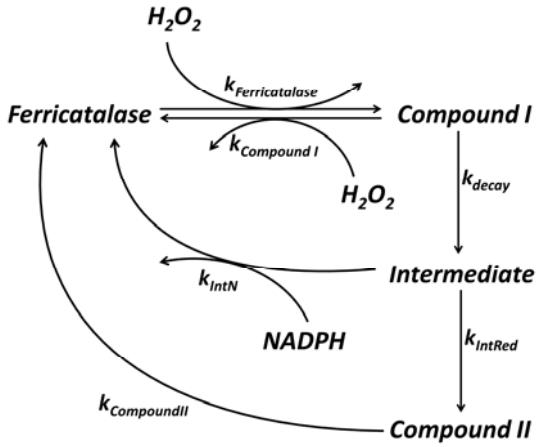

Figure 5.3 – Simplified representation of the catalytic cycle of catalase based on observations by (Chance et al., 1952; Gaetani et al., 1989; Kirkman et al., 1999). The rate constants of all reactions are represented as k_i.

Some values of the rate constants in Figure 5.3 are found in Table 5.3.

Table 5.3 – Values of parameters in Figure 5.3.

Parameter	Value	Reference
$k_{CompoundI}$	1.6×10^{7} M^{-1} s^{-1}	(Chance et al., 1952)
$k_{CompoundII}$	8×10^{-6} s^{-1}	(Kirkman et al., 1999)
k_{decay}	1.1×10^{-2} s^{-1}	(Nicholls, 1964)
$k_{Ferricatalase}$	0.6×10^{7} M^{-1} s^{-1}	(Chance et al., 1952)

Catalase has still another inactive form, Compound III, but this appears to be very minor even when NADPH is absent in the experiments of (Kirkman et al., 1999). The formation of Compound II is still not completely understood. We will now discuss the conditions under which the accumulation of Compound II may occur, leading to inactivation of catalase.

(Kirkman et al., 1999) assessed the relative abundance of each catalase form *in vitro* in a reaction mixture where there was constant H_2O_2 production (1×10^{-7} to 2×10^{-7} M H_2O_2/s). The authors observed that catalase was found as Ferricatalase, Compound I and II even in the absence of NADPH. When there was no NADPH in the mixture most of catalase was found in Ferricatalase state (40 – 55% total catalase), but there was also accumulation of Compound II (7 – 20% total catalase). On the other hand, there was practically no Compound II present when NADPH (2×10^{-6} M) was added to the mixture. Again, most of catalase is in Ferricatalase form under such conditions. So under which conditions is NADPH able to protect catalase from inactivation? To assess this we built a kinetic model of the reactions depicted in Figure 5.3:

$$\frac{d\,Ferricatalase}{dt} = k_{IntN}\cdot NADPH\cdot Intermediate + k_{CompoundII}\cdot CompoundII + H_2O_2\cdot(k_{CompoundI}\cdot CompoundI - k_{Ferricatalase}\cdot Ferricatalase)$$

$$\frac{d\,CompoundI}{dt} = k_{Ferricatalase}\cdot H_2O_2\cdot Ferricatalase - CompoundI\cdot(k_{CompoundI}\cdot H_2O_2 + k_{decay}) \qquad \textbf{Model 5.2}$$

$$\frac{d\,Intermediate}{dt} = k_{decay}\cdot CompoundI - Intermediate\cdot(k_{IntN}\cdot NADPH + k_{Int\,Red})$$

$$CatalaseT = Ferricatalase + CompoundI + CompoundII + Intermediate$$

We used Model 5.2 to compare the rates of H_2O_2 consumption through Compound I ($v_{CompoundI}$) with the decay of Compound I to Intermediate (v_{decay}) and NADPH consumption ($v_{NADPHcons}$). These rates are respectively represented in Equation 5.7 to Equation 5.9:

$$v_{CompoundI} = k_{CompoundI}\cdot H_2O_2\cdot CompoundI \qquad \textbf{Equation 5.7}$$

$$v_{decay} = k_{decay}\cdot CompoundI \qquad \textbf{Equation 5.8}$$

$$v_{NADPHcons} = k_{IntN}\cdot Intermediate\cdot NADPH \qquad \textbf{Equation 5.9}$$

The total rate of H_2O_2 dismutation by catalase is given by

$$v_{H2O2cons} = H_2O_2\cdot\left(k_{Ferricatalase}\cdot Ferricatalase + k_{CompoundI}\cdot CompoundI\right) \qquad \textbf{Equation 5.10}$$

The formation of Intermediate may compete for Compound I with the reaction in which the latter is used for H_2O_2 dismutation. When this occurs catalase then accumulates in its inactive form. The following ratio allows us to compare the flux of Compound I decay to Intermediate with the flux in which Compound I is used for H_2O_2 dismutation.

$$\frac{v_{CompoundI}}{v_{decay}} = \frac{k_{CompoundI} \cdot H_2O_2}{k_{decay}}$$ **Equation 5.11**

Considering the values of parameters in Table 5.3, Equation 5.11 then becomes

$$\frac{v_{CompoundI}}{v_{decay}} \approx 1.5 \times 10^9 \cdot H_2O_2$$ **Equation 5.12**

Equation 5.12 shows that for $H_2O_2 < 1\times10^{-9}$ M the decay of catalase competes for Compound I with Compound I-mediated H_2O_2 dismutation (i.e. $v_{CompoundI} \approx v_{decay}$). For higher H_2O_2 the rate of reduction of Compound I to Ferricatalase is much larger than the decay of Compound I to Intermediate. This occurs because the pseudo-first order rate constant for reduction of Compound I to Ferricatalase with respect to Compound I (given by $k_{CompoundI} \times H_2O_2$) will be much larger than k_{decay} (i.e. $v_{CompoundI} \gg v_{decay}$).

There may still be accumulation of Compound II if the reduction of Intermediate to Ferricatalase is limited by NADPH availability. But as we now show, Model 5.2 and the parameter estimates above also imply that NADPH is oxidized at much lower rates than those of H_2O_2 dismutation by catalase. Under steady state conditions, solving Model 5.2 in order to the dependent variables and replacing them into Equation 5.9 and Equation 5.10 gives

$$\frac{v_{NADPHcons}}{v_{H2O2cons}} = \frac{k_{decay} \cdot k'_{IntN}}{\left(2 \cdot k_{CompoundI} \cdot H_2O_2 + k_{decay}\right) \cdot \left(k_{IntRed} + k'_{IntN}\right)}$$ **Equation 5.13**

where k_{IntN}' is the pseudo-first order rate constant for Intermediate reduction to Ferricatalase ($=k_{IntN} \times NADPH$). If the NADPH concentration is high enough to make $k_{IntN}' \gg k_{IntRed}$ Equation 5.13 then becomes

$$\frac{v_{NADPHcons}}{v_{H2O2cons}} \approx \frac{k_{decay}}{2 \cdot k_{CompoundI} \cdot H_2O_2 + k_{decay}}$$ **Equation 5.14**

It would be useful to know how high would the NADPH concentration have to be for this approximation be accurate (i.e. for $k_{IntN}' \gg k_{IntRed}$ to be verified). However, we have not found any reports in the literature for the values of k_{IntRed} or k_{IntN}. Nevertheless, we can find a lower estimate for the k_{IntN}' that allows $k_{IntN}' > k_{IntRed}$ as follows. Consider that k_{IntRed} must be higher than or

equal to k_{decay} if accumulation of Intermediate in the absence of NADPH is to be avoided. Making $k_{IntRed} = k_{decay}$, and considering the parameters in Table 5.3, we get $k_{IntN}' > 0.011\ s^{-1}$.

From this pseudo-first order rate constant we may also obtain a rough estimate of k_{IntN}. The total concentration of bound plus unbound NADP is about 40×10^{-6} M (Wagner and Scott, 1994), of which a large fraction is bound to proteins. About 16×10^{-6} M NADPH is catalase-bound (Kirkman et al., 1986) and exchanges with unbound NADPH very slowly (Kirkman and Gaetani, 1984). As per determination by (Wagner and Scott, 1994), unbound NADP comprises about $\approx28\times10^{-6}$ M in the human erythrocyte. Considering NADPH = 28×10^{-6} M and $k_{IntN}' = 0.011\ s^{-1}$ we get $k_{IntN} \approx 390\ M^{-1}s^{-1}$. However, we would like to note that this k_{IntN} represents a lower estimate, and further studies are required to determine a more accurate value for this rate constant.

Considering the values in Table 5.3, Equation 5.14 gives

$$\frac{v_{NADPHcons}}{v_{catalase}} \approx \frac{0.011}{0.011 + 3.2\times10^{7}\cdot H_2O_2} \qquad \textbf{Equation 5.15}$$

Equation 5.15 shows that for $H_2O_2 \ll 10^{-10}$ M the oxidation of NADPH and the total rate of H_2O_2 dismutation occur at comparable rates (i.e. $v_{NADPHcons} \approx v_{catalase}$). This means that under such oxidative loads the rate at which catalase oxidizes NADPH is limited by H_2O_2 availability. On the other hand, for values much higher than 10^{-10} M H_2O_2 the ratio above becomes practically null. This means that when H_2O_2 increases above 10^{-10} M the rate of NADPH consumption by catalase becomes negligible compared to the rate of H_2O_2 dismutation. Therefore, higher oxidative loads will lead to much higher increase in the rate of H_2O_2 dismutation by catalase than in the rate of NADPH oxidation by catalase. Although NADPH is needed to prevent accumulation of inactive catalase, at high oxidative loads catalase likely consumes very little NADPH compared to the antioxidant activity it exerts. This conclusion is in accordance with the experimental observations by (Kirkman et al., 1999). These authors show that 2×10^{-6} M of catalase consumes $\approx13\times10^{-6}$ M H_2O_2/s while oxidizing only $\approx0.006\times10^{-6}$ M NADPH/s, maintaining a steady state H_2O_2 of $\approx3\times10^{-9}$ M. It would be interesting to find if $H_2O_2 < 10^{-10}$ M allows NADPH oxidation to be limited by H_2O_2 availability. Also supporting the assertion that catalase oxidizes NADPH at low rates compared to H_2O_2 consumption is the observation that

catalase oxidizes one NADPH molecule for every 4 to 14 molecules dismutated (Kirkman et al., 1987), the exact ratio depending on the concentrations of superoxide, H_2O_2 and other intracellular reductants. The authors obtained these values in an *in vitro* experiment where H_2O_2 was being generated at 8×10^{-9} to 10^{-7} M H_2O_2/s (2×10^{-6} M catalase, 0.1 M glucose, 0.2×10^{-6} M glucose-6-phosphate dehydrogenase, 4×10^{-6} M NADP). As the rate of H_2O_2 generated increased so did the rate of NADPH consumed.

An important issue that we would like to point out is that NADPH availability may on the other hand affect the dismutase activity of catalase. If catalase accumulates mostly in inactive form there is less enzyme available to dismutate H_2O_2. This occurs if $k_{IntN}' < k_{IntRed}$, making $v_{NADPHcons}$ smaller than the flux of conversion of Intermediate to Compound II (v_{IntRed}, Equation 5.16).

$$v_{IntRed} = k_{IntRed} \cdot Intermediate \qquad \textbf{Equation 5.16}$$

The estimates that led to Equation 5.15 were done by assuming that NADPH does not limit the reduction of Intermediate to Ferricatalase. (Kirkman et al., 1987) observed that $<0.1\times10^{-6}$ M NADPH prevents the accumulation of Compound II when 2×10^{-6} M bovine catalase is exposed to $\approx 3\times10^{-8}$ M H_2O_2/s. However, it could still be interesting to determine the NADPH concentration that prevents accumulation of Compound II for higher oxidative conditions. Again the issue of having just a lower estimate of k_{IntN} and k_{IntRed} prevent us from finding such concentration. Yet, from our estimates above we find that a $k_{IntN}' > 0.011$ s^{-1} allows $v_{NADPH} > v_{IntRed}$. This value represents a lower estimate for the value of k_{IntN}' required to prevent accumulation of Compound II.

More experiments are required in order to improve these estimates and to analyze under what conditions is the dismutase activity of catalase limited by NADPH. Such experiments could be done *in vitro* to analyze various issues. For instance, some could assess the kinetics of NADPH oxidation by catalase in reaction mixtures where H_2O_2 is being produced at various fluxes. By analyzing such rates one would be able to obtain rate constants for such reactions. Other experiments could determine the kinetics of Intermediate formation and disappearance, in the absence of NADPH. While this is a technically difficult issue given the instability of the Intermediate, some experiments using spectroscopic techniques were already used to identify the presence of this Intermediate in *Proteus mirabilis* and bovine catalases (Ivancich et al., 1996;

Ivancich et al., 1997). Obtaining more insight onto the formation and consumption of the Intermediate would allow us to have more accurate estimates of which conditions lead to catalase inactivation.

The issues above prevent a precise estimate of the conditions in which NADPH prevents the accumulation of inactive catalase. However, given the important role of catalase in the defense of erythrocytes against H_2O_2 (Gaetani et al., 1996; Johnson et al., 2010; Scott et al., 1991) it is unlikely that a large fraction of catalase is inactivated even in erythrocytes facing strong oxidative loads. This is further supported by the experiments of (Johnson et al., 2010), who showed that catalase is not significantly inactivated even under strong oxidative conditions. The authors assessed the intracellular redox state of mice erythrocytes by assaying the redox state of hemoglobin. The authors used erythrocytes collected from Prx2- and GPx1-knockout mice. Those erythrocytes were then exposed to various H_2O_2 boluses and the fraction of oxidized hemoglobin (methemoglobin) was quantified. In the absence of Prx2 and GPx1 the main defense against H_2O_2 was catalase. Due to the higher catalase activity required to compensate for the absence of Prx2/GPx1 it could occur that a larger fraction of catalase would be inactivated. However, these authors show that even in Prx2-mutant erythrocytes exposed to boluses up to 500×10^{-6} M H_2O_2 there is not a significant accumulation of methemoglobin (oxidized form of hemoglobin) in comparison to the wild-type erythrocytes. If there was an increase in methemoglobin levels it could be due to the accumulation of intracellular H_2O_2, as a result of catalase inactivation. If NADPH availability was not preventing catalase inactivation there would be a much larger accumulation of methemoglobin in the mutant erythrocytes. Also, the methemoglobin concentration is similar in wild type erythrocytes subjected to 50×10^{-6} and 500×10^{-6} M H_2O_2 boluses. This suggests that erythrocytes subjected to both oxidative loads have similar abilities to scavenge H_2O_2, hence preventing accumulation of oxidized hemoglobin.

These results suggest that catalase is able to scavenge H_2O_2 even in the absence of Prx2 or GPx1 (Johnson et al., 2010). Yet, one should regard these results carefully as they could easily be influenced by the conditions of the experiment. In the experiments of (Johnson et al., 2010) the ability of Prx2- and GPx1-mutant erythrocytes to scavenge H_2O_2 may be only temporary: the NADPH pool may only be able to protect catalase from inactivation for a short period of time, surpassing the erythrocyte's capacity to produce NADPH and maintain catalase active. Also,

despite the similar ability that wild type and Prx2-mutant erythrocytes have to maintain the redox state of hemoglobin, Prx2-mutant erythrocytes exhibit only ≈80 % catalase activity relatively to the wild types. However, it is not clear if this is due to slower catalytic activity, lower catalase concentration or accumulation of inactive enzyme.

Though these results suggest that catalase alone is able to defend the erythrocyte from H_2O_2, more experiments are needed to study catalase inactivation and how this process affects its antioxidant activity. Such experiments would provide values under which the dismutase activity of catalase is effectively a first-order process with respect to H_2O_2.

In our work we started by considering that catalase activity is not limited by NADPH availability hence disregarding the accumulation of inactive catalase. This was done because we first want to compare the relevance of Prx2, GPx1 and catalase for H_2O_2 scavenging. We want to understand which of these three antioxidants could represent the main H_2O_2 scavenging process where the supply reducing equivalents are not rate limiting.

5.2.1.2.Peroxidase activity of GPx1

GPx1 oxidizes two GSH molecules per H_2O_2 molecule reduced (Reaction 5.1 to Reaction 5.3). In our analyses we considered a pseudo-first order rate constant of 40 s^{-1} (Section 5.1.1.1) for GPx1 activity, with respect to iH_2O_2.

However, under high oxidative loads GSH availability limits the rate of H_2O_2 reduction by GPx1. Glutathione Reductase (GSR) is the enzyme responsible for GSSG reduction, consuming NADPH in this process. In Section 5.1.1.1 we showed that GPx1 has a $K_m^{app}(H_2O_2) \approx 18\times10^{-6}$ M, a value that exceeds plausible iH_2O_2 [which should be $<3\times10^{-9}$ M iH_2O_2 under basal oxidative conditions, and up to $\approx10^{-7}$ M iH_2O_2 in pathological conditions, as per the experiments of (Giulivi et al., 1994; Kirkman et al., 1999)], provided that all of the GSH contents are in reduced form. Under which oxidative loads does GPx1 exhibit first-order kinetics with respect to H_2O_2?

To address this question we started by estimating the iH_2O_2 that yields a kinetic order of 0.5 for the reaction of with respect to H_2O_2, as a function of the fraction of GSSG. Consider that GPx1 reduces H_2O_2 with overall reaction

$$iH_2O_2 + 2GSH \rightarrow 2H_2O + GSSG$$ **Reaction 5.4**

With overall conservation relationship

$$GSH + 2GSSG = GStot$$ **Equation 5.17**

The kinetic order for Reaction 5.4 with respect to iH_2O_2 (f) is

$$f = \frac{d\ \mathrm{Log}[v_{GPx1}]}{d\ \mathrm{Log}[iH_2O_2]}$$ **Equation 5.18**

where v_{GPx1} is the rate of H_2O_2 reduction by GPx1 (Equation 5.1, Section 5.1.1.1). Taking into consideration Equation 5.17 and Equation 5.18 we get

$$f = \frac{1}{1 + \frac{iH_2O_2 \cdot \phi_2}{GStot \cdot \phi_1 \cdot \left(1 - 2\frac{GSSG}{GStot}\right)}}$$ **Equation 5.19**

We compute the iH_2O_2 required for v_{GPx1} to be half saturated with H_2O_2 (i.e. f = 0.5) from Equation 5.19 giving

$$iH_2O_2 = \frac{\phi_1 \cdot GStot \cdot \left(1 - 2\frac{GSSG}{GStot}\right)}{\phi_2}$$ **Equation 5.20**

Under which conditions is GPx1 half saturated with H_2O_2 and half of the erythrocyte's NADPH production capacity is used towards GPx1-mediated H_2O_2 reduction? To assess this we considered parameters from Table 5.1 (Section5.1.1.1), v_{GPx1} from Equation 5.1 (Section 5.1.1.1), the conservation relationship in Equation 5.17, and iH_2O_2 from Equation 5.20. Taking all this into account, we estimated the fraction of GSSG under which $v_{GPx1} = V_{max}^{PPP}/2$ where V_{max}^{PPP} is the maximum rate of NADPH production by the PPP [=1.9×10^{-6} M/s, as determined using methylene blue as NADPH oxidant (Albrecht et al., 1971; Gaetani et al., 1974)]. Under these conditions we find that >99% of $GStot$ is oxidized, and would correspond to ≈4.7×10^{-8} M iH_2O_2 as estimated through Equation 5.20.

Under such an oxidative load, Prx2 would consume H_2O_2 at a rate $v_{Prx2} = k_{Prx2}\times iH_2O_2$ ≈ 1.7×10^{-3} M/s (considering k_{Prx2} = 37 000 s^{-1}, Section 5.1.1.3). This rate largely surpasses the erythrocyte's capacity to produce NADPH [=1.9×10^{-6} M/s, (Albrecht et al., 1971; Gaetani et al., 1974)]. Therefore, Prx2's activity is limited by NADPH supply under these conditions and the

contribution of this protein for H_2O_2 consumption is negligible (Section 5.1.2). Most of iH_2O_2 is consumed by catalase, as per our analysis in Section 5.1.2.

The steady state eH_2O_2 that would achieve such an oxidative load (4.7×10^{-8} M iH_2O_2) may be computed as follows. Considering only GPx1 and catalase consume iH_2O_2 we get

$$v_{influx} = v_{catalase} + v_{GPx1} \quad \textbf{Equation 5.21}$$

where

$$v_{influx} = k_p \cdot eH_2O_2 \quad \textbf{Equation 5.22}$$

$$v_{catalase} = k_{catalase} \cdot iH_2O_2 \quad \textbf{Equation 5.23}$$

$$v_{GPx1} = \frac{V_{max}^{PPP}}{2} \quad \textbf{Equation 5.24}$$

The parameters of Equation 5.22 to Equation 5.24 are found in Table 5.4.

Table 5.4 – Parameters considered to compute the eH_2O_2 under which GPx1 is not saturated with iH_2O_2.

Parameter	Value	Notes/Reference
$k_{catalase}$	218 s^{-1}	Pseudo-first order rate constant for H_2O_2 consumption by catalase (Section 5.1.1.2)
k_p	8 s^{-1}	Estimated after considering $k_p = \kappa \cdot A_S / V_e$ where κ is the H_2O_2 permeability constant [$=6\times10^{-5}$ dm/s (Nicholls, 1965)]; A_S is the erythrocyte surface area [$=1.35\times10^{-8}$ dm^2(Evans and Fung, 1972)]; and V_e is the erythrocyte volume [10^{-13} dm^3 (Evans and Fung, 1972)]
V_{max}^{PPP}	1.9×10^{-6} M/s	Maximum rate of NADPH production by the PPP (Albrecht et al., 1971; Gaetani et al., 1974)

After considering parameters from Table 5.4 we estimate that $\approx1.9\times10^{-6}$ M eH_2O_2 would be enough to maintain a steady state 4.7×10^{-8} M iH_2O_2, and would correspond to $v_{influx} \approx 1.1\times10^{-5}$ M/s.

These conditions thus represent the load under which GPx1 is not saturated with iH_2O_2. In the analyses below we considered that GPx1 exhibits first-order kinetics with respect to iH_2O_2 and zeroth-order kinetics with respect to GSH. This would pertain to low oxidative loads ($\approx1.3\times10^{-6}$ M eH_2O_2 and 4.7×10^{-8} M iH_2O_2), where $2\,GSSG/GSH$ is low (Cohen and Hochstein, 1963).

5.2.1.3.Endogenous H_2O_2 production and basal intracellular H_2O_2

A few studies addressed what are the basal levels of H_2O_2 in the erythrocyte cytoplasm. In the studies of (Kirkman et al., 1999) and (Giulivi et al., 1994) the authors found values between 2×10^{-10} and 3×10^{-9} M iH_2O_2. However, we believe that these values may overestimate those *in vivo* for the reasons we discuss below.

First, we cannot disregard the possibility that the H_2O_2 found in both studies represents the detection limit of the methods used, which are not sensitive to sub-nanomolar concentrations. Second, both studies use indirect methodologies to quantify H_2O_2 which may be associated with methodological imprecision. Third, the contribution of Prx2 (and other antioxidants) for H_2O_2 scavenging was not accounted for. We will now discuss these issues.

(Giulivi et al., 1994) determined the rate of H_2O_2 dismutation by catalase in bovine erythrocyte (5% hematocrit). Catalase dismutates H_2O_2 according to Reaction 5.5 and Reaction 5.6

$$\text{Ferricatalase} + H_2O_2 \rightarrow \text{Compound I} + H_2O \qquad \textbf{Reaction 5.5}$$

$$\text{Compound I} + H_2O_2 \rightarrow \text{Ferricatalase} + H_2O + O_2 \qquad \textbf{Reaction 5.6}$$

The authors determined the rate of catalase inactivation by 3-amino-1,2,4-triazole to determine the rate at which catalase is consuming H_2O_2: a higher rate of H_2O_2 dismutation by catalase leads to higher flux of formation of Compound I. Because aminotriazole binds to Compound I and inactivates catalase (Reaction 5.7), a higher rate of catalase inactivation corresponds to a higher rate of H_2O_2 consumption by catalase.

$$\text{Compound I} + \text{3-Amino-1,2,4-Triazole} \rightarrow \text{Inactive Compound} \qquad \textbf{Reaction 5.7}$$

The authors observed a constant decrease in catalase activity after 4 hours of incubation, which they attributed to a steady state of H_2O_2 (estimated as $\approx2\times10^{-10}$ M iH_2O_2). They also determined an endogenous production of $\approx4\times10^{-10}$ M iH_2O_2/s. We will now discuss the reliability of these determinations.

(Giulivi et al., 1994) determined the rate of H_2O_2 produced endogenously as per the method of (Aebi, 1984): using the absorbance of H_2O_2 at 240nm, they determined the pseudo-first order rate constant for H_2O_2 dismutation by catalase. Larger iH_2O_2 thus corresponds to higher catalase activity, which leads to higher catalase inactivation by aminotriazole. As catalase is

progressively inactivated by aminotriazole, H_2O_2 accumulates if catalase is the main H_2O_2 scavenger. GPx1 and Prx2 have a minor contribution for H_2O_2 consumption because NADPH production was prevented by adding no glucose to the incubation medium in their experiments, and iodoacetamide was added. Iodoacetamide is an inhibitor used to prevent formation of disulfide bonds, thus inhibiting Prx2 and GPx1.

Using Equation 5.25 we estimate the steady state iH_2O_2 that would be attained under basal loads, consideringthe rate of H_2O_2 production determined by the authors ($\boldsymbol{\Phi}$= 4×10^{-10} M H_2O_2/s). Consider Prx2 the main H_2O_2 scavenger (Section 5.1.2) with k_{Prx2} = 37 000 s^{-1} (Section 5.1.1.3).

$$\frac{d\ H_2O_2}{dt} = \Phi - H_2O_2 \cdot k_{Prx2} = 0 \qquad \textbf{Equation 5.25}$$
$$\Leftrightarrow H_2O_2 \approx 10^{-14}\,\text{M}$$

This suggests that if we consider the peroxidase activity of Prx2 we would obtain a much lower iH_2O_2.

On the other hand, the authors also estimated the steady state H_2O_2 that would correspond to the above catalase activity (=4×10^{-10} M/s). Considering catalase as the only H_2O_2 scavenger they determined 2×10^{-10} M H_2O_2 under steady state basal oxidative loads. However, a few issues prevent us from considering this as the steady state H_2O_2 found under basal oxidative conditions as we now discuss.

Considering that Prx2 consumes practically all of the iH_2O_2 under basal loads (Section 5.1.2), a very high endogenous production of H_2O_2 would be required to maintain a steady state 2×10^{-10} iH_2O_2. Considering 2×10^{-10} M iH_2O_2 and k_{Prx2} = 37 000 s^{-1} (Section 5.1.1.3), the rate of H_2O_2 production in the erythrocyte ($\boldsymbol{\Phi}$) in steady state conditions is 7.4×10^{-6} M H_2O_2/s.

H_2O_2 dismutation by Prx2 is stoichiometrically coupled with NADPH oxidation through the Trx/TrxR cycles. So the NADPH supply must cope with such rate of H_2O_2 reduction. However, a $\boldsymbol{\Phi}$=7.4×10^{-6} M H_2O_2/s surpasses the erythrocyte's capacity to produce NADPH via the Pentose Phosphate Pathway [=1.9×10^{-6} M NADPH/s (Albrecht et al., 1971)]. Thus, part of the rate of H_2O_2 production determined likely is produced by the medium. These issues prevent us from taking into consideration the above steady state iH_2O_2.

(Kirkman et al., 1999) on the other hand, determined a 3×10^{-9} M H_2O_2 through an *in vitro* assay which tried to reproduce the conditions found in human erythrocytes (such as enzyme

concentrations, pH, temperature, etc.). The authors quantified H_2O_2 by following the disappearance of catalase fluorescence by spectrophotometric methods at 240 nm. They also used bovine catalase as an antioxidant, disregarding the contributions of Prx2 or GPx1 for H_2O_2 consumption. Considering 3×10^{-9} M H_2O_2 and k_{Prx2} = 37 000 s^{-1} we obtain $\boldsymbol{\Phi}$ = 10^{-4} M H_2O_2/s through Equation 5.25. This value is again implausibly high under physiological conditions because it also largely surpasses the erythrocyte's capacity to produce NADPH.

With the above in mind we considered the basal iH_2O_2 as 10^{-12} M. This value would correspond to a basal endogenous production of 3.7×10^{-8} M H_2O_2/s considering k_{Prx2} = 37 000 s^{-1} and Equation 5.25. Assuming that Prx2 consumes all of the iH_2O_2 under basal oxidative loads, NADPH would have to be produced at a rate of 3.7×10^{-8} M NADPH/s in order to regenerate Prx2. This value is ≈50 fold smaller than the erythrocyte's maximal rate of NADPH production by the PPP [=1.9×10^{-6} M NADPH/s (Albrecht et al., 1971)]. Considering 3.7×10^{-8} M/s as the rate of H_2O_2 reduction by Prx2 and k_p = $8s^{-1}$ (Section 5.2.1.2), a steady state iH_2O_2 = 10^{-12} M would be achieved if $eH_2O_2 < 5\times10^{-9}$ M.

Thus, Prx2 activity is not limited by NADPH supply under sustained $eH_2O_2 < 5\times10^{-9}$ M and 3.7×10^{-8} M H_2O_2/s, considered the basal oxidative conditions in agreement with NADPH supply.

5.2.1.4.Kinetics of H_2O_2 efflux and consumption by catalase and GPx1

Even for high oxidative loads, in which Prx2 is mostly oxidized, the pseudo-first order rate constant for H_2O_2 consumption through catalase and GPx1 ($k_c=k_{catalase}+k_{GPx1}$=258 s^{-1}, Table 5.2, Section 5.1.2) is much higher than the first order rate constant for H_2O_2 efflux (k_{efflux}):

$$k_{efflux} = \kappa \cdot \frac{A_s}{V_{ew}} \approx 12\ s^{-1} \qquad \textbf{Equation 5.26}$$

With κ as the H_2O_2 permeability constant [6×10^{-5} dm/s (Nicholls, 1965)], A_S as the erythrocyte surface area [1.35×10^{-8} dm^2 (Evans and Fung, 1972)] and V_{ew} as the erythrocyte water volume [7×10^{-14} dm^3 water/cell, obtained by multiplying the erythrocyte water content $WaterContent_{RBC}$ = 0.7 dm^3 water/dm^3 cells (Savitz et al., 1964) with the erythrocyte volume of ≈10^{-13} dm^3 (Evans and Fung, 1972)].

The comparison of the value of k_c and k_{efflux} shows that antioxidant-mediated decomposition of intracellular H_2O_2 is much higher than H_2O_2 efflux. Further, if Prx2 is also contributing for H_2O_2 scavenging, the difference between the rate constants for intracellular H_2O_2 decomposition by antioxidants and membrane efflux will be even larger. So, we neglected the contribution of H_2O_2 efflux for H_2O_2 clearance from the erythrocyte.

5.2.1.5.Peroxidase activity and concentration of Prx2

Regarding the antioxidant action of Prx2, we considered the following reactions:

$$Prx_{red} + H_2O_2 \xrightarrow{k_{PrxRed}} PSSP + H_2O \qquad \textbf{Reaction 5.8}$$

$$PSSP + TrxRed \xrightarrow{k_{PSSP}} Prxred + TrxOx \qquad \textbf{Reaction 5.9}$$

In these reactions we assume that Prx2 oxidation leads directly to the formation of disulfide bonds, whose reduction is coupled with the oxidation of Trx. We also consider that each of the above reactions occurs simultaneously in all monomers.

Although the formation of the inactive sulfinylated form of Prx2 may occur under high oxidative loads, it is negligible in human erythrocytes (Low et al., 2007). Therefore we neglected Prx2 sulfinylation. In a later part of this work we address the sulfinylation of Prx2 and its influence on the catalytic cycle of Prx2 (Section 5.7).

(Manta et al., 2009) reported a value of 10^8 $M^{-1}s^{-1}$ for the rate constant of H_2O_2 reduction by Prx_{red} (k_{PrxRed}). At this stage we have considered that Reaction 5.8 happens in a single step. PSSP is then reduced by Trx_{Red} (Reaction 5.9), with a second order rate constant $k_{PSSP} = 2.1\times10^5$ $M^{-1}s^{-1}$ (Manta et al., 2009).

Because only two oxidation states of Prx2 will be considered initially (Prx_{Red} and PSSP), the following conservation relationship is obtained:

$$Prxtot = Prx_{red} + PSSP \qquad \textbf{Equation 5.27}$$

The total concentration of Prx2 used ($Prxtot = 3.7\times10^{-4}$ M) was estimated in Section 5.1.1.3.

5.2.1.6.Total concentration of Trx

Two oxidized states of Trx are considered: a reduced state (Trx_{Red}) and an oxidized state (Trx_{Ox}). Accordingly, the following conservation relationship is obtained

$$Trxtot = Trx_{Red} + Trx_{Ox}$$ **Equation 5.28**

Because the total concentration of Trx in human erythrocytes (*Trxtot*) is unknown, we used a value obtained for bovine erythrocytes. The following equation was used to estimate the concentration of Trx:

$$Trxtot = \frac{Trx_{Holmgren}}{WaterContent_{RBC} \times MW_{Trx} \times Density_{RBC}}$$ **Equation 5.29**

In which $Trx_{Holmgren}$ is the concentration of Trx [37×10^{-3} g Trx/Kg erythrocyte wet weight (Holmgren and Luthman, 1978)]; MW_{Trx} is the molecular weight of Trx [12 kDa (Cha and Kim, 1995)]; $Density_{RBC}$ is the erythrocyte density [1.094 Kg/L (Raftos et al., 1999)] and $WaterContent_{RBC}$ as the erythrocyte water content [0.7 dm^3 water/dm^3 erythrocytes (Savitz et al., 1964)]. Replacing these values into Equation 5.29 yields a Trx concentration of $\approx4.8\times10^{-6}$ M.

5.2.1.7.TrxR concentration

We estimated the concentration of TrxR as follows:

$$TrxR = \frac{TrxR_{Méplan}}{MW_{TrxR}}$$ **Equation 5.30**

with $TrxR_{Méplan}$ as the concentration of TrxR 1 in human erythrocytes [3.5×10^{-3} g TrxR/dm^3 erythrocyte lysate (Méplan et al., 2007)] and with MW_{TrxR} as the molecular weight of the same enzyme [116 kDa (Tsang and Weatherbee, 1981)]. Replacing these values into the above equation yields a concentration of $\approx30\times10^{-9}$ M TrxR.

5.2.1.8.Estimate of the rate constants for H_2O_2 permeation and endogenous production in the experiments of (Low et al., 2007)

To determine the value of k_{TrxR} we considered the experiments of (Low et al., 2007). But before we could estimate the value of that rate constant we had to estimate the values of k_p and the endogenous production of H_2O_2 in those experiments.

The authors assessed the time course of H_2O_2 consumption after exposing 5×10^9 erythrocytes/dm^3 to 5×10^{-6} M H_2O_2 boluses [Figure 4B of (Low et al., 2007)]. To frame our problem we studied the time course of H_2O_2 consumption, represented in Figure 5.4.

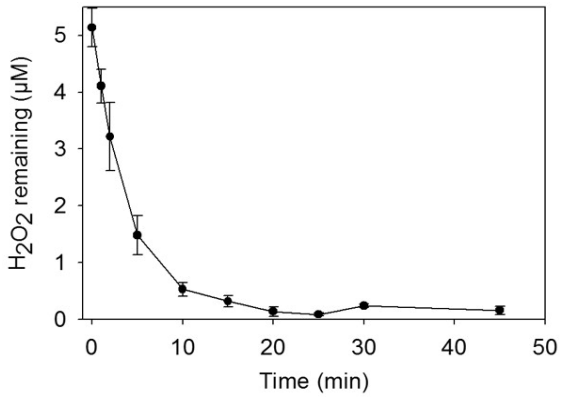

Figure 5.4 – Time course of H_2O_2 consumption by 5×10^6 erythrocytes/ml after a 5×10^{-6} M H_2O_2 bolus. Taken from Figure 4B of (Low et al., 2007).

The hydrogen peroxide concentration decreases quickly in the first 10 minutes of the experiment and then settles to a steady value of about 10^{-7} M. This steady state suggests that H_2O_2 is constantly being produced by the medium (or by the cellular membrane of erythrocytes)[3]. We estimated this production (Φ) and the first-order rate constant for hydrogen peroxide permeation through erythrocytes (k_p) by fitting Equation 5.31 to the time course of H_2O_2 consumption in Figure 5.4.

$$\frac{d\ eH_2O_2}{dt} = \Phi - k_p \cdot eH_2O_2 \qquad \textbf{Equation 5.31}$$

We computed the values of Φ and k_p that minimize the error function $\varepsilon(\Phi, k_p) = \sum_{i=1}^{N}\left(1 - \frac{y_{comp}(\Phi, k_p)}{y_{exp}(t_i)}\right)^2$, where $y_{comp}(\Phi, k_p, t_i)$ stands for the computed value of eH_2O_2 at time t_i as per Equation 5.31, $y_{\exp}(t_i)$ stands for the experimental value of eH_2O_2 at time t_i from Figure 5.4, and *N* stands for the number of points. The values that allowed the best fit were $k_p = 4.2\times10^{-3}$ s^{-1}, $\Phi = 69\times10^{-11}$ M/s (Figure 5.5). This value of Φ is low enough to be a plausible estimate of the spontaneous H_2O_2 generation in an experimental preparation exposed to

[3] **However, the possibility that the apparent steady state is an artifact due to the attainment of the detection limit of the method used by (Low et al., 2007) to determine H_2O_2 cannot be discarded.**

O_2 at atmospheric pressure, was not subject to treatments to remove transition metals and may contain a few activated phagocytes.

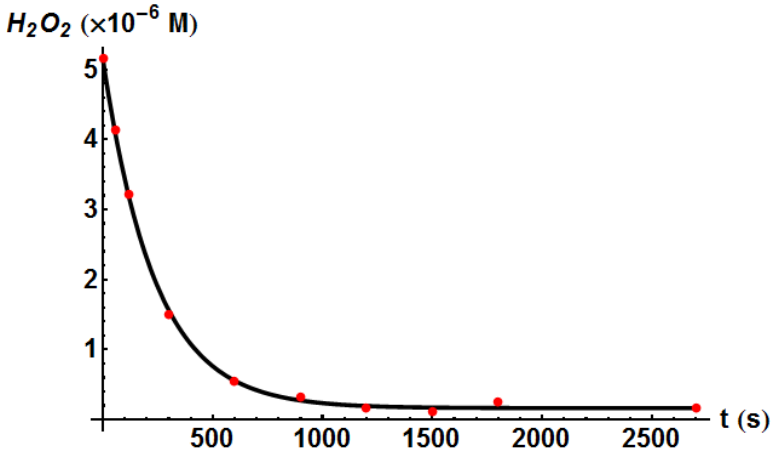

Figure 5.5 – Best-fit time course of H_2O_2 consumption of the experimental data (dots) from Figure 4B of (Low et al., 2007).

(Low et al., 2007) claim that the settling observed 10 minutes after the H_2O_2 bolus is not a steady state but the detection limit of the experiment. If this is what is occurring there would be a steeper decrease in the H_2O_2 concentration and possibly the value of k_p would be higher.

To reinforce our confidence in the obtained value of k_p, we compare this value with the k_p computed through Equation 5.32.

$$k_p = \kappa \frac{n \cdot A_s}{V_o - n \cdot V_e} \qquad \textbf{Equation 5.32}$$

The parameters of this equation are found in Table 5.5.

Table 5.5 - Parameters used for computing the pseudo-first order rate constant for H_2O_2 permeation across erythrocytes membranes, for the experiments of (Low et al., 2007).

Parameter	Value	Notes/Reference
κ	6×10^{-5} dm/s	H_2O_2 permeability constant (Nicholls, 1965)
A_S	1.35×10^{-8} dm^2	Erythrocyte surface area (Evans and Fung, 1972)
n	5×10^{9} cells/dm^3	Number of erythrocytes per volume unit under the experimental conditions of (Low et al., 2007)
V_e	10^{-13}dm^3	Erythrocyte volume (Evans and Fung, 1972)
V_o	10^{-3} dm^3	Extracellular volume. Experimental conditions of (Low et al., 2007)

Because the hematocrit used by the authors was very low (i.e. $n \cdot V_e \ll V_o$), Equation 5.32 becomes

$$k_p = \kappa \frac{n \cdot A_s}{V_o}$$ **Equation 5.33**

Replacing the values of Table 5.5 into Equation 5.33 we get $k_p \approx 4.0\times10^{-3}$ s^{-1}. With this approach we further reinforce our confidence in the value of k_p we obtained.

If the constant H_2O_2 concentration found by (Low et al., 2007) towards the end of their experiment is not due to the detection limit of the techniques used, it could only be explained by additional H_2O_2 production. If we neglect H_2O_2 production by the medium the time-course of H_2O_2 depletion in Figure 5.4 could only be explained by a very high rate of H_2O_2 production from the erythrocytes. We now show our estimate of the rate of endogenous H_2O_2 production (ϕ) that allows H_2O_2 to remain constant. In order to maintain $eH_2O_2 = 10^{-7}$ M (as observed towards the end time of the experiment in Figure 5.4), even for an implausibly high steady state value of $iH_2O_2 = 10^{-6}$ M, ϕ would have to be very high:

$$eH_2O_2 \cdot k_p = \phi - iH_2O_2 \cdot (k_{GPx1} + k_{catalase} + k_p)$$
$$\Leftrightarrow \phi \approx 2\times10^{-6} \text{ M/s}$$ **Equation 5.34**

The above ϕ was determined by considering parameters from Table 5.2 (Section 5.1.2) and $k_p = 4.2\times10^{-3}$ s^{-1} (as estimated above), and not including Prx2 as an antioxidant. If the latter was included, an even higher ϕ would be required to maintain an H_2O_2 efflux rate able to cope with the H_2O_2 influx rate. As per comparison to the experiments of (Giulivi et al., 1994) this ϕ is implausibly high to be achieved by human erythrocytes in physiological conditions. This shows that the settling observed in Figure 5.4 is not due to endogenous production of H_2O_2 by the erythrocytes but is either due to an additional production of H_2O_2 by the medium or due to the detection limit of the methods.

In the next section we estimate the value of k_{TrxR} from the experiments of (Low et al., 2007) by considering $k_p = 4.2\times10^{-3}$ s^{-1} and $\Phi = 69\times10^{-11}$ M/s.

5.2.1.9.Pseudo-first order rate constant for Trx reduction through TrxR

TrxR reduces oxidized Trx (Trx_{Ox}) at the expense of NADPH. We considered that the reduction of Trx (Reaction 5.10) was not limited by NADPH:

$$Trx_{Ox} \xrightarrow{k_{TrxR}} Trx_{Red}$$ **Reaction 5.10**

The rate constant of Trx reduction through TrxR (k_{TrxR}) was estimated from the experiments of (Low et al., 2007). This was done by using Figure 4A, where the authors assess the redox state of Prx2 through immunoblotting at different time points, after exposing 5×10^6 erythrocytes/dm^3 to a bolus of 5×10^{-6} M H_2O_2:

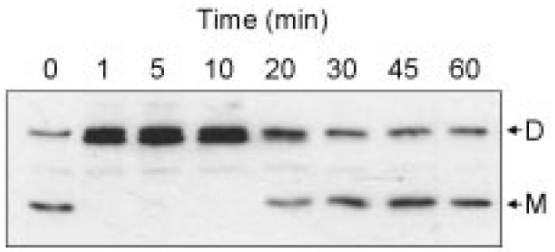

Figure 5.6 – Immunoblot of Prx2, for 5×10^6 erythrocytes/dm^3 exposed to 5×10^{-6} M H_2O_2, taken from Figure 4A of (Low et al., 2007). D – Dimerized (disulfide form) Prx2; M – Monomeric (reduced) Prx2.

We sought to find a value of k_{TrxR} that yields a fraction of reduced Prx2 similar to the one exhibited twenty minutes after the H_2O_2 bolus. We estimated this fraction by comparing Figures 2A and B from (Low et al., 2007) (reproduced in Figure 5.7 below) to the immunoblot in Figure 5.6, proceeding as follows. The intensity of reduced Prx2 (Monomer) in the latter immunoblot is intermediate between those found in Figure 5.7B, which (Low et al., 2007) determined to correspond to 3% and 21% of Prx2 in reduced form. Thus, the mean of these two values, 12%, seems a reasonable estimate for the fraction of Prx2 in reduced form twenty minutes after the H_2O_2 bolus in the immunoblot in Figure 5.6.

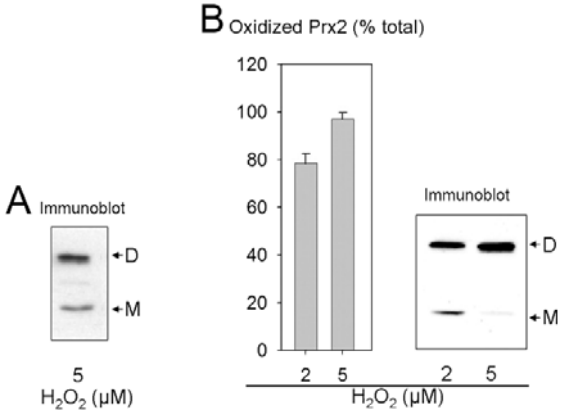

Figure 5.7 – Oxidation of Prx2 in 5×10^6 erythrocytes/ml exposed to different peroxide boluses. A. Immunoblot of the redox state of Prx2, determined 20 minutes after a 5 μM H_2O_2 bolus [Figure 4A of (Low et al., 2007)]; B. Quantification of oxidized Prx2 (left) determined from immunoblots against oxidized state of Prx2 (right), determined 10 minutes after 2 and 5 μM H_2O_2 boluses [Figure 2A and B from (Low et al., 2007)]. D – Dimerized (disulfide form) Prx2; M – Monomeric (reduced) Prx2.

Note that the experiment does not distinguish singly from doubly-crosslinked Prx2 in Figure 5.6.

Therefore, to estimate the value of k_{TrxR} we consider a reaction scheme which takes into account three oxidized states of Prx2: reduced Prx2 (Prx_{Red}), singly-crosslinked (Prx_1) and doubly-crosslinked (PSSP) Peroxiredoxin 2.

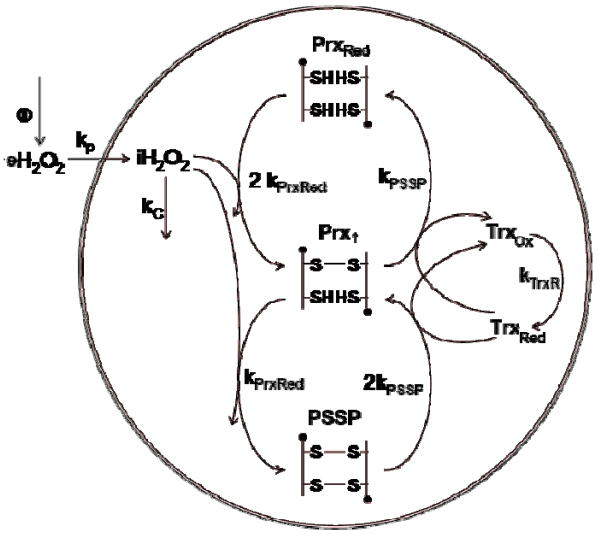

Figure 5.8 – Reactions considered to estimate k_{TrxR} from the data of (Low et al., 2007).

Model 5.3 was built from the scheme above and allows us to estimate the rate constant of Trx reduction.

$$\frac{d\ eH_2O_2}{dt} = \Phi - k_p \cdot eH_2O_2$$

$$\frac{d\ iH_2O_2}{dt} = \kappa \cdot \frac{A_S \cdot n}{V_e} \cdot eH_2O_2 - iH_2O_2 \cdot \left(k_C + k_{PrxRed} \cdot \left(2 \cdot Prx_{Red} + Prx_1\right)\right)$$

$$\frac{d\ Prx_{Red}}{dt} = k_{PSSP} \cdot Trx_{Red} \cdot Prx_1 - 2 \cdot k_{PrxRed} \cdot Prx_{Red} \cdot iH_2O_2$$

$$\frac{d\ Prx_1}{dt} = 2 \cdot k_{PrxRed} \cdot Prx_{Red} \cdot iH_2O_2 + 2 \cdot k_{PSSP} \cdot Trx_{Red} \cdot PSSP - \left(k_{PrxRed} \cdot iH_2O_2 + k_{PSSP} \cdot Trx_{Red}\right) \cdot Prx_1 \qquad \textbf{Model 5.3}$$

$$\frac{d\ Trx_{Red}}{dt} = k_{TrxR} \cdot Trx_{Ox} - k_{PSSP} \cdot Trx_{Red} \cdot \left(2 \cdot PSSP + Prx_1\right)$$

$$Prx_{dimer} = Prx_{Red} + Prx_1 + PSSP$$

$$Trxtot = Trx_{Red} + Trx_{Ox}$$

The meaning of each parameter of the above model is found in Table 5.6.

Table 5.6 – Parameters used to estimate k_{TrxR} through Model 5.3.

Parameter	Value	Meaning/Reference
A_S	1.35×10^{-8} dm^2	Erythrocyte surface area (Evans and Fung, 1972)
k_c	258 s^{-1}	Aggregate pseudo-first-order rate constant of catalase and GPx, obtained through the sum of $k_{catalase}$ and k_{GPx1} (Section 5.1.2)
k_p	4.2×10^{-3} s^{-1}	First-order rate constant for hydrogen peroxide consumption by erythrocytes. Estimated in Section 5.2.1.8
k_{PrxRed}	10^8 M^{-1}s^{-1}	Reactivity between reduced Prx2 and H_2O_2 (Manta et al., 2009)
k_{PSSP}	2.1×10^5 M^{-1}s^{-1}	Reactivity between reduced Trx and PSSP (Manta et al., 2009)
k_{TrxR}	To be estimated	Pseudo-first order rate constant for Trx reduction through TrxR
n	5×10^9 cells/dm^3	Concentration of erythrocytes in the experiments of (Low et al., 2007)
$Prxtot$	3.7×10^{-4} M	Total concentration of Prx2 monomers. Estimated in Section 5.1.1.3
$Trxtot$	4.8×10^{-6} M	Total Trx concentration (from bovine erythrocytes). Estimated in Section 5.2.1.6
V_e	1×10^{-13} dm^3	Erythrocyte volume (Evans and Fung, 1972)
V_{ew}	7×10^{-14} dm^3 water/cell	Erythrocyte water volume. Obtained by multiplying 0.7 dm^3 water/dm^3 cells (Savitz et al., 1964) with the erythrocyte volume of 10^{-13} dm^3 (Evans and Fung, 1972)
V_o	1×10^{-3} dm^3	Extracellular volume. Experimental conditions of (Low et al., 2007)
κ	6×10^{-5} dm/s	H_2O_2 permeability constant (Nicholls, 1965)
Φ	69×10^{-11} M/s	Hydrogen peroxide production, estimated in Section 5.2.1.8

In this model we neglect the intracellular production of hydrogen peroxide. k_{PrxRed} was used as the rate constant for the oxidation of a peroxidatic cysteine in both singly-crosslinked and reduced Prx2; k_{PSSP} was the rate constant for doubly-crosslinked and singly-crosslinked Prx2. We acknowledge the possibility that the reactivity between peroxidatic cysteines and H_2O_2 differs in singly- and doubly-crosslinked monomers, due to conformational changes or allosteric regulation. The same may also occur during Prx2 reduction. However, we did not find any reports confirming or denying such events. We treated thioredoxin reduction as a first-order process. However, because the thioredoxin concentration exceeds the K_M(Trx) of thioredoxin reductase [1.83×10^{-6} M (Turanov et al., 2006)], this assumption is reasonable only at low oxidative loads where a small fraction of the thioredoxin is in oxidized form.

Seeking to find the value of k_{TrxR}, we started by computing the steady state expressions for all the dependent variables in Model 5.3. The obtained expressions were then used as the initial values for the numerical integration of Model 5.3 with exception for eH_2O_2 which had initial value of 5×10^{-6} M. This was done by considering parameters from Table 5.6, leaving k_{TrxR} as the only

unknown parameter. In each trial, we sought to find a k_{TrxR} that yielded 12% of reduced Prx2 20 minutes after a H_2O_2 bolus, and found $k_{TrxR} \approx 0.5\ s^{-1}$.

In turn, we also estimated the k_{TrxR} from the data of (Turanov et al., 2006) through Equation 5.35. TrxR follows ping-pong kinetics to reduce Trx_{Ox}, oxidizing NADPH in the process (Arscott et al., 1997; Williams, 1995), and has the following rate equation

$$v_{TrxR} = \frac{V_{max}^{TrxR}}{1 + \frac{K_m(NADPH)}{NADPH} + \frac{K_m(TrxOx)}{Trx_{Ox}}} \qquad \textbf{Equation 5.35}$$

This equation may be rearranged algebraically giving

$$v_{TrxR} = \frac{Trx_{Ox} \cdot V_{\max}^{app}\left(Trx_{Ox}\right)}{Trx_{Ox} + K_m^{app}\left(Trx_{Ox}\right)} \qquad \textbf{Equation 5.36}$$

Where

$$V_{max}^{app}\left(Trx_{Ox}\right) = \frac{V_{max}^{TrxR}}{1 + \frac{K_m(NADPH)}{NADPH}} \text{ and } K_m^{app}\left(Trx_{Ox}\right) = \frac{K_m(Trx)}{1 + \frac{K_m(NADPH)}{NADPH}}$$

The value of V_{max}^{TrxR} may be computed by the product of the total concentration of enzyme found ($TrxR = 30\times10^{-9}$ M, Section 5.2.1.7) with the catalytic constant [$k_{cat} = 25.8\ s^{-1}$, (Turanov et al., 2006)]. This gives $V_{max}^{TrxR} \approx 77\times10^{-9}$ M/s. (Turanov et al., 2006) found a $K_m(Trx) = 1.83\times10^{-6}$ M for the human Trx. Using the values of V_{max}^{TrxR} and $K_m(Trx)$ one may estimate the pseudo-first order rate constant for Trx reduction through Equation 5.37

$$k_{TrxR} = \frac{V_{max}^{app}\left(Trx_{Ox}\right)}{K_m^{app}\left(Trx_{Ox}\right)} \approx 0.45\,s^{-1} \qquad \textbf{Equation 5.37}$$

This value is close to the 0.5 s^{-1} obtained through the fitting of Model 5.3, but because the experimental conditions in (Turanov et al., 2006) are not completely clear we considered $k_{TrxR} = 0.5\ s^{-1}$ in our next analyses.

5.2.1.10.Estimate of the pseudo-first order rate constant for formation of PSSP

We consider three oxidized states of Prx2: reduced (Prx_{Red}), sulfenic acid form (PSOH) and disulfide form (PSSP). Hydrogen peroxide first oxidizes each peroxidatic cysteine to a sulfenic acid (-SOH) which then reacts with a resolving cysteine to form disulfide bonds. The reduction of these disulfide bonds is accomplished through the oxidation of Trx (Reaction 5.9, Section 5.2.1.5). Thus, we have replaced Reaction 5.8 (Section 5.2.1.5) by the following reactions:

$$Prx_{Red} + H_2O_2 \xrightarrow{k_{PrxRed}} PSOH + H_2O$$ **Reaction 5.11**

$$PSOH \xrightarrow{k_{PSOH}} PSSP$$ **Reaction 5.12**

k_{PrxRed} and k_{PSOH} are the rate constants for each of the reactions. The total concentration of Prx2 is therefore given by the sum of Prx_{Red}, PSOH and PSSP. Note that we assume that any of the above reactions (including Reaction 5.9, Section 5.2.1.5) occurs equivalently in every monomer of the protein. This should approximate what happens *in vivo* unless Prx2 presents cooperativity among its monomers. However, we have not found any evidence in the literature for cooperativity in mammalian peroxiredoxins.

We have estimated k_{PSOH} from the study of (Manta et al., 2009). These authors evaluated the overoxidation (sulfinylation) of Prx2, obtaining the results in Figure 5.9.

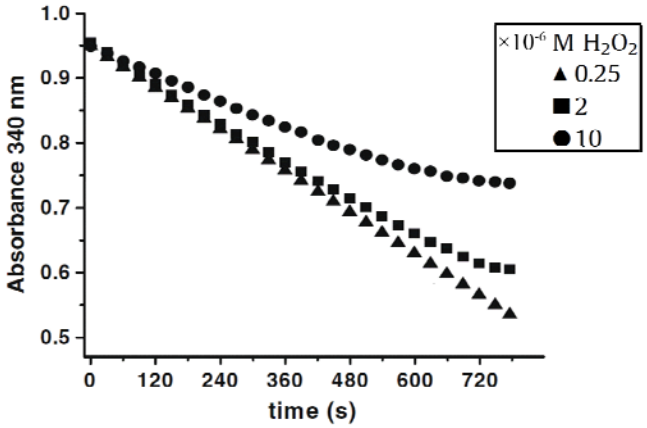

Figure 5.9 – Overoxidation of Prx2. Oxidation of NADPH monitored at 340 nm, as determined by (Manta et al., 2009). Reaction mixture contained 200×10^{-6} M NADPH, 10^{-6} M human TrxR, 8×10^{-6} M human Trx1, 5×10^{-7} M Prx2 and was assayed for the peroxidase activity at the indicated H_2O_2 concentrations in 100×10^{-3} M phosphate buffer, pH 7.4, 1×10^{-3} M DTPA, at 25 ºC. Taken from Figure 5A of (Manta et al., 2009).

These authors assessed NADPH oxidation as a means to determine the overoxidation of Prx2 in an *in vitro* assay. We used the plot corresponding to the lower H_2O_2 because it shows almost no

overoxidation, as noted by the constant rate of NADPH decrease. If the rate of PSSP formation is the limiting step of the system, it will be possible to determine the value of the rate constant of this reaction (k_{PSOH}) from the kinetics of NADPH oxidation above. The reaction scheme of this experiment is the following

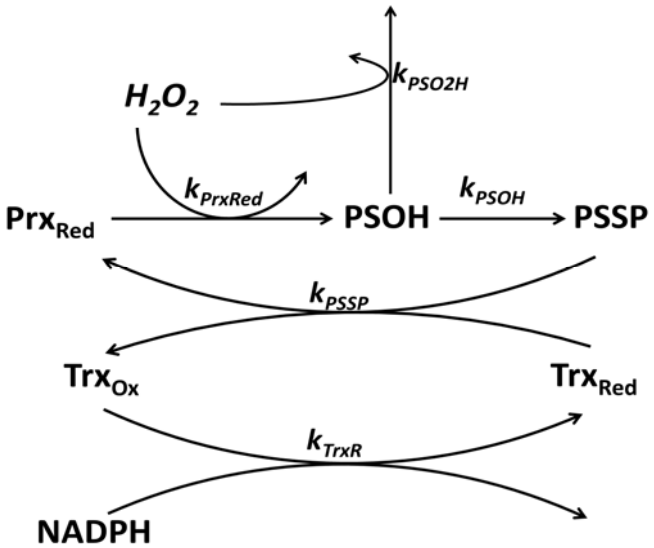

Figure 5.10 – Reaction scheme for the experiment of (Manta et al., 2009).

The initial concentrations of each of the variables in the experiment are represented in Table 5.7.

Table 5.7– Initial conditions of the experiment of (Manta et al., 2009).

Variable	Initial value ($\times 10^{-6}$ M)
NADPH	200
TrxR	1
Trxtot	8
Prxtot	0.5
H_2O_2	250

We now show how we determined which is the limiting step of the experiment. Notice that NADPH is oxidized at a constant rate, which means that the concentrations of the various Prx2 and Trx forms are at steady state.

In order to know if Trx_{Ox} has accumulated, we first determined if NADPH consumption is occurring at the maximal rate of TrxR. We used the plot with the lower H_2O_2 in Figure 5.9 after converting absorbance to NADPH concentration. This was done by first computing a scaling factor (*sf*) from Equation 5.38.

$$sf = \frac{NADPH_{t=0}}{\overline{abs_{t=0}}} = \frac{200\times10^{-6}}{0.9511} \approx 2.10\times10^{-4}\ \text{M} \quad \text{Equation 5.38}$$

,

whereWhere $NADPH_{t=0}$ is the initial NADPH concentration considered in the experiments (200×10^{-6} M) and $\overline{abs_{t=0}}$ is the mean of absorbances registered for the three plots in Figure 5.9 when t=0 (0.951). The data was then normalized by multiplying each registered absorbance by *sf*. A least-squares fit of these experimental results yields the following best-fit line:

$$NADPH\,[\text{t}] \approx 0.11\times10^{-6}\times t + 200\times10^{-6} \quad \text{Equation 5.39}$$

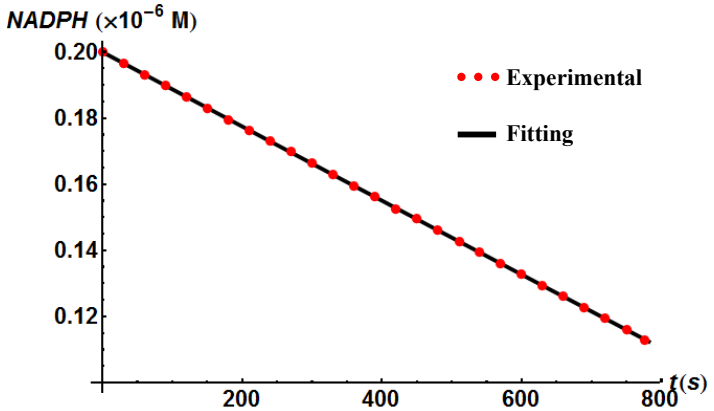

Figure 5.11 – NADPH consumption by hTrxR obtained through the experiment of (Manta et al., 2009) – dots – and fitting to the experimental data through the Method of Linear Least Squares – line.

As Figure 5.11 shows, Equation 5.39 provides an excellent fit ($R^2 \approx 0.99$) to the data by (Manta et al., 2009). The slope of the line indicates that NADPH is oxidized at 11×10^{-6} M/s. Because in the experimental setup designed by the authors only TrxR is oxidizing NADPH, this rate also corresponds to the activity of TrxR (v_{TrxR}, Equation 5.35, Section 5.2.1.9). Note that these authors initially had $NADPH = 2\times10^{-4}$ M, a concentration well above the K_m of TrxR for this substrate [$K_{m,TrxR}$(NADPH)= 6×10^{-6} M, (Urig et al., 2006)]. Because $NADPH \gg K_m(NADPH)$, the rate of TrxR activity (Equation 5.35, Section 5.2.1.9) then becomes

$$v_{TrxR} \approx \frac{V_{max}^{TrxR}}{1+\frac{K_m(TrxOx)}{Trx_{Ox}}} \quad \text{Equation 5.40}$$

If the TrxR activity was limited by *Trx* there would be accumulation of oxidized Trx. This would make $Trx_{Ox} = Trxtot = 8\times10^{-6}$ M (Table 5.7), leading to $v_{TrxR} = 11\times10^{-8}$ M/s. However, replacing the values of $Trx_{Ox} = 8\times10^{-6}$ M, $V_{max}^{TrxR} = 77\times10^{-8}$ M/s (Section 5.2.1.9) and $K_m(Trx_{Ox}) = 1.83\times10^{-6}$

M (Turanov et al., 2006) in Equation 5.35 gives $v_{TrxR} \approx 6\times10^{-7}$ M/s. Because this rate is much higher than the rate of NADPH oxidation observed by the authors, it is not Trx reduction that is the limiting step. Indeed if we consider $v_{TrxR} = 11\times10^{-8}$ M/s, $V_{max}^{TrxR} = 77\times10^{-8}$ M/s and $K_m(Trx_{Ox}) = 1.83\times10^{-6}$ M (Turanov et al., 2006), we get $Trx_{Ox} \approx 3\times10^{-6}$ M (about 4% of the total Trx contents considered in the experiments). Therefore we can assume that Trx is mostly reduced in the experiments of (Manta et al., 2009).

On the other hand, Prx2 reduction may be the limiting step. (Manta et al., 2009) determined a $k_{PSSP} = 2.1\times10^{5}$ $M^{-1}s^{-1}$ in their experiments. Taking this value and the concentrations in Table 5.7 into consideration and assuming that all the Prx2 is in PSSP form, the rate of Prx2 reduction v_{PSSP} is

$$v_{PSSP} = k_{PSSP} \cdot Trxtot \cdot Prxtot \qquad \textbf{Equation 5.41}$$
$$\Leftrightarrow v_{PSSP} \approx 84\times10^{-8} \text{ M/s}$$

Yet, the reaction rate obtained through Equation 5.41 is much higher than the 0.11 µM NADPH/s oxidized (Figure 5.11), indicating that Prx2 reduction is not the limiting step either.

These authors also estimated the reactivity between Prx2 and H_2O_2 and found $k_{PrxRed} = 10^{8}$ $M^{-1}s^{-1}$. Using this value, we find that the pseudo-first order rate constant for Prx_{Red} oxidation under the conditions of the experiment is extremely high ($k = k_{PrxRed} \times H_2O_2 \approx 2.5\times10^{4}$ s^{-1} with H_2O_2 from Table 5.7). Note that this pseudo-first order rate constant is much higher than the pseudo-first order rate constant for Prx2 reduction obtained above ($k_{PSSP}\times Trxtot \approx 1.7$ s^{-1}). Therefore, the limiting step may only be the formation of PSSP.

Because the system is at steady state and Trx is mostly reduced, we get

$$v_{PSSP} = k_{PSSP} \cdot Trx_{Red} \cdot PSSP \qquad \textbf{Equation 5.42}$$
$$\Leftrightarrow v_{PSSP} \approx k_{PSSP} \cdot Trxtot \cdot PSSP \qquad \textbf{Equation 5.43}$$
$$\Leftrightarrow PSSP \approx 66\times10^{-9} \text{ M}$$

with $v_{PSSP} = 11\times10^{-6}$ M/s, $Trxtot = 8\times10^{-6}$ M, $k_{PSSP} = 2.1\times10^{5}$ $M^{-1}s^{-1}$. Because Prx_{Red} oxidation is extremely fast ($k \approx 2.5\times10^{4}$ s^{-1}), the concentration of Prx_{Red} is negligible. Therefore, $Prxtot \approx PSOH + PSSP$, yielding 43×10^{-8} M $PSOH$ if $Prxtot = 5\times10^{-7}$ M (Table 5.7) and PSSP= 66×10^{-9} M.

Under these conditions, we get

$$v_{PSSP} = v_{PSOH} = k_{PSOH} \cdot PSOH \qquad \textbf{Equation 5.44}$$

from which the value of k_{PSOH} = 0.26 s^{-1} is obtained by considering $PSOH$ = 43×10^{-8} M and v_{PSSP} = 11×10^{-8} M/s.

5.2.2. Maximum rates of H_2O_2 decomposition by Prx2 at steady state

The maximum rate of H_2O_2 reduction achieved by Prx2 depends on the redox status of the erythrocyte, not only in terms of iH_2O_2 but also in terms of NADPH supply and Trx oxidation. If either NADPH or Trx supply is limiting Prx2 reduction, the maximum rate achieved by Prx2 is equal to the rate of supply under steady state conditions.

If Trx reduction is limiting the peroxidase activity of Prx2, one may use the maximum rate of Trx reduction to estimate the maximum rate of Prx2 reduction (V_{max}^{Red}). Taking this into consideration, v_{Prx2} reaches its maximum value (V_{max}^{Prx2}) when

$$v_{Prx2} = V_{max}^{Prx2} = V_{max}^{TrxR} \qquad \textbf{Equation 5.45}$$

$$\text{with } V_{max}^{TrxR} = k_{TrxR} \cdot Trxtot \qquad \textbf{Equation 5.46}$$

Considering Equation 5.46, k_{TrxR} = 0.5 s^{-1} (Section 5.2.1.9) and Trx_{Ox} = $Trxtot$ = 4.8×10^{-6} M (Section 5.2.1.6) gives V_{max}^{Red} ≈ 2.4×10^{-6} M/s. This rate is comparable to the maximum rate of NADPH production by the hexose monophosphate shunt under stimulation by methylene blue [1.9×10^{-6} to 2.4×10^{-6} M/s (Albrecht et al., 1971; Gaetani et al., 1974)]. This suggests that NADPH supply and not Trx availability or TrxR activity limit Prx2 reduction.

Other evidence also points this as a likely possibility. The TrxR activity in human erythrocytes determined by (Low et al., 2007) using DTNB as substrate is 7.9×10^{-6} M/s (at 37ºC). The enzyme has a k_{cat} = 33.3 s^{-1} for DTNB at 25ºC (Urig et al., 2006), which tentatively considering a Q_{10} of 1.2 would translate into a k_{cat} = 48 s^{-1} at 37ºC. On the other hand, using the data by (Turanov et al., 2006) we obtain that k_{cat} (Trx) ≈ 0.77 k_{cat} (DTNB), which would correspond to an activity of 0.77×7.9×10^{-6} M/s = 6.1×10^{-6} M/s. This high V_{max}^{TrxR} is 2.5 to 4.7 fold higher than the erythrocyte's capacity for NADPH production [1.9×10^{-6} to 2.4×10^{-6} M/s (Albrecht et al.,

1971; Gaetani et al., 1974)]. This again suggests that NADPH supply may limit Trx (and Prx2) reduction hence affecting the antioxidant activity of Prx2 under high oxidative loads.

However, the estimates above are pinned on some uncertainties. Namely, the value of *Trxtot* in *human* erythrocytes, doubts about the interpretation of the progression curve in Figure 5.5 (Section 5.2.1.8), the imprecise estimate of the fractions of Prx2 in reduced form in Figure 5.6 (Section 5.2.1.9), unclear experimental conditions in the experiments of (Turanov et al., 2006) and doubts about the precise kinetics of Prx2 oxidation and reduction. Clearly, the issue of what limits Prx2 reduction in human erythrocytes requires further experimental investigation with more sensitive and precise methods.

5.3. At what extracellular H_2O_2 concentration does Prx2 remain the main H_2O_2 scavenging process?

As the above sections show, when Prx2 is mostly reduced catalase and GPx1 have negligible contributions for H_2O_2 scavenging as noted by their rate constants (Table 5.2, Section 5.1.2). However, because Trx reduction limits the peroxidase activity of Prx2 under high oxidative loads, it would be interesting to estimate the maximal sustained oxidative load tolerated by the Prx2/Trx cycles.

However, such estimate is associated with a couple problems, some of which were already discussed in Section 5.2.2. Also, NADPH may become scarce at high eH_2O_2, and we have not assessed yet how TrxR and GSR compete for NADPH when the latter is scarce. For these reasons we will instead determine the oxidative load under which the Prx2/Trx cycles are not saturated with H_2O_2, remaining the main H_2O_2 scavenging process in the erythrocyte.

Using Figure 4A of (Low et al., 2007) partially represented in Figure 5.6 (Section 5.2.1.9), we estimated the rate of Prx2 reduction as we now explain. As shown in that figure, the band of reduced Prx2 is much less intense than the band of dimerized Prx2 20 minutes after the erythrocytes were exposed to a 5×10^{-6} M H_2O_2 bolus. 30 minutes after the exposure to the H_2O_2 bolus, the bands of reduced and dimerized Prx2 were about the same intensity.

Tentatively assuming that about 12% and 50% of Prx2 is in reduced form respectively 20 and 30 minutes after the bolus as per the immunoblot in Figure 5.6 (Section 5.2.1.9), we computed the concentrations of Prx2 in each reduced fraction by considering $Prxtot = 3.7\times10^{-4}$ M (Section 5.2.1.2). The values corresponding to each concentration are present in Table 5.8.

Table 5.8 – Approximated fractions of reduced Prx2 in the experiments of (Low et al., 2007), and corresponding concentration of reduced Prx2. Refer to Figure 5.7 (Section 5.2.1.9) and to the text above for more detail on the experiments of (Low et al., 2007).

	20 minutes	**30 minutes**
Prx_{Red} (% of total)	12	50
Corresponding Prx_{Red} ($\times10^{-6}$ M)	44	185

In ten minutes $(185 - 44)\times10^{-6} \approx 1.4\times10^{-4}$ M Prx2 was reduced. This gives a rate of Prx2 reduction of $\approx2.3\times10^{-7}$ M/s. To achieve half of this flux the H_2O_2 influx rate (v_{influx}) would have to be

$$v_{influx} = \frac{2.3\times10^{-7}}{2} \approx 1.2\times10^{-7} \text{ M/s}$$

where

$$v_{influx} = k_p \cdot eH_2O_2 \qquad \textbf{Equation 5.47}$$

Considering $k_p = 8$ s^{-1} (Section 5.2.1.2) we get $eH_2O_2 \approx 2\times10^{-8}$ M. This value represents the oxidative load that may be sustained by a human erythrocyte without leading to saturation of its Prx2/Trx systems.

In Equation 5.47 we are assuming that most of Prx2 is in reduced form, thereby representing the main H_2O_2 scavenger in the cell[4]. This would occur when Prx2 reduction is limited by H_2O_2 availability. The iH_2O_2 that would correspond to such a v_{influx}, considering $k_p = 8$ s^{-1}, $eH_2O_2 = 1.5\times10^{-8}$ M and $k_{Prx2} = 3.7\times10^4$ s^{-1} (Section 5.1.1.3), would be

$$v_{influx} = v_{Prx2}$$
$$\Leftrightarrow k_p \cdot eH_2O_2 = k_{Prx2} \times iH_2O_2 \qquad \textbf{Equation 5.48}$$

[4] In Section 5.1.2 we compared the contributions of Prx2 with those of GPx1 and catalase for H_2O_2 scavenging by considering that each process has pseudo-first order kinetics with respect to H_2O_2.

$$\Leftrightarrow iH_2O_2 \approx 3\times10^{-12}\,\mathrm{M}$$

This value corresponds to the oxidative load under which we may safely assume that the erythrocyte's Prx2/Trx cycles are not saturated with H_2O_2. It may be higher if catalase/GPx1 or other processes are contributing substantially for H_2O_2 scavenging; or if part of the oxidized Prx2 in Figure 5.6 (Section 5.2.1.9) is due to unaccounted oxidation of Prx2 during sample preparation.

To support this estimate we have also computed the load supported by the Prx2/Trx cycles by considering that TrxR activity (and Prx2 reduction) is limited by NADPH supply. We have already presented evidence that suggests that TrxR is likely limited by NADPH, and not by Trx availability, under high oxidative loads (Section 5.2.2). Bearing this in mind, consider that iH_2O_2 scavenging by Prx2 is occurring at half the maximal rate of NADPH production by the erythrocyte. Under such conditions, Prx2 activity is limited by iH_2O_2 availability and not by NADPH supply. The eH_2O_2 that would correspond to such rate, considering again k_p = 8 s^{-1} and V_{max}^{PPP} = 1.9×10^{-6} M/s would be

$$\begin{aligned} & v_{influx} = \frac{V_{max}^{PPP}}{2} \\ & \Leftrightarrow k_p \cdot eH_2O_2 = 9.5\times10^{-7} \\ & \Leftrightarrow eH_2O_2 \approx 10^{-7}\ \mathrm{M} \end{aligned}$$

Equation 5.49

Considering again Equation 5.48 and taking eH_2O_2 = 10^{-7} M, we find that this would correspond to $iH_2O_2 \approx 2\times10^{-11}$ M. This value could represent the $K_m^{app}(iH_2O_2)$ of Prx2 if all of the NADPH produced in the cell was consumed by TrxR at high eH_2O_2. Though, because NADPH may be distributed between TrxR and GSR under such loads, we cannot assume that $K_m^{app}(iH_2O_2)$ of Prx2 is 2×10^{-11} M.

If these values are the basal iH_2O_2 found in the erythrocyte they thus represent the oxidative load under which Prx2 remains mostly reduced. We now proceed to estimate the fractions of Prx_{Red} and Trx_{Red} that would correspond to the iH_2O_2 estimated above. To do so we considered the reaction scheme in Figure 5.12.

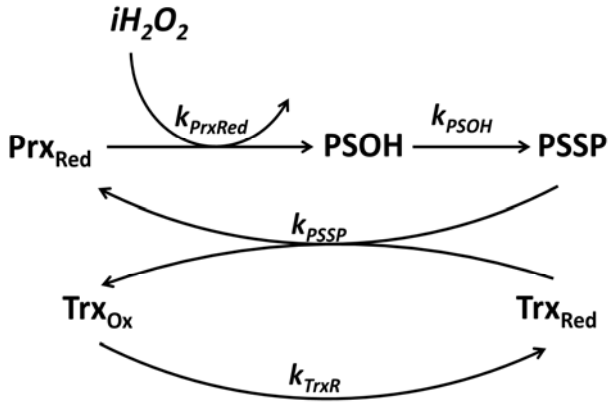

Figure 5.12 – Representation of reactions used to study the fraction of Prx_{Red} under various iH_2O_2.

These reactions led to Model 5.4, whose parameters were estimated in Section 5.2.1:

$$\frac{d\ Prx_{Red}}{dt} = k_{PSSP} \cdot PSSP \cdot Trx_{Red} - k_{PrxRed} \cdot Prx_{Red} \cdot iH_2O_2$$
$$\frac{d\ PSOH}{dt} = k_{PrxRed} \cdot Prx_{Red} \cdot iH_2O_2 - k_{PSOH} \cdot PSOH$$
$$\frac{d\ Trx_{Ox}}{dt} = k_{PSSP} \cdot PSSP \cdot Trx_{Red} - k_{TrxR} \cdot Trx_{Ox}$$
$$Prxtot = Prx_{Red} + PSOH + PSSP$$
$$Trxtot = Trx_{Red} + Trx_{Ox}$$

Model 5.4

In this model, we are disregarding NADPH supply as a possible limiting step for TrxR activity in erythrocytes facing higher oxidative loads. However, NADPH might limit Trx reduction, thus affecting Prx2 activity. Therefore, this model pertains only to oxidative loads in which the NADPH supply can keep up with the demand for reducing equivalents by TrxR and other processes.

Consider k_p = 8 s^{-1} (Section 5.2.1.2**Erro! A origem da referência não foi encontrada.**), k_{TrxR} = 0.5 s^{-1} (Section 5.2.1.9), k_{PSOH} = 0.26 s^{-1} (Section 5.2.1.10) and other values from Table 5.6 (Section 5.2.1.9). In steady state conditions, solving Model 5.4 in order to every dependent variable allows us to estimate the fractions of Prx_{Red} and Trx_{Red} under various iH_2O_2. In Table 5.9 we show the eH_2O_2 and fractions of Prx_{Red} and Trx_{Red} that would correspond to the basal iH_2O_2 estimated above. We also compare them to the iH_2O_2 estimated by (Giulivi et al., 1994) and (Kirkman et al., 1999). These authors respectively estimated 2×10^{-11} and 3×10^{-9} M iH_2O_2 under basal oxidative loads, as discussed in Section 5.2.1.3.

Table 5.9 – eH_2O_2 and fractions of Prx_{Red} and Trx_{Red} that would correspond to the basal iH_2O_2 estimated by us from V_{max}^{PPP} and from the experiments (Low et al., 2007), and iH_2O_2 estimated by (Giulivi et al., 1994) and (Kirkman et al., 1999). eH_2O_2 computed through Equation 5.48; fractions of Prx_{Red} and Trx_{Red} computed through Model 5.4. Consider Prx2 as the main H_2O_2 scavenger in the erythrocyte; $k_p = 8\ s^{-1}$; $k_{Prx2} = 3.7\times10^4\ s^{-1}$.

Source	iH_2O_2 ($\times10^{-9}$ M)	eH_2O_2 ($\times10^{-6}$ M)	Prx_{Red} (% *Prxtot*)	Trx_{Red} (% *Trxtot*)
Estimate using experiments by (Low et al., 2007)	0.003	0.02	>99.8	95.4
Estimate using V_{max}^{PPP}	0.02	0.1	98.9	70
Estimate by (Giulivi et al., 1994)	0.2	0.9	32	0.97
Estimate by (Kirkman et al., 1999)	3	10	2	0.67

According to our estimates, an $eH_2O_2 \approx 10^{-7}$ M (and $iH_2O_2 \approx 2\times10^{-11}$ M) is sustained by the Prx2/Trx cycles, much lower than the basal loads found by (Giulivi et al., 1994; Kirkman et al., 1999). We also found that the basal iH_2O_2 estimated by us allow most of the Prx2 contents to completely reduced, unlike what would be obtained if one considered the basal iH_2O_2 estimated by (Giulivi et al., 1994; Kirkman et al., 1999).We also see that the iH_2O_2 estimated by (Giulivi et al., 1994) and (Kirkman et al., 1999) would lead to most of the Trx contents in the erythrocyte to be in oxidized form. TrxR would then be constantly consuming NADPH in order to reduce such a high (>99% Trx_{Ox}) fraction of oxidized Trx. On the other hand, TrxR would achieve a much lower rate of NADPH consumption if we considered the iH_2O_2 we estimated (2×10^{-11} M or 3×10^{-11} M).

Yet, we found that Trx_{Red} would account for 70% of the total Trx contents considering $iH_2O_2 = 2\times10^{-11}$ M as basal oxidative load. Having Trx_{Ox} = 30% of the total Trx concentration would correspond to a constant NADPH consumption by TrxR of 7.2×10^{-7} M/s by considering $k_{TrxR} = 0.5\ s^{-1}$ (Section 5.2.1.9) and $Trxtot = 4.8\times10^{-6}$ M (Section 5.2.1.6). Although this rate is lower than the maximal rate of NADPH supply by the PPP [1.9×10^{-6} M/s, (Albrecht et al., 1971)], TrxR would still account for a very significant NADPH consumption. Therefore, the basal iH_2O_2 must be lower than 2×10^{-11} M.

Our next analyses will be done by considering steady state conditions. We analyzed not only pathological conditions (such as systemic inflammation) but also low H_2O_2 ($iH_2O_2 \ll 3\times10^{-12}$ M and $eH_2O_2 \ll 2\times10^{-8}$ M) from basal oxidative loads (<9.5×10^{-7} M iH_2O_2/s).

5.4. How does the redox state of Peroxiredoxin 2 vary with Trx or disulfide bond formation rate constants?

In the sections above we estimated and discussed the load sustained by the Prx2/Trx cycles, assuming that NADPH supply may or may not limit Prx2 reduction (Sections 5.2.2 and 5.3). Because Prx2 reduction is affected by the redox status of Trx, it is important to address how the Trx cycle affects the redox status of Prx2. Because we had to estimate the rate constant for the formation of disulfide Prx2, we will now analyze how this rate constant affects the redox state of Prx2. Because we estimated the Trx concentration using data from bovine erythrocytes (Section 5.2.1.6), in this section we also analyze how *Trxtot* affects the redox state of Prx2.

We consider again intracellular H_2O_2 as an independent variable. As we saw in Section 5.1.2, catalase and GPx1 have negligible contributions for H_2O_2 reduction provided that Prx2 is mostly reduced. This simplification is reasonable for $eH_2O_2 < 3\times10^{-12}$ M as per our estimates in Section 5.3. With these simplifications we were able to obtain simpler analytical expressions of the steady-state of each dependent variable in Figure 5.12 (Section 5.3).

Considering steady state conditions, we solved Model 5.4 (Section 5.3) in order to every dependent variable and obtained their respective steady state values. We considered k_{PSOH} = 0.26 s^{-1} (Section 5.2.1.10), and parameters in Table 5.6 (Section 5.2.1.9). We then plotted the fraction of each Prx2 form against various Trx concentrations (Figure 5.13) under basal iH_2O_2 (= 10^{-12} M, Section 5.2.1.3)

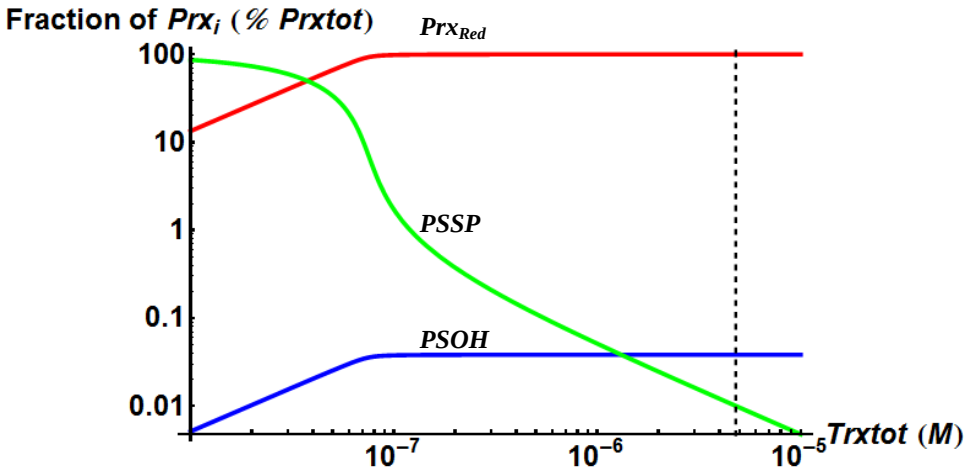

Figure 5.13 – Log-log plots of the steady state fraction of Prx_{Red} (red), *PSOH* (blue) and *PSSP* (green) for various *Trxtot* ($iH_2O_2 = 10^{-12}$ M). The dashed line represents the *in vivo* concentration ≈ 4.8×10^{-6} M *Trxtot* (Section 5.2.1.6). See text above for more details.

The above figure shows that for low *Trxtot*, practically all Prx2 is in the PSSP form. This is expected to happen when the oxidative load is above the capacity of the Trx/TrxR cycle to keep reducing Prx2 (i.e. there is not enough Trx to keep reducing Prx2). On the other hand, a larger *Trxtot* allows these cycles to endure larger oxidative loads, leading to the accumulation of reduced Prx2. The shift from a "high capacity" system (i.e. Prx_{Red} accumulates) to a "low capacity" system (i.e. *PSSP* accumulates) depends on the oxidative load (iH_2O_2) and on *Trxtot*. If iH_2O_2 is very large *PSSP* accumulates. If *Trxtot* increases, the maximal oxidative load supported by the Prx2/Trx cycles increase as well, allowing a larger V_{max}^{TrxR}.

In Figure 5.14 we plot how *PSOH* and Prx_{Red} change with *Trxtot.* This figure shows that, up until a certain breakpoint value of *Trxtot* (which we refer as "crossover" from now on), *PSOH* and Prx_{Red} increase with *Trxtot*. After the crossover, further increasing *Trxtot* does not significantly change *PSOH* nor Prx_{Red}. Notice however that PSOH represents <0.1% of the total Prx2 contents, a value obtained for larger *Trxtot*.

Because the estimate of k_{PSOH} was done by considering a series of assumptions we also analyzed how this parameter affects the redox state of Prx2. As Figure 5.14 shows, neither the fractions of Prx_{Red} or PSSP are affected by k_{PSOH}. In that figure we plotted the steady state value of the fractions of *PSSP,* Prx_{Red} and *PSOH,* against various *Trxtot* and k_{PSOH}. We again considered $k_{PSOH} = 0.26\ s^{-1}$ (Section 5.2.1.10), and parameters in Table 5.6 (Section 5.2.1.9).

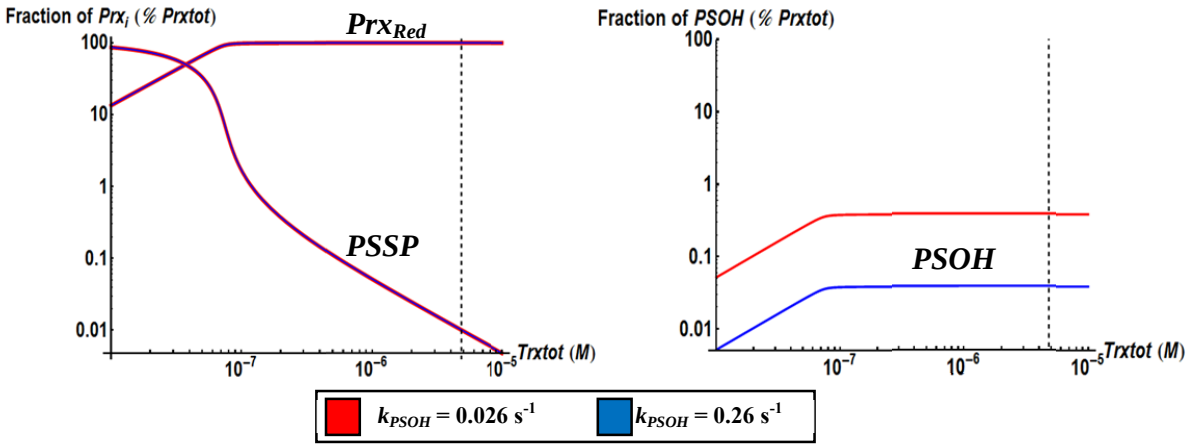

Figure 5.14 – Log-log plot of the steady state fraction of *PSSP* and Prx_{Red} (left) or *PSOH* (right) with *Trxtot*. k_{PSOH} = 0.026 s^{-1} (Red), or 0. 26 s^{-1} (Blue). The dashed line represents the assumed *in vivo* concentration ≈ 4.8×10^{-6} M *Trxtot* (Section 5.2.1.6). See text above for more details.

The figure above shows that decreasing the value of k_{PSOH} does not significantly change the fraction of Prx_{Red} nor *PSSP* (note that the plots for the same Prx_i are superimposed for both k_{PSOH}). However, decreasing k_{PSOH} increases the fraction of PSOH due to the slower formation of disulfide bonds. These results show that *Trxtot* controls the fraction of oxidized Prx2 for a given oxidative load. The fraction of PSOH, but not Prx_{Red} nor PSSP, is affected by k_{PSOH}.

5.5. What is the concentration of each Prx2 form in limit situations and how does it change with system's parameters?

In this section we estimated the fraction of each redox form of Prx2 under low and high oxidative loads. We also estimated how each redox form changes with the parameters from the model. In this section we describe these estimates.

5.5.1. Fraction of each Prx2 form under low and high oxidative loads

Using Model 5.4 (Section 5.3) we computed the fraction of Prx_{Red}, *PSOH* and *PSSP* when *Trxtot* tends to be very large (Equation 5.50). The values obtained in the equations below were computed after we had obtained the analytical expressions for the steady state concentration of each Prx2 form. We again considered k_{PSOH} = 0.26 s^{-1} (Section 5.2.1.10), iH_2O_2 = 10^{-12} M (Section 5.2.1.3) and parameters from Table 5.6 (Section 5.2.1.9).

$$\lim_{Trxtot\to\infty}\frac{PSOH}{Prxtot}=\frac{k_{PrxRed}\cdot iH_2O_2}{k_{PrxRed}\cdot iH_2O_2+k_{PSOH}}\approx 0.28\ \%$$ **Equation 5.50**

The limit in Equation 5.50 shows that when *Trxtot* increases much, *PSOH* tends to only depend on iH_2O_2. This happens because the availability of iH_2O_2 and not of Trx_{Red} affects the rates of Prx_{Red} oxidation and PSSP formation.

In such conditions and as Equation 5.51 shows, Prx_{Red} accumulates:

$$\lim_{Trxtot\to\infty}\frac{Prx_{Red}}{Prxtot}=\frac{k_{PSOH}}{k_{PrxRed}\cdot iH_2O_2+k_{PSOH}}\approx 100\ \%$$ **Equation 5.51**

On the other hand if *Trxtot* is very little (or if the oxidative load is much larger than the value supported by the Prx2/Trx cycles), practically no Prx2 is found in *PSOH* or Prx_{Red} form because *PSSP* accumulates (Equation 5.52):

$$\lim_{Trxtot\to 0}\frac{PSSP}{Prxtot}=100\ \%$$ **Equation 5.52**

For lower *Trxtot*, the availability of Trx_{Red} limits the oxidation of Prx_{Red} oxidation and PSSP formation.

The limits obtained above are in agreement with the analysis we made in Section 5.1.2 as well as what was found through Figure 5.14 (Section 5.4) above. Those limits suggest that Prx2 accumulates in PSSP form or Prx_{Red}, depending on whether or not the Trx cycle is able to reduce Prx2: a very high *Trxtot* allows a larger rate of Prx2 reduction thus leading to Prx_{Red} accumulation; on the other hand, a very low *Trxtot* leads to accumulation of *PSSP*. But the redox status of Prx2 depends not only on *Trxtot* but also on the oxidative load that the cell is facing as we now show.

Take into consideration the reaction scheme in Figure 5.15, mathematically expressed through Model 5.5. These reactions include the antioxidant activity of Prx2 but also the contributions of catalase and GPx1 for iH_2O_2 consumption. It also includes H_2O_2 influx across the cellular membrane.

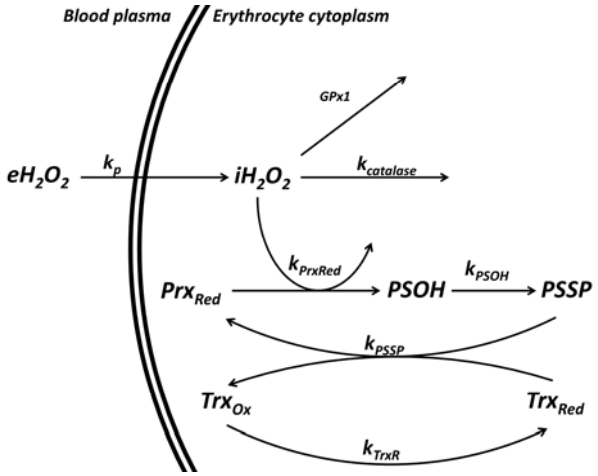

Figure 5.15– Reaction scheme used to address how various parameters of the system affect the redox status of Prx2.

$$\frac{d\ iH_2O_2}{dt} = k_p \cdot eH_2O_2 - iH_2O_2 \cdot (k_{PrxRed} \cdot Prx_{Red} + k_{catalase} + k_{GPx1})$$

$$\frac{d\ Prx_{Red}}{dt} = k_{PSSP} \cdot PSSP \cdot Trx_{Red} - k_{PrxRed} \cdot Prx_{Red} \cdot iH_2O_2$$

$$\frac{d\ PSOH}{dt} = k_{PrxRed} \cdot Prx_{Red} \cdot iH_2O_2 - k_{PSOH} \cdot PSOH$$

Model 5.5

$$\frac{d\ Trx_{Ox}}{dt} = k_{PSSP} \cdot PSSP \cdot Trx_{Red} - k_{TrxR} \cdot Trx_{Ox}$$

$$Prxtot = Prx_{Red} + PSOH + PSSP$$

$$Trxtot = Trx_{Red} + Trx_{Ox}$$

The model above includes the parameters found in Table 5.10.

Table 5.10 – Parameters used for Model 5.1. Refer to Table 5.6 (Section 5.2.1.9) for values and meaning of parameters here referred.

Parameter	Value	Meaning/Reference
$k_{catalase}$	218 s^{-1}	Pseudo-first-order rate constant for H_2O_2 consumption by catalase, Section 5.1.1.2
k_{GPx1}	40 s^{-1}	Pseudo-first order rate constant for H_2O_2 consumption by GPx1, Section 5.1.1.1
k_p	8 s^{-1}	First-order rate constant for hydrogen peroxide consumption by erythrocytes (estimated in Section 5.2.1.2)
k_{PrxRed}	10^8 $M^{-1}s^{-1}$	Reactivity between reduced Prx2 and H_2O_2 (Manta et al., 2009)
k_{PSOH}	0.26 s^{-1}	First order rate constant for formation of PSSP (Section 5.2.1.10)
k_{PSSP}	2.1×10^5 $M^{-1}s^{-1}$	Reactivity between reduced Trx and PSSP (Manta et al., 2009)
k_{TrxR}	0.5 s^{-1}	Pseudo-first order rate constant for Trx reduction through TrxR (Section 5.2.1.9)
Prxtot	3.7×10^{-4} M	Total concentration of Prx2 monomers (Section 5.1.1.3)
Trxtot	4.8×10^{-6} M	Total Trx concentration (from bovine erythrocytes, 5.2.1.6)

Using Model 5.5 we plotted the steady state fraction of Prx_{Red} in cells facing various eH_2O_2, after taking into consideration parameters from Table 5.10:

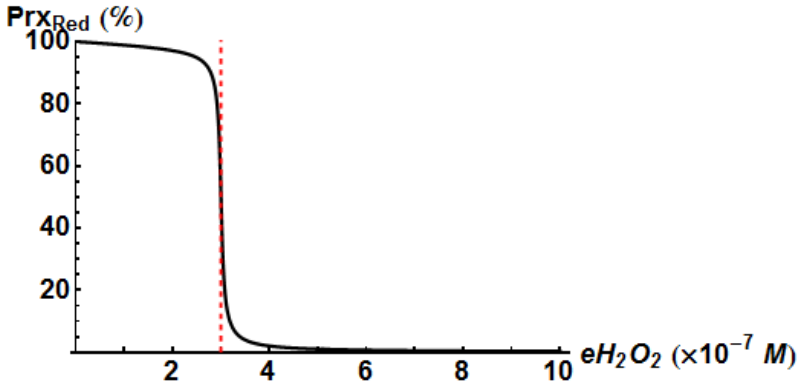

Figure 5.16 – Fraction of Prx_{Red} in erythrocytes exposed to various eH_2O_2. Obtained by computing the steady state fraction of Prx_{Red} through Model 5.5 and Table 5.10. The dashed line marks $eH_2O_2 = 3\times10^{-7}$ M. See text below for details.

The figure above shows the existence of a "*crossover*", from oxidative loads in which most of the Prx2 contents are in reduced form ("*pre-crossover*") to an oxidative load that leads to *PSSP* accumulation ("*post-crossover*"). The dashed line marks this crossover and corresponds to $eH_2O_2 = 7\times10^{-7}$ M. In the next section we study how this value may be obtained analytically and how the rate of H_2O_2 influx and *Trxtot* affect the redox status of Prx2.

5.5.2. How H_2O_2 influx and Prx2 reduction affect the redox status of Prx2

In this section we will obtain analytical expressions for the redox status of each Prx2 form and analyze how each parameter affects its concentration. We approached this issue in a simplified way by considering limit cases.

Under low oxidative loads ($eH_2O_2 < 3\times10^{-12}$ M, Section 5.3), the contributions of catalase and GPx1 for iH_2O_2 consumption are negligible (Section 5.1.2), and H_2O_2 consumption by Prx2 (v_{Prx2}) is limited by the rate of H_2O_2 influx (v_{influx}).

$$v_{influx} = k_p \cdot iH_2O_2 \qquad \textbf{Equation 5.53}$$

$$v_{Prx2} = k_{PrxRed} \cdot iH_2O_2 \cdot Prx_{Red} \qquad \textbf{Equation 5.54}$$

Thus, under these oxidative loads $v_{Prx2} = v_{influx}$. Model 5.5 (Section 5.5.1) becomes

$$\frac{d\ Prx_{Red}}{dt} = k_{PSSP} \cdot PSSP \cdot Trx_{Red} - k_p \cdot eH_2O_2$$

$$\frac{d\ PSOH}{dt} = k_p \cdot eH_2O_2 - k_{PSOH} \cdot PSOH$$

$$\frac{d\ Trx_{Ox}}{dt} = k_{PSSP} \cdot PSSP \cdot Trx_{Red} - k_{TrxR} \cdot Trx_{Ox}$$

Model 5.6

$$Prxtot = Prx_{Red} + PSOH + PSSP$$

$$Trxtot = Trx_{Red} + Trx_{Ox}$$

Further, in order to simplify the expressions obtained, we considered $v_{influx} \ll v_{max}^{TrxR}$ where v_{max}^{TrxR} is the maximal rate of Trx reduction by TrxR (= $k_{TrxR} \times Trxtot$). This assumption verifies in erythrocytes facing low sustained oxidative loads that allow Trx to remain mostly reduced, i.e. $<2\times10^{-8}$ M eH_2O_2 or $<3\times10^{-12}$ M iH_2O_2 as per our estimates in Section 5.3.5.3. After taking these considerations in mind, we computed the steady state concentrations of each redox form of Prx2:

$$Prx_{Red} = Prxtot - k_p \cdot eH_2O_2 \left(\frac{1}{k_{PSOH}} + \frac{1}{k_{PSSP} \cdot Trxtot}\right)$$ **Equation 5.55**

$$PSOH = \frac{k_p \cdot eH_2O_2}{k_{PSOH}}$$ **Equation 5.56**

$$PSSP = \frac{k_p \cdot eH_2O_2}{k_{PSSP} \cdot Trxtot}$$ **Equation 5.57**

From the equations above we see that the accumulation of the various Prx2 forms depend on the eH_2O_2 which the erythrocyte is subjected to. Most of the Prx2 contents are in Prx_{Red} (Equation 5.55) given that eH_2O_2 is very low. *PSOH* and *PSSP* are directly proportional to v_{influx}, whereas Prx_{Red} decreases with v_{influx}.

The equations above also show that the accumulation of Prx_{Red} and *PSSP* depend on the balance between v_{influx} and the pseudo-first order rate constant for Prx2 reduction (=$k_{PSSP} \times Trxtot$ given that Trx is in reduced form under these oxidative loads). Decreasing *Trxtot* leads to the accumulation of *PSSP* and decreases the concentration of Prx_{Red}.

On the other hand, at high eH_2O_2 the redox status of Prx2 is differently affected by parameters of the system. Under these loads the reduction of Prx2 is limited by the rate at which TrxR is reducing Trx, thus occurring at a rate equal to the maximum rate of TrxR activity ($v_{\max}^{TrxR}$ = $k_{TrxR} \times Trxtot$). In addition, catalase and GPx1 have a much larger contribution that Prx2 for iH_2O_2

consumption. Therefore, iH_2O_2 depends on v_{influx} and on the rate of iH_2O_2 consumption by the three antioxidants. Model 5.5 (Section 5.5.1) then becomes

$$\frac{d\ iH_2O_2}{dt} = k_p \cdot eH_2O_2 - iH_2O_2 \cdot (k_{PrxRed} \cdot Prx_{Red} + k_{catalase} + k_{GPx1})$$
$$\frac{d\ Prx_{Red}}{dt} = k_{TrxR} \cdot Trxtot - k_{PrxRed} \cdot Prx_{Red} \cdot iH_2O_2$$
$$\frac{d\ PSOH}{dt} = k_{PrxRed} \cdot Prx_{Red} \cdot iH_2O_2 - k_{PSOH} \cdot PSOH$$
$$Prxtot = Prx_{Red} + PSOH + PSSP$$

Model 5.7

When the oxidative load surpasses the capacity of the TrxR/Trx to cope with the demand for Trx_{Red} (i.e. for eH_2O_2 » 2×10^{-8} M or iH_2O_2 » 3×10^{-12} M as per estimates in Section 5.3) $v_{influx} \gg v_{\max}^{TrxR}$. Under these conditions, after taking Model 5.7 into consideration, the steady state concentrations of each Prx2 form are given by

$$Prx_{Red} = \frac{k_{catalase} + k_{GPx1}}{k_{PrxRed}} \cdot \frac{k_{TrxR} \cdot Trxtot}{k_p \cdot eH_2O_2} \qquad \textbf{Equation 5.58}$$

$$PSOH = \frac{k_{TrxR} \cdot Trxtot}{k_{PSOH}} \qquad \textbf{Equation 5.59}$$

$$PSSP = Prxtot - k_{TrxR} \cdot Trxtot \cdot \left(\frac{1}{k_{PSOH}} + \frac{k_{catalase} + k_{GPx1}}{k_{PrxRed} \cdot k_p \cdot eH_2O_2} \right) \qquad \textbf{Equation 5.60}$$

Again, these equations show that a balance between v_{influx} and the rate of Trx reduction affects the concentration of each Prx2 form under high eH_2O_2. Whereas *PSSP* increases with v_{influx}, the concentration of Prx_{Red} decreases with v_{influx}. The accumulation of *PSSP* decreases with catalase and/or GPx1 activity, leading to a higher Prx_{Red}. Additionally, $v_{\max}^{TrxR}$ (=$k_{TrxR}\times Trxtot$) greatly affects the concentration of each Prx2 form. Increasing $v_{\max}^{TrxR}$ increases Prx_{Red} and *PSOH*, and decreases *PSSP*.

Altogether, these results show that the parameters of the system affect the redox status of Prx2 differently at low and high oxidative loads. Under low oxidative loads we found that: 1. *PSSP* and *PSOH* are directly proportional to v_{influx}, and Prx_{Red} decreases with v_{influx}; 2. Prx_{Red} increases with *Trxtot,* decreasing the fraction of Prx2 in PSSP form*;* 3. *PSOH* is only affected by v_{influx} and k_{PSOH}. On the other hand, at high eH_2O_2 we have 1. a higher catalase and/or GPx1 activity allows

lower accumulation of *PSSP* and larger Prx_{Red} concentrations; 2. *PSOH* is no longer dependent on v_{influx} but now depends on $v_{\max}^{TrxR}$.

These analyses again show that the redox status of Prx2 depends on the balance between the oxidative load and on the ability of the Trx/TrxR cycle to reduce Prx2. As suggested in this section, this balance also affects the point at which the crossover occurs. In the next section we analyze what variables and parameters determine the eH_2O_2 at which the crossover occurs.

5.6. What determines the eH_2O_2 at which the crossover occurs?

For better framing how we obtain an analytical expression for the crossover between Prx2 oxidation regimes let us first consider how PSOH accumulates with increasing oxidative loads. Using Model 5.5 and parameters from Table 5.10 (both from Section 5.5.1), we plotted the steady state value of *PSOH* by considering various eH_2O_2:

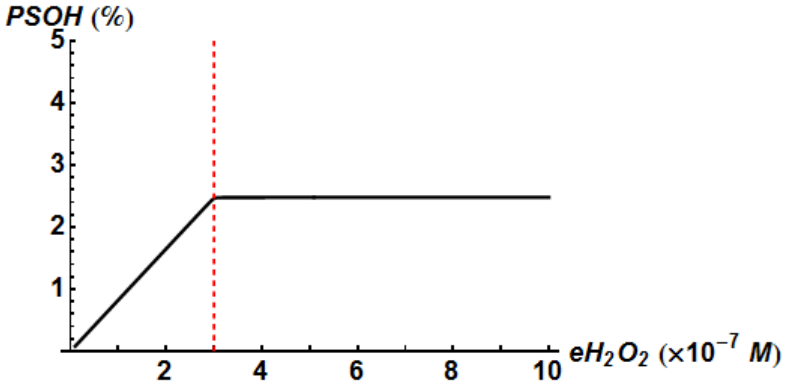

Figure 5.17 – Steady state concentration of *PSOH* under various oxidative loads. Estimated by considering Model 5.5 and parameters from Table 5.10, both found in Section 5.5.1. The dashed line marks $eH_2O_2 = 3\times10^{-7}$ M.

The figure above illustrates that at the low oxidative loads regime *PSOH* increases with increasing eH_2O_2, as evident from Equation 5.56 (Section 5.5.2). In turn, at the high oxidative regime *PSOH* does not change with eH_2O_2, as expressed by Equation 5.59. The crossover between these two regimes is defined as the eH_2O_2 where the regimes merge together, which can be found by equating Equation 5.56 to Equation 5.59:

$$\frac{k_p \cdot eH_2O_2}{k_{PSOH}} = \frac{k_{TrxR} \cdot Trxtot}{k_{PSOH}} \qquad \textbf{Equation 5.61}$$

$$\Leftrightarrow eH_2O_2 = \frac{k_{TrxR} \cdot Trxtot}{k_p} \qquad \textbf{Equation 5.62}$$

Taking into consideration the parameters from Table 5.10 (Section 5.5.1) we get $eH_2O_2 \approx 3\times10^{-7}$ M, the oxidative load that marked the crossover in Figure 5.16 (Section 5.5.1) and Figure 5.17.

As Equation 5.62 shows, the eH_2O_2 at which the crossover occurs depends on the rate of Trx reduction. TrxR reduces Trx at a maximum rate of $k_{TrxR}\times Trxtot$. If the activity of this enzyme is increased, so will the eH_2O_2 at which the crossover occurs: larger TrxR or Trx concentrations allow a higher rate of Trx reduction, shifting the crossover to higher oxidative loads.

In the analyses above we assumed that NADPH supply does not limit TrxR activity. However, we may still draw some conclusions about how *NADPH* availability affects the eH_2O_2 at which the crossover occurs. A low NADPH/$NADP^+$ is associated with oxidative stress (Gaetani et al., 1974). Therefore, NADPH availability TrxR activity at high eH_2O_2, shifting the crossover to lower eH_2O_2.

Equation 5.62 also allows us to address how eH_2O_2 affects the separation of the two oxidative regimes: a low oxidative regime where Prx2 consumes practically all of the iH_2O_2; and a high oxidative regime where catalase becomes the main scavenger of iH_2O_2. In Figure 5.18 we plotted the relative contributions of Prx2, catalase and GPx1 for H_2O_2 scavenging under various eH_2O_2. This was obtained by computing the rates of H_2O_2 consumption by Prx2, catalase and GPx1 through Model 5.5 (Section 5.5.1) and considering parameters from Table 5.10 (Section 5.5.1).

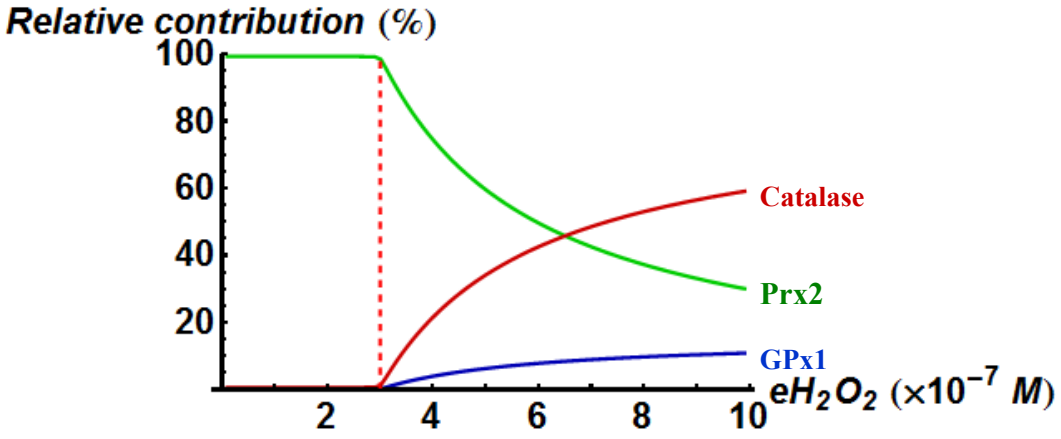

Figure 5.18 –Relative contribution of Prx2 (green), catalase (red), and GPx1 (blue) for iH_2O_2 consumption under steady state conditions. Obtained through Model 5.5 (Section 5.5.1), considering parameters from Table 5.10 (Section 5.5.1). The dashed line corresponds to $eH_2O_2 = 3\times10^{-7}$ M.

Figure 5.18 shows that *post-crossover* eH_2O_2 affect the contribution of Prx2 for H_2O_2 consumption. As we showed in Section 5.5.1, the contribution of Prx2 for H_2O_2 consumption is affected at high eH_2O_2 due to the accumulation of *PSSP*. When PSSP accumulates catalase becomes the main scavenger of H_2O_2.

Overall, these results show that a balance between *Trxtot* and eH_2O_2 must occur for Prx2 to remain mostly reduced. Under *pre-crossover* eH_2O_2, Prx2 remains the main H_2O_2 scavenger because the Trx/TrxR cycle maintains Prx2 mostly reduced. When the crossover occurs, Prx2's contribution for H_2O_2 consumption is affected. A higher *Trxtot* shifts the crossover to higher eH_2O_2 (Equation 5.62), allowing Prx2 to remain the main scavenger for higher eH_2O_2. Under *post-crossover* loads catalase becomes the main H_2O_2 scavenger.

5.7. Is the sulfinylation of Prx2 physiologically relevant?

Prx2 is inactivated through sulfinylation of its peroxidatic cysteines. In this process PSOH is oxidized by H_2O_2. If very prevalent, the inactivation of Prx2 may influence the antioxidant activity of Prx2.

In this Section we studied the sulfinylation of Prx2 because 1. it consumes H_2O_2, thus contributing for antioxidant protection; 2. it inactivates Prx2, leading to a state in which this protein cannot scavenge H_2O_2.

In order to understand if sulfinylation of Prx2 may potentially compete with the formation of PSSP for PSOH we need the value of the rate constant for the sulfinylation of Prx2 (k_{PSO2H}). The pseudo-first order rate constant for the sulfinylation of Prx2 ($=k_{PSO2H}\times iH_2O_2$) may then be compared with k_{PSOH}. We now explain the considerations we made in order to analyze the kinetics of inactivation of Prx2.

The experiments of (Manta et al., 2009) were previously used to determine k_{PSOH} (Section 5.2.1.10). We used these again to estimate k_{PSO2H}. As discussed in Section 5.2.1.10, the majority of Trx is in reduced form in the conditions considered by the authors. In the same section we also showed that the rate of Prx_{Red} oxidation is extremely fast. The limiting step in those conditions is the formation of PSOH. Because we want to estimate the rate constant for the sulfinylation of Prx2 we used the data from the plot in which the authors initially had considered H_2O_2=*2 mM*

(Figure 5.9, Section 5.2.1.10). This plot shows a slower NADPH oxidation towards the end of the experiment, indicative of sulfinylation of Prx2. Yet, this slowing down is not very pronounced, meaning that Trx is still mostly reduced. With this in mind we used the reaction scheme in Figure 5.19 and corresponding Model 5.8 for analyzing this experiment.

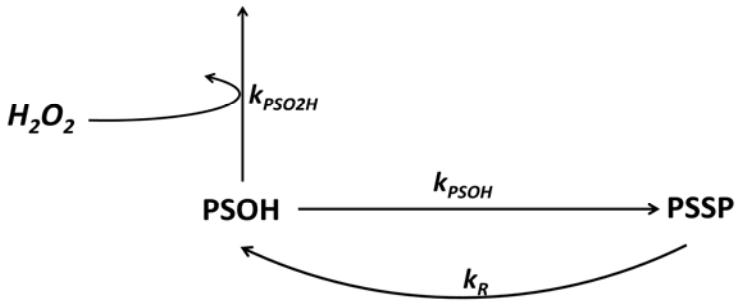

Figure 5.19 – Reaction scheme used to estimate k_{PSO2H} from the data of (Manta et al., 2009), using Model 5.8.

$$\frac{d\ PSOH}{dt} = k_R \cdot PSSP - PSOH \cdot (k_{PSOH} + H_2O_2 \cdot k_{PSO2H})$$

$$\frac{d\ PSSP}{dt} = PSOH \cdot k_{PSOH} - k_R \cdot PSSP$$ **Model 5.8**

with initial values:

$PSSP[0] = PSSP0$ and $PSOH[0] = PSOH0$

The parameters of this system of equations are the following:

Table 5.11 – Parameters and initial values considered to estimate k_{PSO2H} from the experiments of (Manta et al., 2009)

Parameter	Value	Meaning/Reference
k_R	$= k_{PSSP} \times Trx_{Ox} \approx 1.7\ s^{-1}$	Rate constant for Prx2 reduction. With $k_{PSSP}=2.1\times10^5\ M^{-1}\ s^{-1}$ (Table 5.6) and Trx_{Ox} = Trxtot = 8×10^{-6} M [experimental conditions of (Manta et al., 2009)].
k_{PSOH}	$0.26\ s^{-1}$	Estimated in Section 5.2.1.10.
PSOH0	43×10^{-8} M	Estimated in Section 5.2.1.10.
PSSP0	66×10^{-9} M	Estimated in Section 5.2.1.10.
H_2O_2	200×10^{-6} M	Experimental conditions of (Manta et al., 2009).

We wanted to find a function that would follow the NADPH oxidation profile found in the experiment (Figure 5.9), with k_{PSO2H} as the only free parameter of the fitting. As we saw in Section 5.2.1.10, the system is at a quasi-steady state and the rate of NADPH oxidation is approximately equal to the rate of PSSP reduction (Equation 5.64):

$$v_{PSSP} = k_{PSSP} \cdot Trx_{Red} \cdot PSSP$$ **Equation 5.63**

$$\Leftrightarrow v_{PSSP} \approx k_{PSSP} \cdot Trxtot \cdot PSSP \qquad \textbf{Equation 5.64}$$

To find the expression of *PSSP[t]*, we integrated Model 5.8. The expression found was then replaced into Equation 5.64, and this equation was then integrated from $t=0$ to $t=\tau$ giving *NADPH[t],* the function that defines the time course of NADPH oxidation. The value of *NADPH* when $t=\tau$ is the result of the difference between the initial amount of NADPH (*NADPH0*= 200×10^{-6} M) and *NADPH[t]*. The values of all parameters in the obtained expression were available with exception to k_{PSO2H}. We then sought to find the value of k_{PSO2H} that would lead to the best fit of this expression to the experimental time points in the plot with the lower H_2O_2 of Figure 5.9 (Section 5.2.1.10). Similarly to what was done in Section 5.2.1.10, the time points were converted from absorbance units to NADPH concentration by considering Equation 5.38 (Section 5.2.1.10). Figure 5.20 represents our fitting to the experimental data.

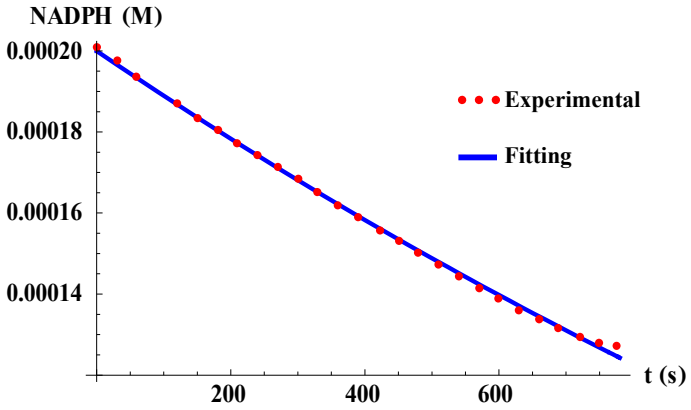

Figure 5.20 – NADPH concentration (M) as determined by (Manta et al., 2009) – dots – and fitting of *NADPH[t]* determined above (see text) – line. k_{PSO2H}=0.23 $M^{-1}s^{-1}$, H_2O_2 = 200×10^{-6} M and parameters from Table 5.11.

The value which led to the best fit ($R^2\approx0.98$) was approximately k_{PSO2H}=0.23 $M^{-1}s^{-1}$. With this rate constant, our fitting correctly followed the kinetics of NADPH reduction by TrxR in the conditions of the experiment. However, using the same parameters for higher oxidative loads (H_2O_2 = 10^{-2} M) gives a poorer fitting:

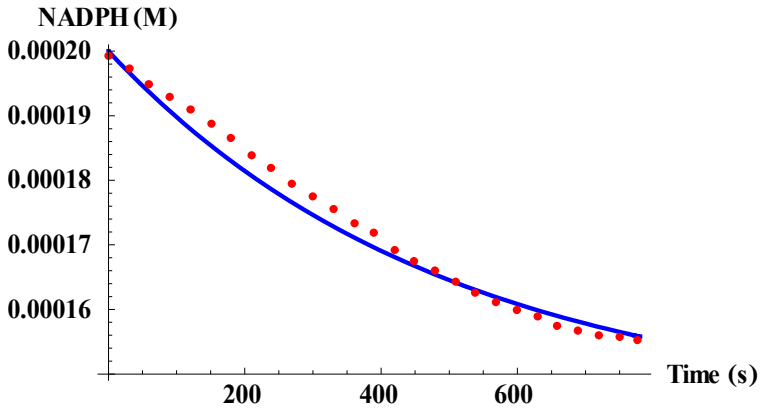

Figure 5.21 – NADPH concentration (M) as determined by (Manta et al., 2009) – dots – and our fitting – line - considering k_{PSO2H}=0.23 $M^{-1}s^{-1}$, H_2O_2 = 10^{-2} M and parameters from Table 5.11.

Despite having a poorer fitting for higher oxidative loads, the lack of data related with the sulfinylation of Prx2 led us to use the estimated k_{PSO2H} value.

For the sulfinylation of Prx2 to compete with the formation of PSSP, the pseudo-first order rate constant for the sulfinylation of Prx2 must be similar to the first order rate constant for the formation of PSSP:

$$k_{PSO2H} \cdot iH_2O_2 \approx k_{PSOH} \qquad \textbf{Equation 5.65}$$

Replacing the equation above with k_{PSO2H}=0.23 $M^{-1}s^{-1}$ and k_{PSOH}=*0.26* s^{-1} (Section 5.2.1.10) gives iH_2O_2≈1.1 M, an implausibly high value which does not occur *in vivo*. With this estimate in mind we may consider that the rate of sulfinylation of Prx2 is negligible compared to the rate of PSSP formation.

(Low et al., 2007) observed that Prx2 is not detectably sulfinylated in human erythrocytes even when exposed to higher eH_2O_2 boluses. Although using the estimated k_{PSO2H} does not allow an exact fitting of the experimental data of (Manta et al., 2009) in all iH_2O_2 considered, the estimated rate constant is consistent with the observations of (Low et al., 2007).

According to the observations of (Low et al., 2007) and to our estimate of k_{PSO2H}, the sulfinylation of Prx2 seems to have a negligible effect on the capacity of this protein to reduce hydrogen peroxide in the human erythrocyte.

5.8. Is Prx2 essential for plasma H_2O_2 scavenging by erythrocytes?

Could the accumulation of PSSP affect the ability of the erythrocyte to scavenge plasma H_2O_2? Is the activity of Prx2 as an iH_2O_2 scavenger essential for erythrocytes to keep consuming plasma H_2O_2?

In order to address this question we considered the reaction scheme represented in Figure 5.22.

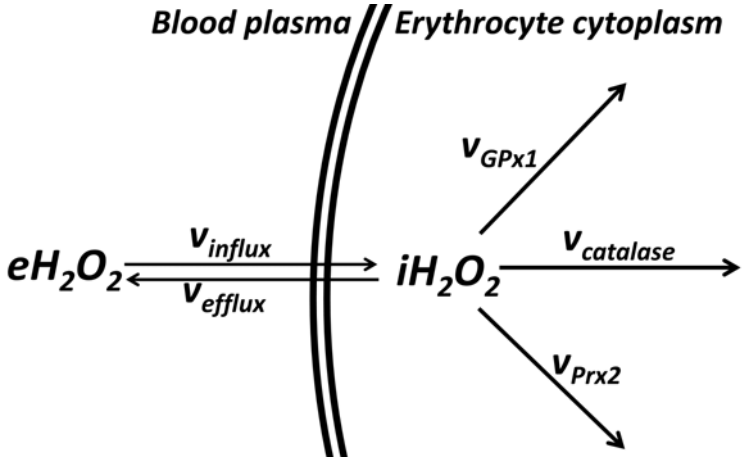

Figure 5.22– Reaction scheme for the analysis of plasma H_2O_2 consumption by erythrocytes and iH_2O_2 consumption by GPx1, catalase and Prx2.

The formation and consumption of iH_2O_2 may be expressed through Equation 5.66

$$\frac{d\ iH_2O_2}{dt} = v_{influx} - (v_{GPx1} + v_{catalase} + v_{Prx2} + v_{efflux}) \qquad \textbf{Equation 5.66}$$

Where the rate of H_2O_2 influx (v_{influx}) and the rates of iH_2O_2 consumption by each process are expressed as

$$v_{influx} = k_p \cdot eH_2O_2 \qquad \textbf{Equation 5.67}$$

$$v_{GPx1} = k_{GPx1} \cdot iH_2O_2 \qquad \textbf{Equation 5.68}$$

$$v_{catalase} = k_{catalase} \cdot iH_2O_2 \qquad \textbf{Equation 5.69}$$

$$v_{efflux} = k_{efflux} \cdot iH_2O_2, \qquad \textbf{Equation 5.70}$$

And the total rate of iH_2O_2 consumption is given by

$$v_{consumption} = v_{GPx1} + v_{catalase} + v_{Prx2} + v_{efflux} \quad \textbf{Equation 5.71}$$

In Section 5.3 we found that an eH_2O_2 «10^{-7} M (or $iH_2O_2 < 10^{-11}$ M) allows most of the Prx2 contents to remain reduced. If an erythrocyte is facing an oxidative load much higher than this value, most of the Prx2 is converted to PSSP form and Prx2 has a negligible contribution for H_2O_2 consumption. Under these conditions Equation 5.71 becomes

$$v_{consumption} = iH_2O_2 \cdot (k_{GPx1} + k_{catalase} + k_{efflux}) \quad \textbf{Equation 5.72}$$

Considering Equation 5.72, we computed the steady state iH_2O_2 after solving Equation 5.66 in order to iH_2O_2. This gives

$$iH_2O_2 = \frac{k_p \cdot eH_2O_2}{k_{catalase} + k_{GPx1} + k_{efflux}} \quad \textbf{Equation 5.73}$$

What is the relative contribution of each process for H_2O_2 consumption in erythrocytes facing very high oxidative loads? We estimated their relative rate of iH_2O_2 consumption by computing the ratio between its rate of iH_2O_2 consumption (Equation 5.68 to Equation 5.70) and the total rate of iH_2O_2 consumption (Equation 5.71). Values in Table 5.12 were considered for these estimates.

Table 5.12 – Parameters used for comparison of rates of iH_2O_2 consumption by catalase and Prx2, at high eH_2O_2.

Parameter	Value	Meaning/Reference
k_p	8 s^{-1}	First-order rate constant for hydrogen peroxide consumption by erythrocytes (estimated in Section 5.2.1.2)
$k_{catalase}$	218 s^{-1}	Pseudo-first-order rate constant for H_2O_2 consumption by catalase (Section 5.1.1.2)
k_{GPx1}	40 s^{-1}	Pseudo-first-order rate constant for H_2O_2 consumption by GPx1 (Section 5.1.1.1)
k_{efflux}	12 s^{-1}	Pseudo-first order rate constant for H_2O_2 efflux (Estimated in Section 5.2.1.4)

Considering 10^{-5} M eH_2O_2 (which corresponds ≈ 2×10^{-7} iH_2O_2), we find that catalase consumes practically all of the iH_2O_2 (Figure 5.23).

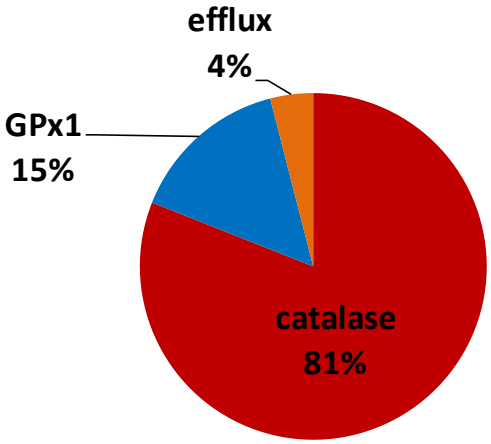

Figure 5.23 – Relative iH_2O_2 consumption by catalase, GPx1 and membrane efflux of H_2O_2 for an $eH_2O_2 = 10^{-5}$ M. See the text below for details on the estimates.

The figure above shows that catalase consumes about 80% of the iH_2O_2, followed by GPx1. The efflux of H_2O_2 has a negligible contribution for the consumption of H_2O_2, because $k_{efflux} \ll k_{catalase}+k_{GPx1}$.

Bear in mind that by considering the reaction scheme represented in Figure 5.22 we are assuming that H_2O_2 consumption by catalase and GPx1 are first-order reactions with respect to iH_2O_2. This may be different under high oxidative loads, when poor NADPH availability limits GPx1 activity or leads to accumulation of inactive catalase (as discussed in Sections 5.2.1.1 and 5.2.1.2). Under these conditions the relative contribution of catalase and GPx1 for iH_2O_2 consumption would be lower than shown in Figure 5.23. However, catalase likely exhibits pseudo-first order kinetics with respect to iH_2O_2: as discussed in Section 5.2.1.1, catalase-associated NADPH oxidation occurs at rates much slower than the rate of H_2O_2 consumption by catalase.

Could plasma H_2O_2 scavenging by erythrocytes be impaired when Prx2's contribution for iH_2O_2 consumption is affected? To answer this question we will consider the situation where a limited NADPH supply limits Prx2's and GPx1's contribution for H_2O_2 scavenging. Under these conditions, only catalase and H_2O_2 efflux consume iH_2O_2. The rate of H_2O_2 consumption Equation 5.72 then becomes

$$v_{consumption} = iH_2O_2 \cdot (k_{catalase} + k_{efflux}) \qquad \textbf{Equation 5.74}$$

For the erythrocyte's plasma H_2O_2 consumption to be affected, the rates of H_2O_2 influx (Equation 5.67) and efflux (Equation 5.70) equal each other. This would occur if a limited NADPH supply lead to accumulation of inactive catalase, giving $k_{catalase} \ll k_{efflux}$.

It is very unlikely that catalase inactivation allows $k_{catalase} \ll k_{efflux}$, as we now show. To attain $k_{catalase}$ = 1.2 s^{-1}, a rate constant ten-fold smaller than k_{efflux} (Table 5.12), the concentration of catalase would have to be $\approx 7.5\times10^{-8}$ M (with $k_{CompoundI} = 1.6\times10^{7}$ $M^{-1}s^{-1}$ as per Table 5.3, Section 5.2.1.1). This corresponds to ≈98% of inactive catalase if we consider 3.4×10^{-6} M catalase [as determined by (Hartz et al., 1973) in the human erythrocyte]. However, such an extensive catalase inactivation is not likely to occur as suggested by the *in vitro* experiments of (Kirkman et al., 1999) with bovine catalase. The authors observed that even in the absence of NADPH, >65% of the total catalase contents (=3×10^{-6} M catalase) were in Ferricatalase or Compound I forms even after one hour of incubation with a system generating $\approx 2.5\times10^{-7}$ M H_2O_2/s. Although a substantial (<35%) of the catalase contents had been inactivated, this evidence suggests that catalase inactivation occurs very slowly, even under high oxidative loads and no added NADPH. In the human erythrocyte, this slow rate of catalase inactivation would allow most of the catalase to remain active. Also, even if NADPH production by PPP is slow, it may still large enough to prevent inactivation of catalase under strong oxidative loads, thus maintaining $k_{catalase} \gg k_{efflux}$.

If catalase remains mostly active, its activity is limited by the rate of H_2O_2 influx. Under these conditions, H_2O_2 consumption by catalase surpasses the rate of H_2O_2 efflux. Thus, erythrocytes remain plasma H_2O_2 sinks even when Prx2's (and GPx1's) contribution for H_2O_2 consumption is limited.

Another possibility for Prx2 to affect plasma H_2O_2 scavenging by erythrocytes would be if Prx2 oxidation would affect H_2O_2 permeation. There is few evidence of membrane association of Prx2 [<3 % of *Prxtot* (Moore et al., 1991; Rocha et al., 2009)], but we found no reports of effects of Prx2 on the permeability of cellular membranes to H_2O_2. Possibly, the membrane association of Prx2 is related with the relevance of Prx2 for acting as an activator of the Gardos channel, a potassium channel (Moore et al., 1991; Moore et al., 1990).

Altogether these results show that Prx2 does not affect plasma H_2O_2 consumption by erythrocytes. This process is limited by membrane permeability even when Prx2 is completely oxidized.

5.9. Could Prx2 be replaced by catalase or GPx1?

Could erythrocytes rely only on catalase and GPx1 for their protection against H_2O_2? What would have to be the increase in concentration of each of these defenses if they were to replace the antioxidant activity of Prx2? And would it be possible to replace catalase or GPx1 by Prx2? In this section we analyze these questions and show why the erythrocyte needs Prx2 in spite of its high demand for reducing equivalents in comparison to catalase.

To do so we have considered the reactions represented in Figure 5.24. In it we have iH_2O_2 being consumed by GPx1, catalase and Prx2 (Figure 5.24, left) and being formed at rate φ. If Prx2 was not present the only H_2O_2 defenses would be GPx1 and catalase (Figure 5.24, right).

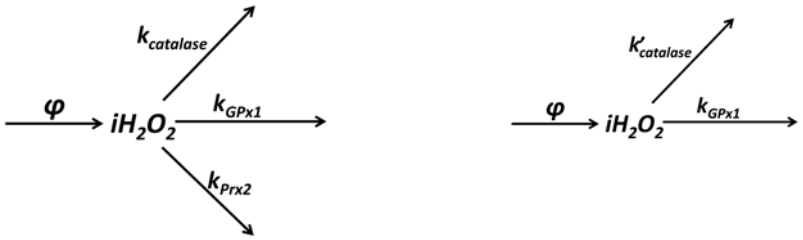

Figure 5.24 – Reactions producing and consuming iH_2O_2 in the normal erythrocyte (left) or in erythrocytes in which Prx2 is not present (right). k - pseudo-first order rate constants of consumption of iH_2O_2 by the three antioxidants. k' – pseudo-first order rate constant for iH_2O_2 consumption by catalase in order to compensate for the absence of Prx2.

If catalase or GPx1 were to compensate for the absence of Prx2 what would have to be the increase in the concentration of each defense in order to maintain the same iH_2O_2 and response time as normal cells? We now analyze this issue by considering that the concentration of antioxidant i would have to increase by a factor of ε_i to compensate for the absence of another antioxidant.

Hemoglobin is the most abundant protein in the human erythrocyte. Because erythrocytes use this protein to carry out their main role in the body (transport of oxygen and carbon dioxide) we compared the concentrations of antioxidant proteins with that of hemoglobin. With this in mind we considered the data in Table 5.13 in order to do the following analyses.

Table 5.13 –Pseudo-first order rate constants, molecular weight and concentrations of Prx2, catalase, GPx1 and Hemoglobin. All values are per erythrocyte except where stated otherwise.

Protein	Parameter	Value	Source
Prx2	k_{Prx2} (s^{-1})	37 000	Estimated in Section 5.1.1.3
	MW_{Prx2} (Da)	22 000	Per monomer (Moore and Shriver, 1994; Schroder et al., 2000)
	Concentration (M)	3.7×10^{-4}	Estimated in Section5.2.1.5
Catalase	$k_{catalase}$ (s^{-1})	218	Estimated in Section 5.1.1.2
	$MW_{catalase}$ (Da)	64 000	Per monomer (Bonaventura et al., 1972)
	Concentration (M)	3.4×10^{-6}	(Hartz et al., 1973), with an heme occupancy of 0.4
GPx1	k_{GPx1} (s^{-1})	40	Estimated in Section 5.1.1.1
	MW_{GPx1} (Da)	23 000	Per monomer (Awasthi et al., 1975)
	Concentration (M)	9.7×10^{-7}	Estimated in Section 5.1.1.1
Hemoglobin	Concentration (g/l packed cells)	340	(Beutler, 1984)
	Concentration (g/l erythrocyte water)	486	Estimated from the concentration determined by (Beutler, 1984) and 0.7 L erythrocyte water/L erythrocytes (Savitz et al., 1964)
	Molecular weight (Da)	64 450	Tetramer weight (Guidotti, 1967)
	Total mass (g)	34×10^{-12}	Estimated using 486 g Hemoglobin/L erythrocyte water and $V_{ew} = 7\times10^{-14}$ L (Table 5.6, Section 5.2.1.9)

At steady state, the rates of production and consumption of iH_2O_2 are equal. Considering Figure 5.24 left gives

$$iH_2O_2 \cdot \left(k_{GPx1} + k_{catalase} + k_{Prx2}\right) = \varphi \qquad \textbf{Equation 5.75}$$

$$\Leftrightarrow iH_2O_2 = \frac{\varphi}{k_{GPx1} + k_{catalase} + k_{Prx2}} \qquad \textbf{Equation 5.76}$$

If Prx2 was not present we would obtain from Equation 5.75:

$$iH_2O_2 = \frac{\varphi}{k'_{GPx1} + k'_{catalase}} \qquad \textbf{Equation 5.77}$$

Where $k_i^{'}$ represents the pseudo-first order rate constant for iH_2O_2 consumption by antioxidant i if one of the antioxidants is not present.

In order for iH_2O_2 to have the same value with and without Prx2, Equation 5.76 must equal Equation 5.77, giving

$$k_{GPx1} + k_{catalase} + k_{Prx2} = k'_{GPx1} + k'_{catalase}$$ **Equation 5.78**

First we want to assess what would have to be the increase in catalase activity. With this in mind consider $k_{GPx1} = k'_{GPx1}$, and $k'_{catalase}$ ($= \varepsilon_{catalase} \cdot k_{catalase}$) as the rate constant for catalase activity adapted to compensate for the absence of Prx2. $\varepsilon_{catalase}$ represents the increase in catalase concentration required to make catalase to compensate for the absence of Prx2. Taking these values into consideration we get from Equation 5.78 that

$$k'_{catalase} = k_{catalase} + k_{Prx2}$$

$$\Leftrightarrow \varepsilon_{catalase} = \frac{k_{catalase} + k_{Prx2}}{k_{catalase}}$$ **Equation 5.79**

Using the values from Table 5.13 we obtain $\varepsilon_{catalase} \approx 171$. Thus the catalase concentration would have to increase to ≈6×10^{-4} M [considering the catalase concentration in normal erythrocytes as 3.4×10^{-6} M (Hartz et al., 1973)]. Such a concentration would totalize ≈11×10^{-12} g catalase (considering the molecular mass of tetrameric catalase = 2.56×10^{5} g/mol, Table 5.13; and V_{ew} = 7×10^{-14} L/cell, Table 5.6, Section 5.2.1.9), which represents ≈32 % of the hemoglobin contents in the erythrocyte (considering 34×10^{-12} g of hemoglobin in the cell, as estimated in Table 5.13).

Using a similar reasoning we determined ε_i for GPx1. This was also done by considering that catalase or GPx1 could also be absent (Table 5.14). A 926 fold increase in GPx1 is required to compensate Prx2 absence, corresponding to ≈6×10^{-12} g GPx1 if we consider the values in Table 5.13 for tetrameric GPx1.

Table 5.14 – Fold increase (ε_i) in the concentration of protein *i* and % of Hemoglobin concentration after such increase, required to maintain the same iH_2O_2 concentration as in normal erythrocytes.

	Normal erythrocytes	Prx2 absent		Catalase absent		GPx1 absent	
	% Hemoglobin	ε_i	% Hemoglobin	ε_i	% Hemoglobin	ε_i	% Hemoglobin
Prx2	1.7	–	–	1.006	1.7	1.001	1.7
Catalase	0.18	171	32	–	–	1.2	0.21
GPx1	0.02	926	18	6.5	0.12	–	–

The table above shows that much higher $\varepsilon_{catalase}$ and ε_{GPx1} would be required to compensate for the absence of Prx2, than ε_{Prx2} if any of the two other defenses were absent. Having such increase in the concentrations of catalase or GPx1 could impair the main role of the erythrocyte in performing gaseous exchanges. A big part of the hemoglobin contents would have to be replaced by these enzymes, thus reducing the ability of the cell to transport oxygen or carbon dioxide. The erythrocyte could also increase in size in order to have a larger amount of these antioxidants. But this could also reduce its mobility within capillaries, whose diameter is approximately that of an erythrocyte.

Although only very small increases in Prx2 concentration would be required to compensate the absence of catalase or GPx1, such increase could alter the behavior of the Prx2/Trx cycles when erythrocytes face oxidative stress. Increasing Prx2 concentration may lead to a higher rate of NADPH oxidation by TrxR. However, the rate of NADPH oxidation would only increase 1.006-fold at most, considering the values presented in Table 5.14. Also, there would only be a larger rate of NADPH oxidation if the concentration of Trx is not limiting the TrxR-mediated consumption of NADPH.

But why is there such a difference in the values of ε_i of the three proteins? We reason that this is due to the specific activity of each antioxidant. This may be computed by the ratio in Equation 5.80:

$$\text{specific activity} = \frac{k_i}{MW_i} \qquad \textbf{Equation 5.80}$$

In which k_i and MW_i are respectively the pseudo-first order rate constant and molecular weight of protein i. Considering the values in Table 5.13 we obtain the following specific activities.

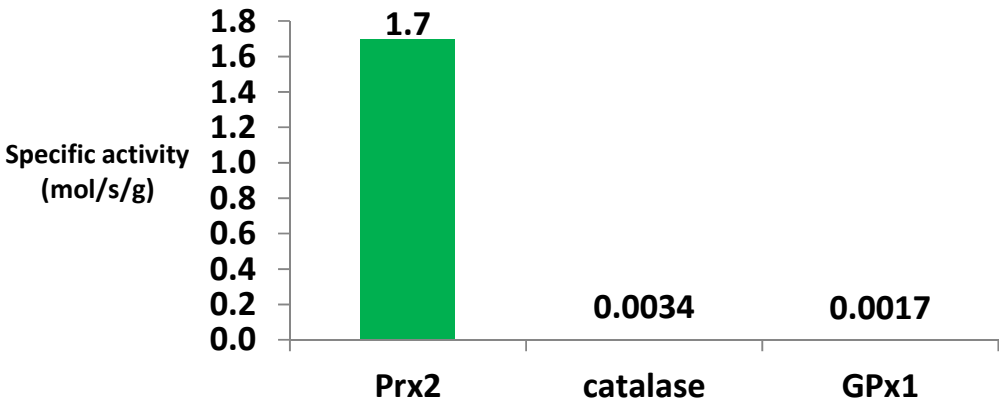

Figure 5.25 – Specific activities of Prx2, GPx1 and catalase in human erythrocytes. Estimated through Equation 5.80 and Table 5.13.

The figure above shows that Prx2 has a much higher specific activity than GPx1 or catalase, which explains why a much larger amount of catalase or GPx1 would be needed to replace Prx2 than the amount of Prx2 needed to replace catalase or GPx1.

Due to the higher specific activity of Prx2 cells can achieve a suitably low iH_2O_2 with much less protein than would be necessary should it have to rely solely on catalase or GPx1. By using Prx2, the cell therefore saves on the biosynthetic costs of defense against H_2O_2, and on the fraction of its cytoplasmic contents devoted to defense against H_2O_2.

These reasons would explain why the human erythrocyte needs Prx2 in spite of having catalase, a defense with much smaller requirement for reducing equivalents. However, the analyses in this section did not take into consideration what happens when Prx2 becomes oxidized, concomitantly affecting its antioxidant activity. Also, they do not explain why human erythrocytes have such a high amount of Prx2, nor why do these cells still need catalase or GPx1 if they have a defense with such a high specific activity. We will address the issues in the next sections of this work.

Results Part II

Analysis of defenses against H_2O_2 in erythrocytes crossing inflammation sites

Some situations such as systemic inflammation of the organism lead to sustained exposure of erythrocytes to H_2O_2, as we studied in the first part of the results. We showed that Prx2 is the main defense of the human erythrocyte against H_2O_2 provided that the oxidative load does not surpass the erythrocyte's capacity to reduce Prx2. However, under less severe pathological conditions and under physiological situations, erythrocytes are exposed to pulses of H_2O_2. In this part of the results we focus on what occurs under those circumstances.

During their flow across the vasculature, erythrocytes may face brief exposure to H_2O_2. These may occur by interaction with monocytes or atherosclerotic lesions for instance. The frequency and duration of the exposure to H_2O_2 depends on the location of the inflammation and type of interaction. For large vessels, the exposure to H_2O_2 from atherosclerotic lesions is likely to be very brief due to the large diameter and blood flow rate of the vessels. However, this may not be the case while erythrocytes cross smaller blood vessels. Most of the gaseous exchanges are done at the capillary level, the blood vessels that have the slowest blood flow rate and smallest diameter - practically of the diameter of an erythrocyte (Marieb and Hoehn, 2007). While crossing a capillary, erythrocytes are thus very prone to oxidation by nearby inflammation sites.

Could an erythrocyte be exposed to several inflammation foci in a time period shorter than the time scale of Prx2 reduction? If so, PSSP might accumulate over time, decreasing the contribution of Prx2 for the defense against H_2O_2. Below we investigate how these localized inflammation sites influence the antioxidant activity of Prx2. But before addressing these issues we will review the relevant physiological aspects of the human circulatory system. This will allow us to then analyze the properties of the Prx2/Trx cycles in physiological context.

5.10. Physiological aspects of human circulatory system and estimates for erythrocytes facing pulses of H_2O_2

5.10.1. Human blood contents and blood flow velocities

The average volume of human blood is about 5.5 dm^3 in a person weighing about 70 Kg (Widmaier et al., 2008). The volume and cellular contents of human blood vary greatly with the organism and physiology of the individual. In the analyses below we considered the average

cellular contents of human blood (Table 5.15), and hematocrit of 45% (Marieb and Hoehn, 2007).

Table 5.15 – Average volume occupied by different cell types in human blood. Adapted from (Widmaier et al., 2008). * Consider the erythrocyte volume of 10^{-13} dm^3 (Evans and Fung, 1972), meaning that human blood has about 2.25×10^{13} erythrocytes.

	Volume occupiedby each fraction (dm^3)
Erythrocytes	2.25*
Leukocytes and Platelets	0.05
Plasma	2.7

The human heart is responsible for pumping an average 5 dm^3 blood per minute in a resting individual. Yet, the blood flow is distributed between a very large number of blood vessels. In capillaries the blood flow is very slow [$\approx47\times10^{-5}$ m/s (Stucker et al., 1996)] which facilitates gaseous exchanges in these blood vessels. If we consider the average length of a capillary as 1 mm (Marieb and Hoehn, 2007) erythrocytes thus take about 2 seconds to cross a capillary. This value is in the range of the erythrocytes' residence time as determined by various studies. In lung capillaries, the transit time is <1 s (Roughton, 1964). In rat muscle, the capillary transit time is ≈4 s (Honig et al., 1977) while in hamster muscle it is ≈3 to 4 s (Sarelius, 1986). In our analyses below we will consider 2 s as the residence time of an erythrocyte in a capillary.

Because inflammation induces vasodilation the blood flow rate within a capillary is increased [this was first showed in rats through an imaging assay by (Shinkarenko, 1983)] and the residence time thus become shorter. Although we have not found values of the transit time in inflamed capillaries, a couple determinations done in inflamed venules may give us some insight onto the effects of inflammation on the capillary transit time. (Lindner et al., 2000) determined the blood flow rates in control (1906×10^{-6} m/s) and inflamed (1778×10^{-6} m/s) venules from mice. Later they again determined these blood flows in mice and found 2055×10^{-6} m/s in control conditions, as opposed to 2442×10^{-6} m/s found in inflamed venules (Lindner et al., 2001). These blood velocities correspond to ≈7 – 19% increase in the blood flow velocity in inflamed venules. If we consider a similar increase in blood flow in capillaries we obtain 50×10^{-5} to 56×10^{-5} m/s, after considering the blood flow 47×10^{-5} m/s (Stucker et al., 1996). Under these conditions, erythrocytes would take about 1.7 s to cross a 1 mm length capillary.

In the subsequent analyses we will consider that an erythrocyte may be exposed to H_2O_2 while crossing a capillary. We believe that this location, rather than other blood vessels, is where this cell is potentially more prone to suffer strong oxidative stress for the following two reasons. First, the average blood flow rate in arterioles [≈100 mm/s (Marieb and Hoehn, 2007)], venules [≈60 mm/s (Marieb and Hoehn, 2007)] and larger blood vessels is much higher than the one observed in capillaries. In those vessels blood flows across atherosclerotic lesions or other inflammatory focus much faster than in the case of capillaries. This makes the duration of exposure to H_2O_2 while crossing such foci practically negligible when compared to the exposure when crossing capillaries. Second, it is in the capillary that the closest contact between erythrocytes and the endothelium occurs. This makes erythrocytes more prone to interact with inflammation focus that may exist nearby the endothelium.

With this in mind, consider that an erythrocyte faces exposure to an extracellular source of H_2O_2 (from an inflammation focus) while it is crossing capillaries (≈2 s) in inflammation foci. In the next section we estimate the frequency with which erythrocytes cross two consecutive inflammation sites.

5.10.2. Frequency of crossing inflammation sites

In order to address what happens when erythrocytes face consecutive exposures to H_2O_2 we need a rough estimate of the frequency of such exposure. To do so we estimated the average time between successive crossings of inflamed capillaries.

The number of inflammatory foci as well as their distribution is highly dependent on various factors such as type of inflammation foci, immune response, age, and other physiological aspects of the individual. For instance, the number of atherosclerotic plaques was shown to vary with age and gender (Ben-Haim et al., 2004; Wasselius et al., 2009). So the estimate we show below should be taken only as a rough approximation of the frequency of crossing an inflammation site.

To do such estimate we started by computing the average volume of the human body that is occupied by blood. As a rough simplifying assumption we considered that human blood bathes all tissues equally. Discarding the total volume occupied by the human skeleton and extracellular fluids (such as interstitial fluids and blood plasma) from the total body volume we get the approximate volume of tissue bathed by blood. Table 5.16 presents some volumes related with this issue and how they were estimated.

Table 5.16 – Relevant volumes of the human body. Values for an average body weight of 70 kg and body density of 1 kg/dm^3 (Roche et al., 1996).

Parameter	Meaning	Volume (dm^3)	Notes
V_{total}	Total body volume	70	
$V_{skeleton}$	Skeleton volume	5.5	The human skeleton accounts for ≈15 % of the body weight (Flindt, 2006). The value of $V_{skeleton}$ was obtained by considering a bone density of 1.9 kg/dm^3 (Cameron et al., 1999).
$V_{interstitial}$	Volume of interstitial fluids	14	The extracellular cavities are mainly filled with fluids. These extracellular fluids represent 14 dm^3 of the body volume (Guyton, 1984) from which 2.7 dm^3 are blood plasma [(Widmaier et al., 2008)].
$V_{blood\ cells}$	Total volume of human blood cells	2.3	Computed from the approximate volume of erythrocytes and leukocytes in Table 5.15, Section 5.10.1
V_{bathed}	Volume of human body that is bathed with blood	To estimate	

Using the data above we get the volume of tissues bathed by blood V_{bathed}

$$V_{bathed} = V_{total} - V_{skeleton} - V_{interstitial} - V_{blood\ cells} \approx 48\ \text{dm}^3 \qquad \textbf{Equation 5.81}$$

This value was then used to compute the average time it takes for the same erythrocyte to pass by capillaries in inflamed regions. Consider that a portion of inflamed tissue with volume $V_{inflammation}$ is located in a random part of the body where it is irrigated by blood vessels. Such volume exposes the capillaries around it to H_2O_2. Using this volume and the value of V_{bathed} estimated above, we compute the period T of crossing an inflammation site as

$$T = \frac{f_h}{\frac{V_{inflammation}}{V_{bathed}}} \qquad \textbf{Equation 5.82}$$

$$\Leftrightarrow T = \frac{f_h}{i} \qquad \textbf{Equation 5.83}$$

where f_h is the average time taken by the same erythrocyte to pass by the heart twice, $V_{inflammation}$ is the volume of inflamed tissue, V_{bathed} is the volume of body tissue bathed by blood and i is the fraction of the body occupied by inflamed tissue. The following table shows the values considered for each of these parameters.

Table 5.17 – Parameters used to compute the frequency in which an erythrocyte crosses the same inflamed site.

Parameter	Value	Meaning
f_h	60 s	Average time taken by the same erythrocyte to pass by the heart twice, in resting conditions (Widmaier et al., 2008)
i		Fraction of body volume occupied by inflamed tissue.
$V_{inflammation}$		Volume of inflamed tissue.
V_{bathed}	48 dm^3	Volume of body tissue bathed by blood (computed through Equation 5.81)

Using these values we estimated the time taken to cross an inflammatory site by considering that inflamed tissue occupies various fractions of the body volume (i).

Table 5.18 – Average time (T) it takes for the same erythrocyte to pass by two consecutive inflammatory focus. i is the fraction of total body volume occupied by inflamed tissue (%).

i (%)	T
0.001	1667 h
0.1	17 h
1	1.7 h
10	10 min
20	5 min
30	3 min
50	2 min

The table above shows that crossing of two consecutive inflammation sites takes many days if one considers low volumes of inflamed tissue. An i = 0.001% (that would pertain to inflamed tissue with volume 48×10^{-5} dm^3, such as a wound for instance) would require about 1667 hours (≈70 days) to be crossed twice by the same erythrocyte. Only when a significant volume of the body is occupied by inflamed tissue does T decrease to the minute range.

Although this is not an exact determination, because of the large branching of the vasculature it is very likely that it takes an erythrocyte at least several hours to pass by two consecutive inflammatory foci under most plausible conditions.

5.10.3. Basal intracellular and extracellular values of H_2O_2

In Section 5.2.1.3 we discussed the determinations of (Giulivi et al., 1994; Kirkman et al., 1999) of the iH_2O_2 under basal oxidative loads. Again we will consider 10^{-12} M iH_2O_2 as the basal oxidative load in the erythrocyte, as per our analyses in Sections 5.2.1.3 and 5.3.

Regarding the basal plasma H_2O_2 we considered a $eH_2O_2 = 10^{-8}$ M. A few lines of evidence support this value: 1. The basal oxidative contents of the blood plasma should not be very high or

may lead to several hazardous effects on endothelial cells and circulating cells, among other processes. 2. Blood plasma also possesses antioxidant defenses (Avissar et al., 1989; Frei et al., 1988; Jones et al., 1995; Jones et al., 2002; Maddipati et al., 1987; Maddipati and Marnett, 1987; Schwertassek et al., 2007). These likely prevent the accumulation of reactive oxygen species to levels that may be toxic to cells interacting with the vasculature. 3. As per our estimates (Section 5.3) values up to $\approx 10^{-7}$ M eH_2O_2 allow the Prx2/Trx cycles to remain mostly reduced. We considered 10^{-8} M eH_2O_2 because it allows Prx2/Trx to remain in reduced form and is not very far from the values estimated above.

Although the results that will follow in the next Sections are highly dependent on the oxidative load we believe that the same results will occur even if other basal iH_2O_2 or eH_2O_2 are considered. Even if such loads found *in vivo* are different from the values we are considering, we will still get the same redox response of the Prx2/Trx cycles, given that these proteins should remain mostly reduced under basal oxidative conditions [as was showed by (Low et al., 2007), human erythrocytes assessed under atmospheric pressure have most of their Prx2 contents in reduced form].

5.10.4. H_2O_2 production in pathological conditions and cell tolerance to H_2O_2

Much effort has been done in order to determine accurate levels of H_2O_2 levels in various pathological conditions. Leukocytes are one of the sources of H_2O_2 during inflammation. These cells are recruited to inflammatory sites, become activated and produce H_2O_2 at rates which depend on the conditions. Table 5.19 presents some of these values as well as approximated rates by single leukocytes (v_{prod}).

Table 5.19 – H_2O_2 production by opsonized leukocytes and estimates of H_2O_2 production per cell.

Observed production	Production ($\times 10^{-12}$ mol/min/cell)	Source cell and reference
0.8×10^{-9} mol/min/10^6 cells	8×10^{-4}	Maximal rate by monocytes (Reiss and Roos, 1978)Maximal rate by monocytes (Reiss and Roos, 1978)
4×10^{-9} mol/min/10^6 cells	4×10^{-3}	Maximal rate by neutrophils (Reiss and Roos, 1978)Maximal rate by neutrophils (Reiss and Roos, 1978)
0.2×10^{-9} mol/min/2.6×10^6 cells	8×10^{-5}	Neutrophils and eosinophils, respectively (Kazura et al., 1981)Neutrophils and eosinophils, respectively (Kazura et al., 1981)
1001×10^{-9} mol/60 min/10^7 cells	2×10^{-3}	Maximal rate by monocytes (Nakagawara et al., 1981)Maximal rate by monocytes (Nakagawara et al., 1981)
15×10^{-9} mol/30 min/10^6 cells	5×10^{-4}	Neutrophils (Minczykowski et al., 2001)Neutrophils (Minczykowski et al., 2001)

The reports above used different techniques and molecules to stimulate the production of H_2O_2 by leukocytes. The values present in Table 5.19 represent reference values and depend on many conditions: the degree of leukocyte stimulation with antigen, leukocyte cell volume, type of antigen, and so on.

Leukocytes are also recruited by tumors, remaining in the periphery of the cancerous mass (Dvorak, 1986). The production of H_2O_2 nearby tumors depends on the number of leukocytes recruited (Szatrowski and Nathan, 1991). The rate of production of H_2O_2 by different tumors can reach up to 5×10^{-8} mol/10^4 cells/hour, comparable to rates by polymorphonuclear neutrophils (Szatrowski and Nathan, 1991).

But could we use such rates by tumors or leukocytes to estimate the H_2O_2 which erythrocytes are exposed to? A few issues prevent a precise estimate. Leukocyte recruitment in inflammation sites depends on a large number of chemokines, cytokines and other molecules (Springer, 1994; Worthylake and Burridge, 2001) which also depend on the pathological conditions. This affects the number of leukocytes present in those locations and the H_2O_2 produced by those cells. Further, the timeframe considered for the determination of some of the rates in Table 5.19 range up to an hour, which does not allow a very precise estimate for lower timescales.

Other issues preventing this relate with the pathology of the inflammatory focus. For instance, it is known that during inflammation many leukocytes interact with (Cohnheim, 1877) and cross (Marchesi and Florey, 1960) the endothelium. Therefore, the endothelium may represent a barrier between the H_2O_2 produced within the inflammation focus and the bloodstream, given that activated leukocytes do not interact directly with blood plasma. Further, even if the H_2O_2 produced by leukocyte would directly flow to the plasma, one would also have to account with its dilution in the bloodstream.

With the above in mind, we chose to focus on the H_2O_2 production in an inflammatory location such as a wound rather than having a precise value for the H_2O_2 produced by leukocytes alone. A study by (Niethammer et al., 2009) used fluorescent methods in order to determine the H_2O_2 levels in wound-inflicted zebrafish. The authors report values between 5×10^{-7} and 5×10^{-5} M

extracellular H_2O_2 in wound margin cells. These values, although not assessed in mammals, may be used as reference H_2O_2 levels in inflammatory locations.

But are these loads tolerated by endothelial cells neighboring inflammatory sites? The cytotoxicity of H_2O_2 to endothelial cells was assessed in several *in vitro* studies. For instance, (Ager and Gordon, 1984) observed that a 3×10^{-4} M , but not 1×10^{-4} M H_2O_2 bolus was sufficient to induce lysis of pig aortic endothelial cells in cultures (10^6 cells per well). The authors also observed that cell culture ($\approx10^4$ cells/well) with xanthine oxidase generating 5×10^{-6} M H_2O_2/s for 1 hour did not induce cell lysis. (Harlan et al., 1984) also assessed the lysis of endothelial cells using bovine aorta ($2\text{-}3\times10^6$ cells). These authors observed that cell culture did not significantly increase cell lysis as assessed 4 hours after cells had been exposed to a 10^{-5} M H_2O_2 bolus. These reports indicate that endothelial cells in culture can survive exposure to a 10^{-5} M H_2O_2 bolus. This value is not very far from the H_2O_2 concentrations determined by (Niethammer et al., 2009) in zebra fish, although the latter H_2O_2 are probably sustained because are being measured close to inflammation sites.

As a comparison we may look at similar analyses done in human erythrocytes. (Masuoka et al., 2006) observed that erythrocytes (2% hematocrit) exposed to a 10^{-4} M H_2O_2 bolus would not present significant hemolysis, 5 and 30 minutes after cells had been exposed to H_2O_2. (Nascimento et al., 2010) also addressed this issue and found that erythrocytes (2% hematocrit) would not undergo hemolysis even when incubated with a 10^{-3} M H_2O_2 bolus, as assessed 4 hours after incubation with H_2O_2. These values are 10 to 100 fold smaller than the values obtained by (Ager and Gordon, 1984) and (Harlan et al., 1984).

The studies above suggest that erythrocytes and endothelial cells survive oxidative loads in the range of the strongest determined near inflammation sites of other organisms (Niethammer et al., 2009). However, the conditions which the endothelium and erythrocytes are subject *in vivo* differs greatly from the well-controlled conditions in which cells are grown or assessed, nutrient- and physiologically-wise. Such differences may be crucial for cell survival upon oxidative stress. Due to these uncertainties and to the unclear conditions in which the experiments performed above were done, we considered several orders of magnitude for the H_2O_2 that erythrocytes face up to 10^{-5} M eH_2O_2.

5.11. How do different eH_2O_2 pulses affect the redox state of Prx2?

We estimated in Section 5.10.1 that the exposure of erythrocytes to H_2O_2 lasts about 2 s if such exposure happens while crossing capillaries. In this section we study how different eH_2O_2 affect the redox state of Prx2 when erythrocytes pass by such inflammatory sites.

We used Model 5.9 (represented in Figure 5.26 and based on Model 5.4, Section 5.3) to analyze the redox state of Prx2 when erythrocytes face H_2O_2 pulses with various intensities.

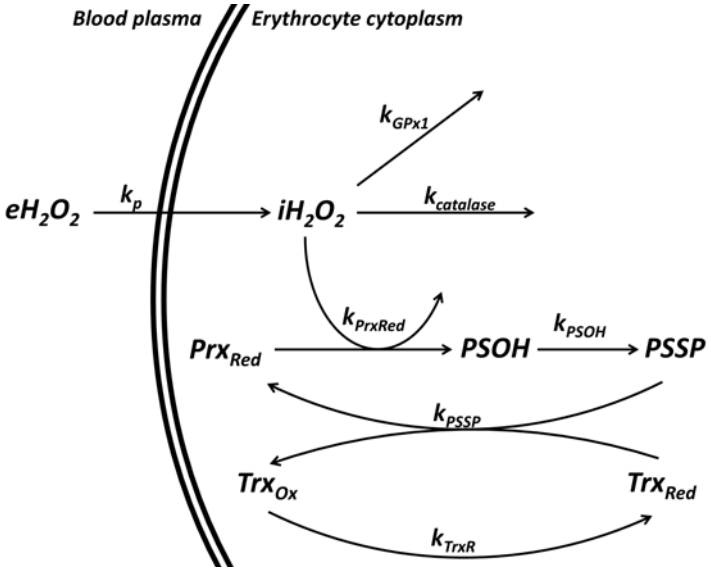

Figure 5.26– Reaction scheme considered to analyze how different eH_2O_2 affect the redox state of Prx2 at the end of a pulse.

$$\frac{d\ iH_2O_2}{dt} = k_p \cdot eH_2O_2 - iH_2O_2 \cdot (k_{PrxRed} \cdot Prx_{Red} + k_{catalase} + k_{GPx1})$$

$$\frac{d\ Prx_{Red}}{dt} = k_{PSSP} \cdot PSSP \cdot Trx_{Red} - k_{PrxRed} \cdot Prx_{Red} \cdot iH_2O_2$$

$$\frac{d\ PSOH}{dt} = k_{PrxRed} \cdot Prx_{Red} \cdot iH_2O_2 - k_{PSOH} \cdot PSOH \qquad \textbf{Model 5.9}$$

$$\frac{d\ Trx_{Ox}}{dt} = k_{PSSP} \cdot PSSP \cdot Trx_{Red} - k_{TrxR} \cdot Trx_{Ox}$$

$$Prxtot = Prx_{Red} + PSOH + PSSP$$

$$Trxtot = Trx_{Red} + Trx_{Ox}$$

The model above includes the parameters found in Table 5.20.

Table 5.20 – Parameters used for Model 5.9.

Parameter	Value	Meaning/Reference
k_p	8 s^{-1}	First-order rate constant for hydrogen peroxide consumption by erythrocytes (estimated in Section 5.2.1.2)
$k_{catalase}$	218 s^{-1}	Pseudo-first order rate constant for H_2O_2 consumption by catalase (Section 5.1.1.2)
k_{GPx1}	40 s^{-1}	Pseudo-first order rate constant for H_2O_2 consumption by GPx1 (Section 5.1.1.1)
k_{PrxRed}	10^8 $M^{-1}s^{-1}$	Reactivity between reduced Prx2 and H_2O_2 (Manta et al., 2009)
k_{PSOH}	0.26 s^{-1}	First order rate constant for formation of PSSP (Section 5.2.1.10)
k_{PSSP}	2.1×10^5 $M^{-1}s^{-1}$	Reactivity between reduced Trx and PSSP (Manta et al., 2009)
k_{TrxR}	0.5 s^{-1}	Pseudo-first order rate constant for Trx reduction through TrxR (Section 5.2.1.9)
Prxtot	3.7×10^{-4} M	Total concentration of Prx2 monomers (Section 5.1.1.3)
Trxtot	4.8×10^{-6} M	Total Trx concentration (from bovine erythrocytes, 5.2.1.6)

We considered that both Prx2 and Trx are fully reduced before crossing a capillary that passes by an inflammatory focus. This approaches what happens when erythrocytes are facing basal oxidative conditions (Sections 5.3 and 5.5). We also considered that the contributions of catalase and GPx1 for H_2O_2 scavenging have first order kinetics with respect to H_2O_2, an assumption discussed in Sections 5.2.1.1 and 5.2.1.2. The initial value of iH_2O_2 was 10^{-12} M as per our analysis in Sections 5.2.1.3 and 5.3.

Bearing these considerations in mind we evaluated what is the minimum fraction of Prx_{Red} at the end of a 2 s eH_2O_2 pulse. This was done through numerical integration of Model 5.9 and determination of the fraction of reduced Prx2 when t = 2 s, considering parameters from Table 5.20. Figure 5.27 represents the minimum fraction of Prx_{Red} obtained for various eH_2O_2 pulses.

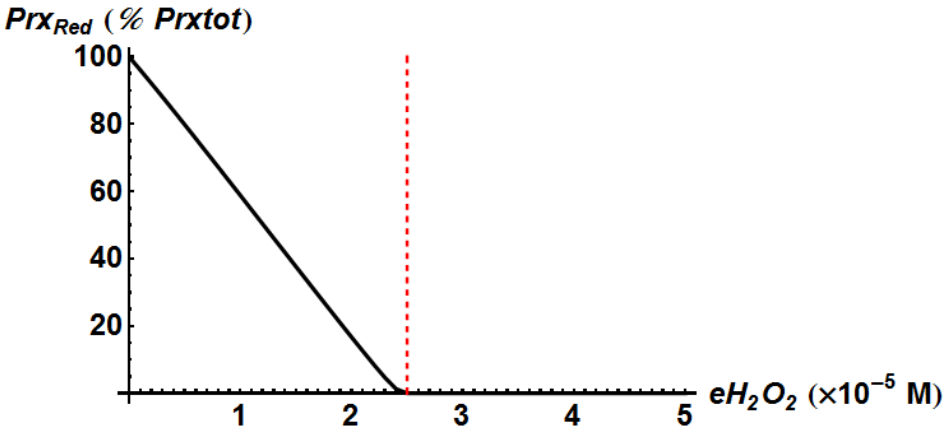

Figure 5.27 – Minimum fraction of Prx_{Red} obtained after an eH_2O_2 pulse (2 s), for H_2O_2 pulses with various eH_2O_2. The dashed line represents the load in which less than 1% of the Prx2 contents are in Prx_{Red} form (eH_2O_2 = 2.5×10^{-5} M). Obtained by computing the fraction of Prx_{Red} after an eH_2O_2 pulse of 2 s, through Model 5.9 and Table 5.20.

The figure above shows that only pulses stronger than ≈2.5×10^{-5} M eH_2O_2 lead to full Prx_{Red} depletion (the dashed line in Figure 5.27 shows the eH_2O_2 in which < 1% of Prx2 in Prx_{Red} form). This eH_2O_2 would correspond to ≈7×10^{-6} M iH_2O_2 at the end of the pulse.

Such high eH_2O_2 is conceivable in inflammatory foci such as wounds, but likely approach the maximum oxidative conditions tolerated by nearby cells (see Section 5.10.4 for values of H_2O_2 nearby wounds and a values tolerated by endothelial cells). This suggests that the high Prx2 concentration in the cell is sufficient to protect erythrocytes against high oxidative loads found nearby inflammation sites during the estimated 2 s residence time.

5.12. What is the role of catalase in defense against eH_2O_2 pulses?

In the section above we saw that only very high eH_2O_2 pulses lead to full Prx2 oxidation. As we showed in the first part of our results, when Prx2 accumulates in PSSP form catalase becomes the main H_2O_2 defense (Section 5.6). In this section we further explore the role of catalase in the defense against H_2O_2 by addressing its contribution for H_2O_2 consumption when erythrocytes face eH_2O_2 pulses.

Using Model 5.9 and parameters from Table 5.20 (Section 5.11) we computed the relative contribution of Prx2 and catalase for H_2O_2 consumption:

$$\text{relative Prx2 contribution} = \frac{v_{Prx2}}{v_{H2O2}} \qquad \textbf{Equation 5.84}$$

$$\text{relative catalase contribution} = \frac{v_{catalase}}{v_{H2O2}} \qquad \textbf{Equation 5.85}$$

Where v_{Prx2} and $v_{catalase}$ are the rates of iH_2O_2 consumption by Prx2 and catalase and v_{H2O2} is the total rate of iH_2O_2 consumption:

$$v_{Prx2} = k_{PrxRed} \cdot iH_2O_2 \cdot Prx_{Red} \qquad \textbf{Equation 5.86}$$

$$v_{catalase} = k_{catalase} \cdot iH_2O_2 \qquad \textbf{Equation 5.87}$$

$$v_{H2O2} = iH_2O_2 \cdot \left(k_{PrxRed} \cdot Prx_{Red} + k_{catalase} + k_{GPx1}\right)$$ **Equation 5.88**

Considering 10^{-8} M eH_2O_2 before and after the pulse, and 10^{-12} M iH_2O_2 before the pulse, we estimated the relative contribution of Prx2 and catalase for iH_2O_2 consumption through the equations above.

During a 3×10^{-5} M eH_2O_2 pulse the contribution of Prx2 for H_2O_2 consumption becomes practically null due to complete Prx2 oxidation (Section 5.11). When this occurs catalase becomes the main H_2O_2 scavenger (Figure 5.28):

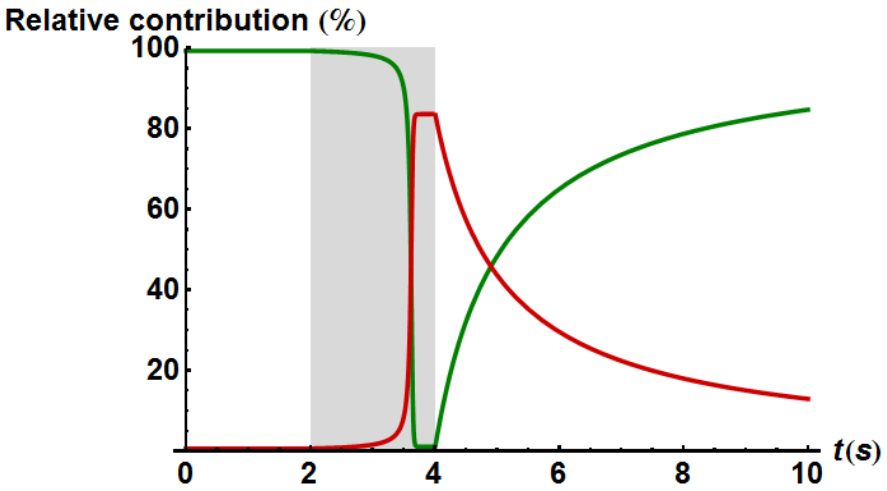

Figure 5.28 - Relative contribution of Prx2 and catalase for H_2O_2 consumption during a 2 s pulse (gray area) of 3×10^{-5} M eH_2O_2. Estimated using Model 5.9 and parameters from Table 5.20 (Section 5.11).

Prx2 becomes again the main H_2O_2 scavenger after the pulse as it is regenerated (Section . But what is the importance of catalase for the defense against iH_2O_2 and under which conditions is it more important?

To address this issue we estimated the iH_2O_2 at the end of various eH_2O_2 pulses, in the presence and absence of catalase, by considering again Model 5.9 and parameters from Table 5.20 (Section 5.11):

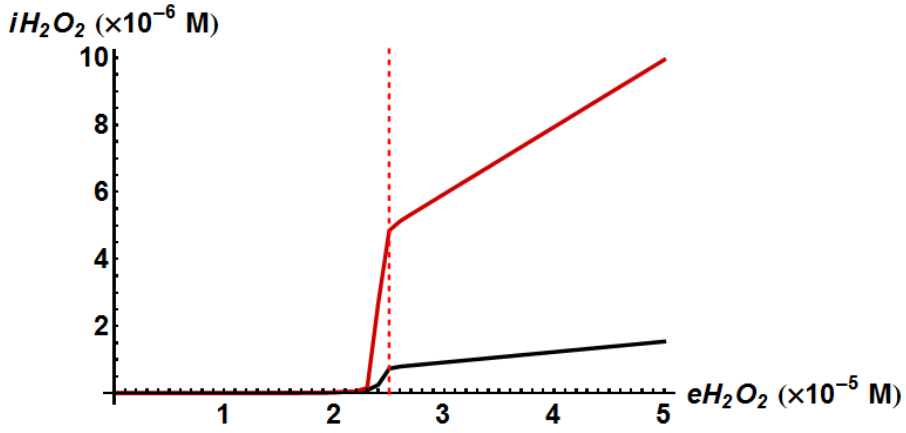

Figure 5.29 – iH_2O_2 found at the end of a 2 s pulse of various eH_2O_2 concentrations, in the presence (black) and absence (red) of catalase.Estimated considering Model 5.9 and the parameter values in Table 5.20 (Section 5.11). The dashed line refers to $eH_2O_2 = 2.5\times10^{-5}$, a eH_2O_2 pulse that at the end of which <1 % of the Prx2 is in reduced form.

The figure above shows that a low iH_2O_2 is maintained at the end of a pulse for $<2.5\times10^{-5}$ M eH_2O_2 pulses, regardless of catalase presence. This occurs because Prx2 consumes most of the iH_2O_2 under such oxidative loads.

However, the situation is different when the erythrocyte is subjected to higher eH_2O_2 pulses. There is a much higher accumulation of iH_2O_2 in the absence of catalase than in its presence for pulses $>2.5\times10^{-5}$ M eH_2O_2. Under such loads most of the Prx2 contents are in PSSP form (Section 5.11). This makes catalase essential to maintain a low iH_2O_2 under those conditions.

These results show that catalase becomes the main antioxidant defense against H_2O_2 when the cell crosses inflammation sites that lead to full Prx2 oxidation. Under such conditions, catalase is important to maintain a low iH_2O_2.

5.13. Could there be accumulation of PSSP due to consecutive crossing of inflammatory sites?

How long would it take for Prx2 to be reduced back after facing such intense oxidative stress? Is it plausible that an erythrocyte may cross consecutive oxidative pulses before there is time for Prx2 to be fully reduced? If so, this could impair the antioxidant ability of Prx2. To answer these questions we used Model 5.9 and Table 5.20 (both from Section 5.11) and considered that the antioxidant activity of catalase and GPx1 is not impaired by the oxidative insult (we addressed

under which conditions this is plausible in Section 5.2.1.1 and 5.2.1.2). Because we want to analyze how long it takes for Prx2 to be fully reduced we considered that initially all Prx2 and Trx are oxidized. This was done because Trx reduction limits Prx2 reduction when erythrocytes face high oxidative loads, as discussed in Section 5.2.2. As for the oxidative conditions, we considered that the cell is facing basal eH_2O_2 (10^{-8} M, Section 5.10.3). This simulates what occurs right after an erythrocyte crosses an inflammation site.

The iH_2O_2 at the end of such a pulse is expected to be higher than the basal concentration (which was considered as 10^{-12} M iH_2O_2). However, the value of iH_2O_2 at the end of a pulse also depends on the eH_2O_2 the erythrocyte is subjected to while crossing an inflammation site. For this reason we considered that iH_2O_2 is initially 7×10^{-7} M, which would correspond to a 25×10^{-6} M eH_2O_2 pulse, as estimated in Section 5.11. Although lower iH_2O_2 may be found *in vivo,* considering other initial iH_2O_2 does not change greatly the time taken to reduce Prx2: even if we only consider the antioxidant activities of catalase and GPx1 (Section 5.1.2), the half-life of iH_2O_2 is

$$t_{1/2}(H_2O_2) = \frac{\ln(2)}{k_{GPx1} + k_{catalase}} \approx 3 \text{ ms} \qquad \textbf{Equation 5.89}$$

Were GPx1 activity impaired due to a low NADPH availability and catalase the only active antioxidant we would still get a similar $t_{1/2}(H_2O_2)$. Due to such small $t_{1/2}(H_2O_2)$, changing the initial value of iH_2O_2 practically does not affect our estimate of the time taken to reduce Prx2.

After taking the above into consideration, we numerically integrated Model 5.9 and solved it in order to every dependent variable. Figure 5.30 represents the fraction of Prx_{red} over time.

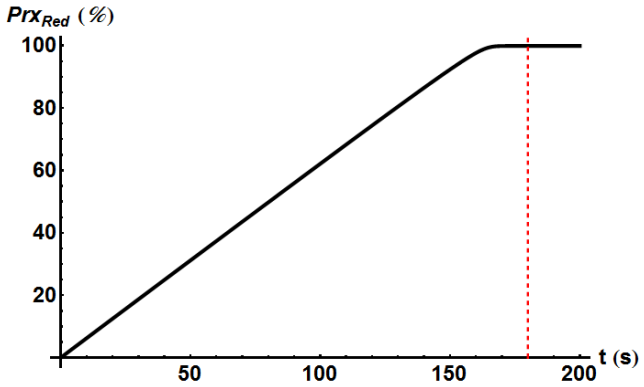

Figure 5.30 – Fraction of Prx_{red} over time (s) using Model 5.9 and the parameter values in Table 5.20 (Section 5.11). See the text above for assumptions. The dashed line marks 3 minutes.

The figure above shows that it takes less than 3 minutes for Prx2 to be fully reduced back to Prx_{Red}. This represents a limit situation for the oxidative conditions considered. The initial eH_2O_2 and iH_2O_2 considered (taken from our analysis in Section 5.11) represent oxidative loads close to maximum values found *in vivo* in pathological conditions (see Section 5.10.4 for a discussion of these values). Because of this, an inflammatory focus that does not lead to full oxidation of Prx2 also allows Prx2 to be fully reduced back to Prx_{Red} even faster than above. However, we acknowledge that the time taken to fully reduce Prx2 may differ from the above estimate. Prx2 reduction depends on other factors besides the intensity of the pulse. It is mostly limited by Trx reduction as discussed in Sections 5.2.2 and 5.3. Different *Trxtot* values or limiting *NADPH* levels would affect the rate of Prx2 reduction. In this analysis we are still considering that NADPH availability is not limiting TrxR activity, which may not be the case in erythrocytes facing higher oxidative loads.

Could an erythrocyte cross more than one inflammatory focus in less than 3 minutes, hence leading to the cumulative oxidation of Prx2? We addressed the time taken to interact with two consecutive inflammatory foci in Section 5.10.2. Taking into consideration our estimates of the time required for Prx2 to be fully reduced back (<3 minutes), what would the volume fraction of inflammed tissue (*i*) (Table 5.17, Section 5.10.2) have to be so that the mean period between consecutive crossings of inflammation sites became less than 3 minutes? As per our estimates (Table 5.17, Section 5.10.2), *i* would have to be at least 30%.

The number and size of inflammatory foci in the body is highly dependent on the individual and the pathological conditions found in the body. Various diseases may lead to extensive inflammation in the body, such as bacterial infection, vasculitis, and metastatic cancer. Under severe cases of these pathologies, it is possible that the total volume of inflamed permits for frequent crossing of multiple inflamed foci: (Wasselius et al., 2009) observed that a few hundred atherosclerotic plaques are present in the aorta of asymptomatic individuals over 60 years old. Nevertheless, values of *i* as high as 30% are only plausible under severe cases of bacterial infection like cellulitis or erysipelas for instance. On the other hand, localized inflammatory sites may occur in less pathological conditions. It is the case of wound healing or localized pathogen infection. These occur constantly throughout the body and are fought by our immune system. Because these are usually very localized inflammatory regions, the frequency of crossing such sites is very low.

To this extent, it very likely that in between crossing two inflammatory foci there is enough time for the complete reduction of Prx2. Taken together, these results show that the erythrocyte is likely able to fully reduce Prx2 between two consecutive oxidative pulses, in most physiological conditions.

5.14. Why is Prx2 so abundant in the human erythrocyte?

As we saw above, Prx2 has the highest contribution for H_2O_2 consumption among the main H_2O_2 scavengers in the human erythrocyte. The results in Section 5.11 show that only very strong oxidative pulses lead to full Prx2 oxidation. When Prx2 accumulates in PSSP form its contribution for defense against H_2O_2 decreases. Under these conditions catalase becomes the main H_2O_2 scavenger, maintaining a low iH_2O_2. But then why is Prx2 one of the most abundant proteins in the human erythrocyte?

The results in Section 5.11 indicate that Prx2 is present in human erythrocytes at approximately the concentration that is necessary to protect them during the residence time in capillaries against pulses $<2.5\times10^{-5}$ M eH_2O_2, in the range of the strongest oxidative loads (5×10^{-5} M H_2O_2) found by (Niethammer et al., 2009) in inflammation *foci* in other organisms. This result suggests that the selective pressure that mediates the evolutionary maintenance of such high Prx2 concentrations is the need to avoid a large iH_2O_2 accumulation as erythrocytes cross capillaries that are located within inflammation *foci*.

To further investigate the extent of protection conferred by Prx2 in these circumstances we proceeded as follows. Assuming that H_2O_2-induced damage (D) accumulates over time and is proportional to iH_2O_2 we can write:

$$\frac{dD}{dt} = k_D \cdot iH_2O_2 \quad \text{,} \qquad \textbf{Equation 5.90}$$

where k_D is a proportionality constant for the damaging effects of iH_2O_2 to the cell. This constant must be much lower than 1 or D would accumulate greatly overtime. During eH_2O_2 pulses there is higher iH_2O_2, which leads to higher damage (D_p). In order to estimate the D_p that would be accumulated at the end of an eH_2O_2 pulse in presence or absence of Prx2 we added Equation

5.90 to Model 5.9 (Section 5.11), and integrated this extended model using the parameter values from Table 5.20 (Section 5.11). Because we are only interested in addressing the influence of Prx2 on the value of D, not on the physiological accurate value of D, we assumed $k_D = 1$ (Equation 5.90). We considered that by the beginning of a pulse, Prx2 and Trx are fully reduced. The initial value of iH_2O_2 considered was 10^{-12} M and the basal $eH_2O_2 = 10^{-8}$ M. We then plotted D_p at the end of an eH_2O_2 pulse, in presence and in absence of Prx2 (Figure 5.31).

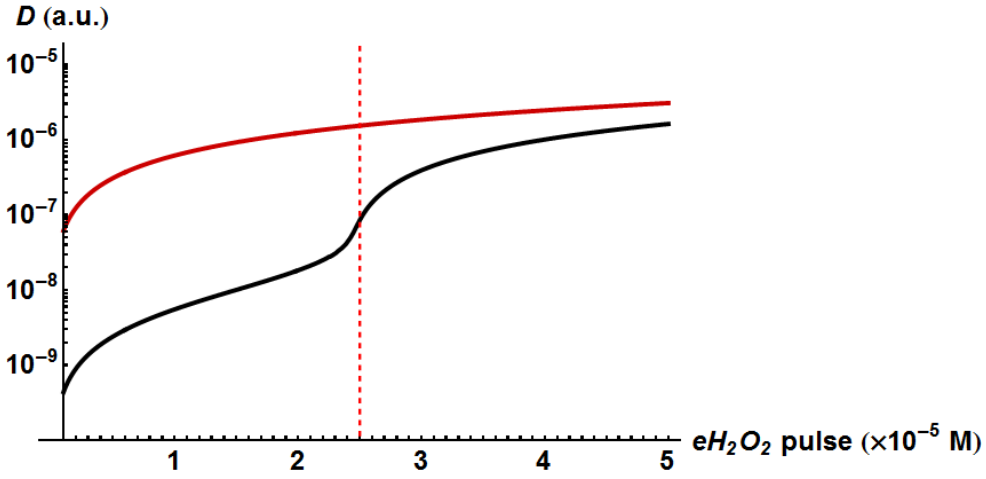

Figure 5.31 – Accumulated damage at the end of 2 s eH_2O_2 pulses of various intensities, in the presence (black) or absence (red) of Prx2. The dashed line represents the eH_2O_2 pulse at the end of which <1 % of the total Prx2 contents is in Prx_{Red} form (Section 5.11).

The results shows that D_p accumulates much more in the absence of Prx2 than in the presence of physiological concentrations of this protein.

6. Discussion

In this work we analyzed the role of the main antioxidant systems of the human erythrocyte to defend this cell against H_2O_2: glutathione peroxidase 1, catalase, and peroxiredoxin 2. It was previously suggested that GPx1 is mainly used to protect this cell from organic peroxides (Gaetani et al., 1996; Johnson et al., 2002), casting out a distinct role for catalase and Prx2: catalase protects erythrocytes from high H_2O_2 concentrations (Gaetani et al., 1996; Johnson et al., 2000; Mueller et al., 1997a) whereas Prx2 protects only against low H_2O_2 (Low et al., 2007). As hypothesized by (Low et al., 2007) this may be related with the different requirements that these two systems have for reducing equivalents. Whereas H_2O_2 scavenging by Prx2 is stoichiometrically coupled to NADPH oxidation, H_2O_2 consumption by catalase practically does not entail NADPH oxidation. Then why do these cells need Prx2? Why do not human erythrocytes rely only on catalase for their defense against H_2O_2? Is Prx2 redundant in the protection of these cells from H_2O_2?

We used kinetic analyses and mathematical modeling to answer these questions. In this section we discuss the results that allowed us to answer these questions, addressing a few improvements and analyses that may further develop this work. We then discuss the relevance of this work for various areas of research. We will start by addressing our analyses of the redox behavior of Prx2/TrxR/Trx cycles when erythrocytes are under sustained exposure to basal and high eH_2O_2. This allows us to examine what occurs when the organism is under systemic inflammation.

6.1. Prx2 is the main scavenger of low/mild H_2O_2

We started our analyses by estimating the pseudo-first order rate constants for H_2O_2 consumption. Due to the very high Prx2 concentration ($\approx 3.7\times10^{-4}$ M, Section 5.1.1.3) and reactivity with H_2O_2 [$\approx 10^8$ $M^{-1}s^{-1}$ (Manta et al., 2009)], we estimate a k_{Prx2} = 37 000 s^{-1} as the pseudo-first order rate constant for Prx2-mediated H_2O_2 reduction (Section 5.1.1.3). This rate constant largely surpasses the rate constant of GPx1 (=40s^{-1}, Section 5.1.1.1) and catalase (=218s^{-1}, Section 5.1.1.2). Prx2 consumes >99% when the erythrocyte faces oxidative loads up to 9.5×10^{-7} M H_2O_2/s (Sections 5.1.2, 5.3 and 5.6). These differences suggest that Prx2 has a potentially very high contribution for the defense against H_2O_2.

Yet, (Low et al., 2007) observed that Prx2 is extremely sensitive to oxidation by H_2O_2. Based on the accumulation of oxidized Prx2 and low turnover of Prx2, the authors suggested that this protein scavenges only low H_2O_2 levels. In agreement with these observations, (Johnson et al., 2010) later observed that Prx2 is important for controlling endogenously produced H_2O_2. These observations suggested that Prx2 is important for controlling iH_2O_2 only under basal oxidative loads. We will now discuss these and other observations, and their relation with our estimates.

6.1.1. Basal concentration and production of H_2O_2

To estimate the basal endogenous production of iH_2O_2 we considered that all Prx2 is reduced under basal oxidative loads, thus accounting for most of the iH_2O_2 consumption. This estimate was carried out through two approaches (Section 5.3): 1. we estimated the rate of Prx2 reduction ($=2.3\times10^{-7}$ M/s) after accumulation of *PSSP* from the data of (Low et al., 2007) (Figure 5.6, Section 5.2.1.9). From this rate we get that $<1.2\times10^{-7}$ M H_2O_2/s is sufficient for >99% of the Prx2 contents to remain in reduced form; 2. considering the maximal rate of NADPH production by the PPP and assuming that NADPH supply limits Prx2 reduction, we estimate that a load $<9.5\times10^{-7}$ M H_2O_2/s allows ≈99% of the Prx2 to be reduced, thus consuming most of the iH_2O_2. These two independent estimates yielded very close estimates for the basal oxidative loads, which further reinforces the confidence in these estimates.

As discussed in Section 5.2.1.3, (Kirkman et al., 1999) and (Giulivi et al., 1994) determined the rates of H_2O_2 production under atmospheric O_2 pressure and glucose depletion. They respectively determined $\approx3.3\times10^{-8}$ M H_2O_2/s and $\approx4\times10^{-10}$ M H_2O_2/s. What would be physiologically more plausible: to consider the fluxes determined by (Giulivi et al., 1994; Kirkman et al., 1999) as the basal oxidative load *in vivo*, or the author's estimate of steady state H_2O_2?

The rates of H_2O_2 production determined by (Kirkman et al., 1999) and (Giulivi et al., 1994) correspond to the rates at which NADPH is oxidized under basal loads if Prx2 is the main scavenger of iH_2O_2. These rates are >55 fold lower than the maximal rate of NADPH production by the PPP [$V_{max}^{PPP}=1.9\times10^{-6}$ M, (Albrecht et al., 1971)]. On the other hand, the authors' estimate of 2×10^{-10} M and 3×10^{-9} M iH_2O_2 would correspond to a Prx2 activity of 7.4×10^{-6} M/s and

10^{-4} M/s, respectively. These rates are much higher than V_{max}^{PPP}, and thus are not physiologically plausible.

While the experiments of (Kirkman et al., 1999) and (Giulivi et al., 1994) aimed to determine basal oxidative loads experimentally, others aimed to estimate the steady state iH_2O_2 under basal oxidative loads through kinetic modeling (Johnson et al., 2005; Johnson et al., 2010). Using a kinetic model that includes the antioxidant activities of catalase and Prx2, and endogenous production of iH_2O_2 from Hb autoxidation, (Johnson et al., 2005) and (Johnson et al., 2010) respectively estimated steady state $iH_2O_2 = 5.2\times10^{-11}$ and 2.6×10^{-10} M. These iH_2O_2 surpass our estimate of the basal iH_2O_2 ($=10^{-14}$ M) by several orders of magnitude, which may be explained by the following two reasons.

First, in their models (Johnson et al., 2005; Johnson et al., 2010) considered a pseudo-first order rate constant for H_2O_2 reduction by Prx2 of $k_{Prx2}= 24\ s^{-1}$. To estimate this rate constant the authors considered a *Prxtot* = 2.4×10^{-4} M [≈1.5-fold lower than the 3.7×10^{-4} M *Prxtot* considered in this work, Section 5.1.1.3). Although their source reference for this concentration was the same as ours (Moore et al., 1991), it is not clear what was the molecular weight or volume of erythrocyte water considered to estimate a 2.4×10^{-3} M *Prxtot.* Second, to estimate $k_{Prx2} = 24\ s^{-1}$ (Johnson et al., 2010) considered $10^5\ M^{-1}\ s^{-1}$ as the reactivity between Prx2 and H_2O_2. However, this reactivity was determined from microbial peroxiredoxins (Hofmann et al., 2002), and more recent experiments found several fold higher reactivities between *human* peroxiredoxin 2 and H_2O_2 [$=10^7$ - $10^8\ M^{-1}\ s^{-1}$, (Manta et al., 2009; Peskin et al., 2007)]. Thus, the k_{Prx2} considered in the experiments of (Johnson et al., 2005; Johnson et al., 2010) underestimates the contribution of Prx2 for iH_2O_2 consumption.

As per our estimates (Section 5.2.1.3), a 3.7×10^{-8} M iH_2O_2/s is a physiologically plausible oxidative load because it would entail a rate of NADPH oxidation much smaller than the maximal rate of NADPH production by the PPP [$=1.9\times10^{-6}$, (Albrecht et al., 1971)]. To our knowledge, these basal oxidative loads are the first estimates that consider the high contribution that Prx2 has for H_2O_2 scavenging under basal oxidative loads.

6.1.2. Redox status of Prx2 under basal oxidative loads

To estimate the basal oxidative loads above we considered that Prx2 is fully reduced under such conditions. However, the experiments of (Low et al., 2007) suggest that a substantial (40%) fraction of Prx2 could be in PSSP form in erythrocytes not subjected to exogenous H_2O_2. Could the 2×10^{-10} M iH_2O_2 determined by (Kirkman et al., 1999) be physiologically plausible if we consider 40% *PSSP* under basal oxidative loads?

(Low et al., 2007) assessed the redox status of Prx2 from human erythrocytes (≈0.05% hematocrit) ten minutes after incubation with 5×10^{-3} M glucose. Considering 60% of Prx2 in Prx_{Red} form, we estimate a pseudo-first order rate constant for H_2O_2 consumption by Prx2 of $0.6\times k_{Prx2} \approx 22\ 000\ s^{-1}$ (with $k_{Prx2} = 37\ 000\ s^{-1}$, Section 5.1.1.3). This rate constant largely surpasses those of catalase or GPx1 ($k_{catalase}$ =218 s^{-1}, Section 5.1.1.2; k_{GPx1} = 40 s^{-1}, Section 5.1.1.1), showing that Prx2 still consumes most of the iH_2O_2 under these conditions. Considering 2×10^{-10} M iH_2O_2 (Kirkman et al., 1999) and k_{Prx2} = 22 000 s^{-1}, we estimate the rate of Prx2-mediated H_2O_2 reduction:

$$v_{Prx2} = k_{Prx2} \cdot iH_2O_2 \qquad \textbf{Equation 6.1}$$

$$\Leftrightarrow v_{Prx2} \approx 4.4\times10^{-6}\ \text{M/s}$$

Because this rate surpasses the maximum rate of NADPH production by the PPP [$=1.9\times10^{-6}$, (Albrecht et al., 1971)], the 2×10^{-10} M iH_2O_2 estimated by (Kirkman et al., 1999) is implausibly high under basal oxidative loads even if one considers 40% *PSSP*.

Could endogenous H_2O_2 production account for the large fraction of *PSSP* found by (Low et al., 2007) under atmospheric partial O_2 pressure (pO_2 = 160 torr)? As our estimates in Section 2.1.3 suggest, the contribution of Hb autoxidation for H_2O_2 production ($<4.9\times10^{-9}$ M H_2O_2/s) is lower than that coming from GSH autoxidation ($<48\times10^{-9}$ M H_2O_2/s), considering pO_2 (=90 torr) from venous blood. This suggests that GSH autoxidation is the main process of endogenous production of H_2O_2. We estimated the endogenous H_2O_2 production from GSH autoxidation under atmospheric partial O_2 pressure as follows.

Glutathione reacts with O_2 (Reaction 2.2, Section 2.1.1) with a $k_{spon} = 0.1\ M^{-1}s^{-1}$ (Scarpa et al., 1996). Considering atmospheric partial O_2 pressure [1 atm, 1.3×10^{-3} M O_2/atm (Wilhelm et al., 1977)] and total glutathione contents in the erythrocyte [$GSH = GStot = 3.2\times10^{-3}$ M (Thorburn

and Kuchel, 1987)], we get a rate of 4.2×10^{-7} M H_2O_2/s produced from glutathione oxidation. This endogenous production of H_2O_2 yields >99% of reduced Prx2 (as estimated through Model 5.9 from Section 5.11 after considering no eH_2O_2, and parameters from Table 5.20, Section 5.11). Therefore, the large accumulation of *PSSP* found by (Low et al., 2007) in erythrocytes subjected to no exogenous H_2O_2 is not due to endogenous production of H_2O_2 from glutathione autoxidation even under atmospheric pO_2. This is further supported by our estimates in Section 5.2.1.8 where we estimate that endogenous production of $>2\times10^{-6}$ M H_2O_2/s would be required to obtain the $eH_2O_2 = 10^{-7}$ M observed towards the end of the experiment of (Low et al., 2007) (Figure 5.5, Section 5.2.1.8). An endogenous production of 2×10^{-6} M H_2O_2/s is implausibly high because it surpasses the maximal rate of NADPH production in human erythrocytes [$=1.9\times10^{-6}$ M/s (Albrecht et al., 1971)].

These estimates suggest that a substantial fraction of Prx2 is oxidized during sample handling in the experiments (Low et al., 2007), as acknowledged by the authors. Furthermore, pretreatment of erythrocytes with a thiol-blocking agent allowed (Low et al., 2007) to observe only a small fraction of *PSSP* in cells exposed to no H_2O_2. Overcoming the issue of uncontrolled oxidative stress during sample handling is a difficult task, given the large reactivity of Prx2 with H_2O_2. A possible way to avoid such uncontrolled oxidation would be to perform those experiments in a Argon-rich anaerobic atmosphere. While performing those experiments one should also take special care to prevent leukocyte activation.

6.1.3. Prx2 contributes significantly for H_2O_2 consumption under low/mild loads

More than ≈99% of the iH_2O_2 is consumed by Prx2 under oxidative loads $<9.5\times10^{-7}$ M H_2O_2/s that allow most of Prx2 to remain reduced (Sections 5.1.2 and 5.3).

Other studies also assessed the relevance of Prx2 for the redox status of the cell. Based on their studies, (Johnson et al., 2005; Johnson et al., 2010; Low et al., 2007) refer that Prx2 is a scavenger of low H_2O_2. We will now discuss the experiments of these authors.

(Johnson et al., 2005) determined the rate of endogenously produced H_2O_2 in GPx1-knockout mice erythrocytes (5% hematocrit) by determining catalase activity through the method of (Aebi, 1984), as explained in Section 5.2.1.3. Using a kinetic model that included the H_2O_2-scavenging activity of catalase and GPx1, (Johnson et al., 2005) then observed that inclusion of $k_{Prx2} = 24$ s^{-1}

in their model would suffice to fit the model to the experimentally determined catalase activity. These results led the authors to suggest that Prx2 is a scavenger of endogenously generated H_2O_2.

Yet, in our estimates we considered a much higher k_{Prx2} of 37 000 s^{-1} (Section 5.1.2). Then why does k_{Prx2} = 24 s^{-1} suffice to obtain a good fitting of the model of (Johnson et al., 2005) to the rate of endogenously produced H_2O_2? The rate of H_2O_2 production was determined from the rate of catalase inhibition by aminotriazole in GPx1-deficient mice erythrocytes incubated with 10^{-2} M glucose. (Johnson et al., 2005) observed inhibition of ≈3.5% catalase/hour for 4 hours. However, aminotriazole-mediated inhibition of catalase occurs only after other iH_2O_2 scavengers (such as Prx2) have been completely oxidized and are not contributing for iH_2O_2 consumption (Cohen and Hochstein, 1964; Giulivi et al., 1994). Considering that GPx1-defficient erythrocytes were incubated with 10^{-2} M glucose to prevent depletion of the NADPH pool, Prx2's activity is not limited by NADPH supply in the experiments of (Johnson et al., 2005). Under these conditions, Prx2 is likely accounting for most of the iH_2O_2 consumption in their experiments . Thus, aminotriazole-mediated catalase inhibition occurs very slowly and a small k_{Prx2} (=24 s^{-1}) suffices to fit the model to the determined rate of catalase inhibition.

Other studies went further to address the impact of each defense on the redox status of the erythrocyte. (Johnson et al., 2010) compared the contributions of GPx1, catalase and Prx2 for defending mice erythrocytes (5% hematocrit) from H_2O_2. They did so by generating mice strains where each of these defenses had been knocked-out. The erythrocytes were incubated with 10^{-2} M glucose and then assessed the redox status of erythrocytes. This was done by determining the fraction of MetHb (an oxidized form of Hb) in catalase-knockout and wild type erythrocytes. They observed no accumulation of MetHb in catalase-knockout erythrocytes, as assessed 15 minutes after incubation with 10^{-2} M glucose. This suggests that catalase is not contributing significantly for defense against iH_2O_2 under those conditions, in agreement with our results.

The authors then examined the contribution of Prx2 for defense against H_2O_2 by following aminotriazole-mediated catalase inhibition for 3 hours in Prx2-knockout and wild-type erythrocytes. This allowed the authors to determine the rate of iH_2O_2 accumulation due to endogenous production. They observed a slightly higher rate (=10^{-11} M/s) in the knock-outs than in wild-type (6×10^{-12} M/s) erythrocytes. This suggests that Prx2 is important for scavenging endogenously generated iH_2O_2. Yet, by using aminotriazole-associated catalase inactivation to

measure the rate of endogenously generated H_2O_2, the authors may have faced the same issues as (Johnson et al., 2005), as mentioned above.

(Johnson et al., 2005) and (Johnson et al., 2010) also addressed the contribution of Prx2 for H_2O_2 scavenging through kinetic modeling. However, some of the authors' considerations in their model present a few issues. The authors not only underestimate Prx2's contribution for H_2O_2 consumption by considering a k_{Prx2} = 24 s^{-1} (as discussed in Section 6.1.1), but also catalase's contribution for this process. (Johnson et al., 2010) considered a $k_{catalase} \approx 5$ s^{-1}, whereas (Johnson et al., 2005) considered a $k_{catalase}$ = 3.5 s^{-1} (after considering k=10^7 M^{-1} s^{-1} for the reactivity between catalase and H_2O_2, and total catalase concentration ≈5×10^{-7} M). These rate constants are even lower than k_{GPx1} considered [≈6 s^{-1} (Johnson et al., 2010) and =140 s^{-1} (Johnson et al., 2005)]. Taken together, these issues show that although their model fits the experimentally determined rate of catalase inactivation by aminotriazole, the values of some of their parameters need to be re-evaluated.

The study of (Low et al., 2007) further suggests that Prx2's contribution for defense against H_2O_2 is only important under low H_2O_2. (Low et al., 2007) found that ≈60% Prx2 was in *PSSP* form, as assessed ten minutes after erythrocytes (0.05% hematocrit) were exposed to a 5×10^{-7} M H_2O_2 bolus. As discussed in Section 6.1.2, a substantial fraction of Prx2 may have been oxidized during sample handling.

Together with our estimates, the results above show that Prx2 contributes significantly for iH_2O_2 consumption in erythrocytes facing low/mild H_2O_2. This is further supported by the observation that it would be physiologically implausible to replace Prx2 with catalase: in order for catalase (or GPx1) to replace Prx2 and maintain the same responsiveness and iH_2O_2 a 171 fold (926 fold) increase in concentration of enzyme would be required (Section 5.9). These higher concentrations would then account for 32% (18%) of the total Hb concentration in the erythrocyte. However, such increases could impair the erythrocyte's ability to for performing gaseous exchanges. A significant part of Hb would have to be replaced with antioxidant enzyme, affecting the cell's ability to transport oxygen or carbon dioxide. On the other hand, an increase in cell's size would allow for higher intracellular protein concentrations but could affect the erythrocyte's mobility in capillaries, vessels whose diameter is about that of an erythrocyte. Conversely, replacing catalase or GPx1 with Prx2 would require < 1% increase in Prx2's

concentration. These differences are due to the much higher specific activity of Prx2 compared to the specific activities of catalase or GPx1. Through Prx2, the erythrocyte is thus able to defend itself against low/mild H_2O_2 while requiring less protein to do so.

6.2. Catalase becomes the main scavenger of iH_2O_2 under high oxidative stress

Our results showed that Prx2 accounts for most of the iH_2O_2 consumption for $eH_2O_2 < 3\times10^{-7}$ M (Sections 5.5.1 and 5.6). But what occurs under sustained exposure to high eH_2O_2 such as that found during systemic inflammation? As per our estimates, catalase becomes the main scavenger of iH_2O_2 when the erythrocyte is exposed to $> 3\times10^{-7}$ M eH_2O_2, consuming about 80% of the iH_2O_2, whereas GPx1 consumes <15%.

(Johnson et al., 2010) also assessed the contribution of GPx1, catalase and Prx2 for defense against high H_2O_2. The authors assessed the fraction of MetHb in mice erythrocytes where each of these defenses had been knocked out. As assessed 15 minutes after exposure to a 30×10^{-6} M and 300×10^{-6} M H_2O_2 bolus, catalase-knockouts exhibited 10% and 25% MetHb, respectively. On the other hand, wild type erythrocytes did not exhibit higher fractions of MetHb, regardless of H_2O_2 bolus to which they were exposed. These H_2O_2 boluses respectively yield initial rates of H_2O_2 influx of 2.4×10^{-4} M/s and 2.4×10^{-3} M/s, considering $k_p = 8$ s^{-1} (Section 5.2.1.2). These fluxes largely surpass the erythrocyte's maximum rate of NADPH production [1.9×10^{-6} M/s, (Albrecht et al., 1971)]. Therefore, *PSSP* accumulates and the erythrocyte relies mainly on catalase for defense against H_2O_2. Because of this, catalase-knockout erythrocytes present a much higher *MetHb* accumulation than GPx1-knockouts or wild type erythrocytes.

On the other hand, (Johnson et al., 2010) observed that Prx2-knockout erythrocytes exposed to a 50 - 500×10^{-6} M H_2O_2 bolus did not exhibit higher *MetHb* comparatively to wild-type cells. This led the authors to refer that Prx2 does not contribute significantly for the defense of the erythrocyte against exogenous H_2O_2. Could these eH_2O_2 boluses lead to *PSSP* accumulation, explaining why Prx2-knockouts and wild-type erythrocytes have similar *MetHb*? To analyze this

question we considered the reaction scheme in Figure 6.1, Model 6.1 and parameters from Table 6.1.

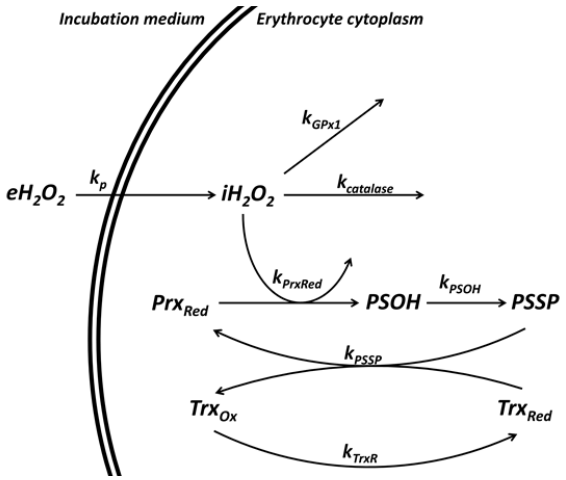

Figure 6.1– Reaction scheme considered to analyze the experiments of (Johnson et al., 2010).

$$\frac{d\ eH_2O_2}{dt} = -k_p \cdot eH_2O_2$$

$$\frac{d\ iH_2O_2}{dt} = k_p \cdot eH_2O_2 - iH_2O_2 \cdot (k_{PrxRed} \cdot Prx_{Red} + k_{catalase} + k_{GPx1})$$

$$\frac{d\ Prx_{Red}}{dt} = k_{PSSP} \cdot PSSP \cdot Trx_{Red} - k_{PrxRed} \cdot Prx_{Red} \cdot iH_2O_2$$

$$\frac{d\ PSOH}{dt} = k_{PrxRed} \cdot Prx_{Red} \cdot iH_2O_2 - k_{PSOH} \cdot PSOH$$

$$\frac{d\ Trx_{Ox}}{dt} = k_{PSSP} \cdot PSSP \cdot Trx_{Red} - k_{TrxR} \cdot Trx_{Ox}$$

$$Prxtot = Prx_{Red} + PSOH + PSSP$$

$$Trxtot = Trx_{Red} + Trx_{Ox}$$

Model 6.1

The parameters of Model 6.1 are expressed in Table 6.1.

Table 6.1 – Parameters used for Model 6.1.

Parameter	Value	Meaning/Reference
k_p	0.42 s^{-1}	First-order rate constant for hydrogen peroxide consumption by erythrocytes. Estimated through Equation 5.32 and considering hematocrit 5%, $V_e = 10^{-13}$ dm^3 (Evans and Fung, 1972), $V_o = 1$ dm^3 and other parameters from Table 5.5 (Section 5.2.1.10) with exception for n.
$k_{catalase}$	218 s^{-1}	Pseudo-first order rate constant for H_2O_2 consumption by catalase (Section 5.1.1.2)
k_{GPx1}	40 s^{-1}	Pseudo-first order rate constant for H_2O_2 consumption by GPx1 (Section 5.1.1.1)
k_{PrxRed}	10^8 $M^{-1}s^{-1}$	Reactivity between reduced Prx2 and H_2O_2 (Manta et al., 2009)
k_{PSOH}	0.26 s^{-1}	First order rate constant for formation of PSSP (Section 5.2.1.10)
k_{PSSP}	2.1×10^5 $M^{-1}s^{-1}$	Reactivity between reduced Trx and PSSP (Manta et al., 2009)

Parameter	Value	Meaning/Reference
k_{TrxR}	0.5 s^{-1}	Pseudo-first order rate constant for Trx reduction through TrxR (Section 5.2.1.9)
Prxtot	37×10^{-4} M	Total concentration of Prx2 monomers (Section 5.1.1.3)
Trxtot	4.8×10^{-6} M	Total Trx concentration (from bovine erythrocytes, 5.2.1.6)

Using Model 6.1 we estimated the fraction of Prx2 in PSSP form for 10 minutes (Figure 6.2), considering the following initial conditions: $eH_2O_2 = 500\times10^{-6}$ M, $iH_2O_2 = 10^{-12}$ M, Prx2 and Trx fully reduced. We also considered that eH_2O_2 is consumed only by permeation across the erythrocyte membrane and no exogenous or endogenous production of iH_2O_2 occurs. Because (Johnson et al., 2010) provided 10^{-2} M glucose to the incubation medium, we also assumed that NADPH is not limiting the activity of Prx2, catalase or GPx1.

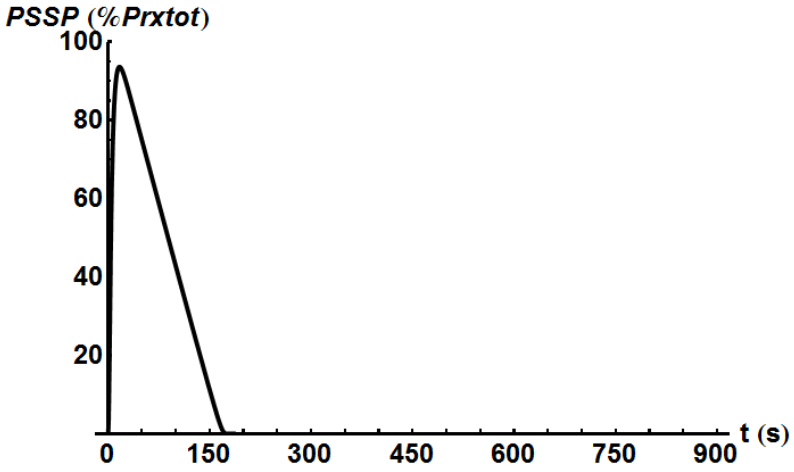

Figure 6.2 – Estimated fraction of *PSSP* in erythrocytes subjected to a 500×10^{-6} M eH_2O_2 bolus in the experiments of (Johnson et al., 2010). Estimated using Model 6.1 and parameters from Table 6.1. See text above for considerations.

Figure 6.2 shows that although *PSSP* initially accumulates, it is completely reduced by the time of assessment of *MetHb* (t=600 s) by (Johnson et al., 2010).

Then why did (Johnson et al., 2010) observe similar *MetHb* in wild-type and Prx2-knockout erythrocytes, regardless of the eH_2O_2 to which erythrocytes were exposed? In their experiments MetHb reduction may have completely regenerated hemoglobin to its native state in both Prx2-knockouts and wild-type erythrocytes. Another possible explanation is that *PSSP* may have accumulated due to uncontrolled oxidation of the erythrocytes during sample preparation.

To clarify this issue the authors could have assessed iH_2O_2 instead of *MetHb*. This would allow understanding if Prx2-knock outs exhibit higher iH_2O_2 when erythrocytes are exposed to eH_2O_2 of various concentrations. Such analysis could then be related with the *MetHb* found by (Johnson

et al., 2010).These points show that further analyses of the iH_2O_2 and NADPH contents in Prx2-deficient erythrocytes are required. To clarify the relevance of Prx2 for defense against iH_2O_2, (Johnson et al., 2010) could have assessed MetHb concentrations after exposure of erythrocytes to lower exogenous H_2O_2.

6.3. The contribution of Prx2 for H_2O_2 consumption is affected by oxidative load and NADPH supply

Under eH_2O_2 higher than a certain threshold (> 3×10^{-7} M, Section 5.6) Prx2 accumulates in PSSP form. This threshold, which we referred to as *crossover*, marks the transition between two regimes: a low oxidative regime (where Prx2 accounts for most of the iH_2O_2 consumption); and a highly oxidative regime (where catalase becomes the main scavenger of iH_2O_2) (Sections 5.1.2 and 5.8). But what affects the eH_2O_2 at which the crossover occurs?

Because Prx2 reduction is coupled with the Trx/TrxR cycle, (Low et al., 2007) hypothesized that accumulation of *PSSP* was affected by a limited TrxR activity. This led the authors to assess TrxR activity. To do so, they used DTNB as a substrate (as discussed in Section 5.2.2) in hemolysates (0.05% dm^3 hemolysate/dm^3). As per our estimates from the authors' data (Section 5.2.2) TrxR is reducing DTNB at a rate of 7.9×10^{-6} M/s, corresponding to a rate of Trx reduction of $\approx6.1\times10^{-6}$ M/s. These rates surpass the maximal rate of NADPH production by the PPP [$=1.9\times10^{-6}$, (Albrecht et al., 1971)], suggesting that NADPH supply and not TrxR activity limits Prx2 regeneration. This is further supported by our estimate of the maximal rate of Trx reduction ($\approx2.4\times10^{-6}$ M/s, Section 5.2.2), in the range of the maximal rate of NADPH produced by the PPP [$=1.9\times10^{-6}$, (Albrecht et al., 1971)].

Yet, determination of the limiting step in Prx2 reduction under high oxidative conditions is associated with some uncertainties. First, the total Trx concentration considered in our estimates was taken from bovine erythrocytes because we have not found reports of concentration in human erythrocytes. Second, our estimate of k_{TrxR} was taken from the immunoblots of the experiments of (Low et al., 2007) (Figure 5.6, Section 5.2.1.9) where the fraction of reduced Prx2 is imprecise. Third, to estimate k_{TrxR} we considered a kinetic model that included singly-

and doubly-crosslinked forms of Prx2 (Figure 5.8, Section 5.2.1.9). Yet, we assumed that reactions leading to Prx2 oxidation would simply occur with rate constant k_{PrxRed}, whereas Prx2 reduction would occur with rate constant k_{PSSP}. However, formation/consumption of singly-crosslinked Prx2 may exhibit different kinetics than those respectively found for the formation/consumption of doubly-crosslinked Prx2.

A more exact determination of *Trxtot* in human erythrocytes could help clarifying the issues above. It could also be interesting to perform the same analyses as (Low et al., 2007) while controlling the rate of NADPH produced by the PPP (by the method of (Gaetani et al., 1989) for instance). One could then relate the rate of NADPH supplied with the redox status of Prx2. However, one should take particular care with uncontrolled oxidation of samples, due to the very high reactivity of Prx2 with H_2O_2.

What would occur if lower k_{TrxR} or *Trxtot* are found in human erythrocytes? In Section 5.6 we determined an analytical expression (Equation 5.62) that allowed us to estimate the conditions under which *PSSP* would accumulate. This analytical expression relates rate of iH_2O_2 influx ($=k_p \times eH_2O_2$) with rate of TrxR activity ($=k_{TrxR} \times Trxtot$) and allows us to draw some predictions of how different k_{TrxR} and *Trxtot* affect the eH_2O_2 at which the crossover occurs. A lower k_{TrxR} due to lower *Trxtot* would shift the crossover to lower eH_2O_2, saving the NADPH pool from depletion by the Prx2/Trx/TrxR cycles. A limited NADPH availability would also lead to lower k_{TrxR}, then decreasing the eH_2O_2 at which the crossover occurs. However, these could also affect Prx2's contribution for iH_2O_2 consumption.

6.4. Prx2's high concentration allows the human erythrocyte to remain protected against H_2O_2 when crossing inflammation sites

The observation that Prx2 is one of the most abundant proteins in the human erythrocyte (Moore et al., 1991) does not seem plausible if Prx2 contributes only for the protection against low (Low et al., 2007) or endogenously generated (Johnson et al., 2010) H_2O_2. Yet, our analyses suggest that a high Prx2 concentration allows protection of human erythrocytes against H_2O_2 from those sites, even if the oxidative insults are relatively strong.

Under mildly pathological conditions such as localized inflammation, erythrocytes are only rarely and briefly exposed to oxidative loads capable of substantially oxidizing Prx2. Most of the gaseous exchanges involving the erythrocyte are done at the capillary level, the blood vessels with smallest diameter and where blood flow is the slowest. This makes capillaries as the locations where erythrocytes are most prone to suffer with oxidation from nearby inflammation sites. As per our estimates, the average residence time of an erythrocyte in a capillary is ≈2 s (Section 5.10.1). Crossing of a capillary may lead to complete Prx2 oxidation if plasma H_2O_2 reaches $>2.5\times10^{-5}$ M (Section 5.11), in the range of the highest H_2O_2 (5×10^{-5} M) found close to wound sites (Niethammer et al., 2009) in other organisms. Therefore, only when erythrocytes cross highly oxidative inflammation foci does Prx2 fully accumulate in PSSP form.

However, a stepwise accumulation of *PSSP* due to crossing of multiple inflammation sites is highly unlikely. We found that erythrocytes are able to regenerate fully oxidized Prx2 to its active form in <3 minutes (Section 5.13) and crossing of multiple inflammation sites takes several hours in between (Section 5.10.2). This allows Prx2 to be completely reduced by the time an erythrocyte crosses another inflammation site (Section 5.10.2). In contrast, (Low et al., 2007) observed that fully oxidized Prx2 takes about 20 minutes to be regenerated back. The differences in time taken for Prx2 reduction may be explained as follows.

In the experiments of (Low et al., 2007) the authors exposed erythrocytes (0.05% hematocrit) to a 5×10^{-6} M H_2O_2 bolus. In less than 1 minute after the exposure they observe full accumulation of PSSP, whereas a large fraction of Prx2 was regenerated in 20 minutes. They also observed that extracellular H_2O_2 is practically fully consumed by erythrocytes in 20 minutes (Figure 5.4, Section 5.2.1.8). These two observations show that erythrocytes were no longer exposed to high oxidative loads, thus allowing Prx2 to be regenerated. The difference between our estimate (<3 min) and the time determined by (Low et al., 2007) for Prx2 reduction could also be due to substantial Prx2 oxidation during sample handling, as discussed above. This difference is also due to the conditions we considered in our estimates: the time taken for Prx2 to be completely reduced was estimated after considering that erythrocytes were exposed to low eH_2O_2 ($=10^{-8}$ M). Yet, even if Prx2 regeneration takes about 20 mins, a stepwise increase in *PSSP* is still highly unlikely.

Altogether, these evidences suggest that a high Prx2 concentration allows crossing of inflammation foci while preventing accumulation of PSSP. Even where Prx2 is completely oxidized, plasma H_2O_2 consumption by erythrocytes is still limited by membrane permeation (Section 5.8). This further supports the claim that human erythrocytes are regarded as the main H_2O_2 sinks in the human blood (Manta et al., 2009; Winterbourn and Stern, 1987).

6.5. Prx2 inactivation and reaction between H_2O_2 and Prx2

In our analyses we considered that sulfinylation of Prx2 may be disregarded as an important process that affects the contribution of Prx2 for H_2O_2 scavenging. This consideration was taken due to the very low reactivity between PSOH and H_2O_2 (k_{PSO2H} = 0.23 M^{-1} s^{-1}, Section 5.7) and is in agreement with previous observations by other authors, as we will now discuss.

(Manta et al., 2009) used an *in vitro* assay (5×10^{-5} M *Prx2*; 8×10^{-6} M *Trx*; 10^{-6} M *TrxR*; 200×10^{-6} M *NADPH*) to determine if Prx2 sulfinylation would be detected in the mixture 10 minutes after beginning of reaction. (Manta et al., 2009) found some sulfinylated Prx2 when a 25×10^{-5} M H_2O_2 bolus was added to the mixture (concentration of sulfinylated Prx2 was not specified).

To examine why (Manta et al., 2009) found accumulation of sulfinylated Prx2 we considered the reaction scheme in Figure 6.3 from which we built Model 6.2.

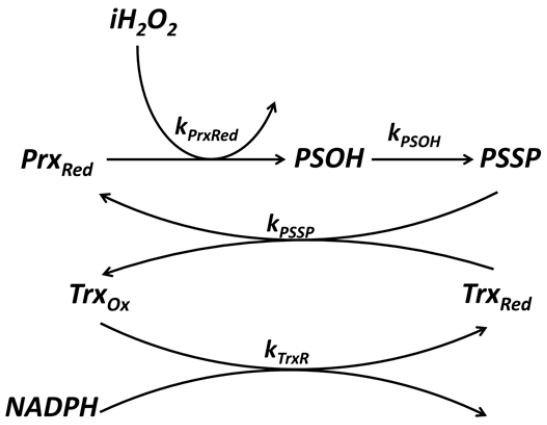

Figure 6.3 – Reaction scheme considered for the analysis of the experiments of (Manta et al., 2009).

$$\frac{d\ H_2O_2}{dt} = -k_{PrxRed} \cdot H_2O_2 \cdot Prx_{Red}$$

$$\frac{d\ Prx_{Red}}{dt} = k_{PSSP} \cdot PSSP \cdot Trx_{Red} - k_{PrxRed} \cdot Prx_{Red} \cdot iH_2O_2$$

$$\frac{d\ PSOH}{dt} = k_{PrxRed} \cdot Prx_{Red} \cdot iH_2O_2 - k_{PSOH} \cdot PSOH$$

$$\frac{d\ Trx_{Ox}}{dt} = k_{PSSP} \cdot PSSP \cdot Trx_{Red} - \frac{V_{max}^{TrxR}}{1 + \frac{K_{m,TrxR}(NADPH)}{NADPH} + \frac{K_m(TrxOx)}{Trx_{Ox}}}$$

Model 6.2

$$\frac{d\ NADPH}{dt} = -\frac{V_{max}^{TrxR}}{1 + \frac{K_{m,TrxR}(NADPH)}{NADPH} + \frac{K_m(TrxOx)}{Trx_{Ox}}}$$

$$Prxtot = Prx_{Red} + PSOH + PSSP$$

$$Trxtot = Trx_{Red} + Trx_{Ox}$$

The parameters of Model 6.2 are expressed in Table 6.2.

Table 6.2 – Parameters used for Model 6.2.

Parameter	Value	Meaning/Reference
$K_m(NADPH)$	6×10^{-6} M	Km of TrxR for NADPH (Urig et al., 2006)
$K_m(Trx)$	1.83×10^{-6} M	Km of TrxR for Trx (Turanov et al., 2006)
k_{PrxRed}	10^8 $M^{-1}s^{-1}$	Reactivity between reduced Prx2 and H_2O_2 (Manta et al., 2009)
k_{PSOH}	0.26 s^{-1}	First order rate constant for formation of PSSP (Section 5.2.1.10)
k_{PSSP}	2.1×10^5 $M^{-1}s^{-1}$	Reactivity between reduced Trx and PSSP (Manta et al., 2009)
$Prxtot$	5×10^{-5} M	Total concentration of Prx2 monomers (Section 5.1.1.3)
$Trxtot$	8×10^{-6} M	Total Trx concentration (from bovine erythrocytes, 5.2.1.6)
V_{max}^{TrxR}	2.58×10^{-6} M/s	Estimated from the product of *TrxR* considered in the experiments of (Manta et al., 2009) ($=10^{-6}$ M) with the catalytic constant k_{cat} = 25.8 s^{-1} (Turanov et al., 2006)

With the aim of understanding the results of (Manta et al., 2009) we aimed to simulate what the authors did through Model 6.2. Using this model we assessed the redox status of Prx2 ten minutes after an initial bolus of 25×10^{-5} M H_2O_2. We considered that H_2O_2 is consumed by Prx2, and that *NADPH* is consumed by TrxR (according to the rate expression in Equation 5.35, Section 5.2.1.9). As per the initial conditions of (Manta et al., 2009) we considered: Prx2 and Trx fully reduced; $NADPH = 200\times10^{-6}$ M; $H_2O_2 = 25\times10^{-5}$ M.

Bearing these considerations in mind, we estimate a iH_2O_2 $\approx1.3\times10^{-4}$ M and a $NADPH \approx 1.8\times10^{-4}$ M when t = 600 s [which corresponds to the time at which (Manta et al., 2009) assessed their mixture for presence of sulfinylated Prx2]. We also found that Prx2 accumulates in PSOH form:

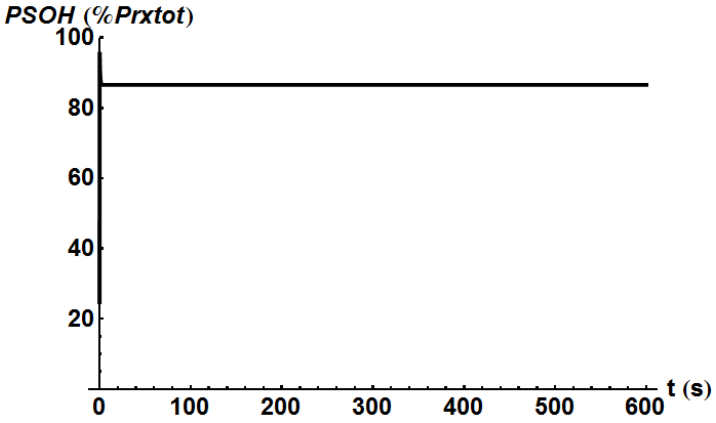

Figure 6.4 – Estimated fraction of *PSOH* in the experiments of (Manta et al., 2009). Estimated through Model 6.2, parameters from Table 6.2. See text above for more considerations.

As the figure above shows, *PSOH* quickly accumulates and remains practically constant until the end of the simulation time. The accumulation of *PSOH* occurs because the pseudo-first order rate constant for Prx_{Red} oxidation, in order to Prx_{Red} ($=k_{PrxRed} \times H_2O_2 \approx 23\ 830\ s^{-1}$) largely surpasses the rate constant for the formation of *PSSP* ($=k_{PSOH} = 0.26\ s^{-1}$, Section 25.2.1.10). Under these conditions, and because there is still plenty *NADPH* and H_2O_2 available, the limiting step in Prx2 activity is the formation of PSSP. Because PSOH accumulates, Prx2 is also prone to accumulate in sulfinylated form. However, iH_2O_2 as high as 25×10^{-5} M largely surpass the physiologically plausible iH_2O_2.

Similarly, (Cho et al., 2010) also addressed whether erythrocytes (50% hematocrit) exposed to 7.5 - 75×10^{-8} M H_2O_2/s would accumulate sulfinylated forms of 2-Cysteine peroxiredoxins, as assessed 3 hours after incubation. The authors found no sulfinylated peroxiredoxin when no exogenous H_2O_2 was provided, which they attributed to sulfiredoxin activity able to regenerate sulfinylated peroxiredoxin under basal oxidative conditions. On the other hand, they found sulfinylated peroxiredoxin when erythrocytes were subjected to 7.5×10^{-8} M H_2O_2/s. However, as acknowledged by the authors, the antibodies used for detecting sulfinylated forms of 2-Cysteine peroxiredoxins do not allow distinction between peroxiredoxins 1 and 2 given their similar catalytic site sequence and size. Because human erythrocytes also possess peroxiredoxin 1 (Marzocchi et al., 2005), the sulfinylated 2-cysteine peroxiredoxin detected may pertain to sulfinylated peroxiredoxin 1, not Prx2.

On the other hand, (Low et al., 2007) found no sulfinylated Prx2 as assessed 10 minutes after human erythrocytes (≈0.05 % hematocrit) were exposed up to $<200\times10^{-6}$ M iH_2O_2 bolus. As per the conditions of the experiment, Prx2 does not accumulate in sulfinylated form because 1. ≈100% of Prx2 was in PSSP form as determined by the authors and 2. because even if Prx2 is in PSSP form, catalase likely prevents accumulation of iH_2O_2 beyond physiologically plausible concentrations that may lead to $k_{PrxRed}\times H_2O_2 > k_{PSOH}$.

Taken together, this evidence suggests that Prx2 sulfinylation is not physiologically relevant for Prx2-mediated H_2O_2 reduction given the very slow rates at which sulfinylated Prx2 accumulates.

6.6. Improvements and experiments needed

Throughout this report we already discussed some of the constraints of our results. We now proceed to further explore some of them and refer some of the studies that could be done to improve our results and answer other questions.

6.6.1. Basal and pathological oxidative loads

As discussed throughout Sections 5.2.1.3, 5.3, 5.10.3 and 5.10.4, the determination of the basal and pathological H_2O_2 loads which erythrocytes face is an experimentally difficult task. Such difficulties come from the sensitivity of the methods used, of the short half-life of H_2O_2, and samples prone to suffer oxidative stress during preparation.

Current methodologies for quantifying H_2O_2 are not sensitive to concentrations much lower than nanomolar. However, our analyses suggest that iH_2O_2 under basal loads should be $< 2\times10^{-11}$ M, allowing most of the Prx2 contents to remain in reduced form. Those methodologies usually rely on coupled reactions to determine the intracellular H_2O_2 loads. It is the case of the catalase inhibition assays employed by (Giulivi et al., 1994) or catalase fluorescence in the work of (Kirkman et al., 1999). If the kinetics of reaction between catalase and inhibitor or between catalase and H_2O_2 are not fast enough, the determination of H_2O_2 concentration is limited by the reactivity between the reactants. Further, if the oxygen which the erythrocytes are exposed to during sample handling is not well controlled, the oxidative stress which these cells may be facing may potentially affect the iH_2O_2 concentration.

A possible way to overcome part of these issues would be to directly quantify H_2O_2 levels from hemolysates in an Argon anaerobic atmosphere, taking special care to minimize leukocyte activation during blood collection. The quantification could be done through H_2O_2 probes that directly quantify H_2O_2 in cells. But these probes are either oxidizable by other substrates (Corbett, 1989; Crow, 1997; Foppoli et al., 2000; Gomes et al., 2005; Wang and Joseph, 1999) or their detection limit does not allow detecting H_2O_2 below the nanomolar range (Zhou et al., 1997). This makes it unfeasible to directly quantify H_2O_2 in erythrocytes.

(Niethammer et al., 2009) developed an H_2O_2 sensor for quantifying H_2O_2. This sensor is introduced onto the embryo of the target organism through mRNA injection, inducing global cytoplasmic expression of the sensor. Later on, the tissue is assessed for the fluorescent excitation of the sensor, whose emission spectra increases upon oxidation by H_2O_2. (Niethammer et al., 2009) used this method in zebrafish to measure the plasma H_2O_2 near wounds and detected $\approx 0.5 - 50\times10^{-6}$ M H_2O_2 in those locations. This sensor was previously used in mammalian cells and was found to be sensitive down to 5×10^{-6} M H_2O_2. Again, despite its potential as an H_2O_2 probe, a couple of problems may arise for using this method to quantify H_2O_2 in mice. First, the ability to use this sensor in mammalian cells was shown in HeLa cells (Belousov et al., 2006). However, this does not guarantee that its insertion in mice embryos is possible, or that the sensor would even be expressed in the erythrocytes' cytoplasm. Second, in order to determine the H_2O_2 levels, blood would have to be collected. This may subject erythrocytes to oxidative stress during handling, due to immune reactions nearby the blood collection site. Thirdly, a higher oxidative stress could result from sample handling (uncontrolled oxygen conditions during handling).

The issues above further show the difficulty in quantification of intracellular and extracellular H_2O_2 levels in blood. Better and more sensitive methods for assaying H_2O_2 concentration are needed in order to obtain more precise determinations of the redox behavior of Prx2/Trx cycles under various conditions.

6.6.2. Catalytic cycle of catalase

In our work we considered that catalase-mediated H_2O_2 consumption is a first order process with respect to H_2O_2. As discussed in Section 5.2.1.1, the accumulation of Intermediate and Compound II forms of catalase is likely not very prevalent, provided that NADPH availability does not lead to accumulation of Compound II.

However, the kinetics of formation and consumption of Intermediate are not completely characterized and further experiments are required to assess them. This is an experimental complicated issue, given the instability of the Intermediate. So instead of assessing the kinetics of formation and consumption of Intermediate, one could analyze the formation of Compound II and kinetics of NADPH consumption by catalase. This could be done *in vitro* with purified enzyme and under controlled NADPH and H_2O_2 conditions.

The rate of NADPH consumption by catalase could be studied under various NADPH and H_2O_2 concentrations. This would allow not only studying the kinetics of NADPH oxidation by catalase but also under which H_2O_2 concentration is NADPH consumption limited by H_2O_2 availability. The concentrations of different catalase forms and NADPH could be determined through spectrophotometric assays as previously described (Hillar et al., 1994; Kirkman et al., 1999). The levels of H_2O_2 could be determined through H_2O_2 probes. However, the probes' sensitivity to H_2O_2 would have to allow measuring H_2O_2 $<10^{-10}$ M (in Section 5.2.1.1 we estimated that catalase-mediated NADPH oxidation is limited by H_2O_2 availability if H_2O_2 is below this concentration). Yet, this H_2O_2 may be too low for quantification by any probe so special care in choosing the H_2O_2 quantification method would have to be taken.

In future studies we intend on including the full catalytic cycle of catalase, considering also catalase inactivation. By doing so we would be able to obtain the conditions in which the dismutase activity is a first-order process with respect to H_2O_2, and address if catalase inactivation may occur *in vivo*.

6.6.3. Frequency of crossing inflammation sites and H_2O_2 induced by crossing inflammation sites

In Section 5.10.2 we estimated the frequency taken by an erythrocyte to cross two consecutive inflammation sites. The value estimated represents a rough approximation and depends on various factors such as number, location and volume of the inflammation foci; capillary density nearby the inflammation foci; heart beat rate; body volume; etc. Yet, could any experiment be designed to determine a more accurate frequency of crossing a localized inflammation site?

If a single erythrocyte could be labeled and exhibit different signal-intensity levels of the label upon exposure to H_2O_2, this could potentially be assessed. Yet, this would require that a whole body analysis method would detect even the small signal intensity emitted by that single cell.

However, this is technically not possible because whole body assays do not permit such a high degree of sensitivity.

Another issue that could help understanding the behavior of Prx2/Trx cycles in human would be to determine the oxidative load which an erythrocyte is subjected to when crossing an inflammation site. A possible way to assess this issue would be to first induce the expression of an H_2O_2 sensor such as the one used by (Belousov et al., 2006) in the cytoplasm of mice erythrocytes. Afterwards, one could induce a wound in the tail of the mouse and inject the modified erythrocytes very close to the wound. By collecting the modified erythrocytes after these have passed by the wound and quantifying the fluorescence of the H_2O_2 sensor, we would be able to measure the H_2O_2 which an erythrocyte is exposed to. However, the mere injection and blood collection could induce an inflammatory response. Thus we would also have to perform the same assay without inducing the wound. The difference in fluorescence in the cytoplasm of the erythrocytes that had crossed the wound versus the erythrocytes that were injected but had no wound would give the H_2O_2 which erythrocytes would be subjected to.

However, a fundamental issue associated with this method is that the mere injection and blood collection could lead to a very high oxidative stress. If the oxidative load was high enough to lead to full oxidation of Prx2, the iH_2O_2 would be much higher than what would be gotten by mere crossing of inflammation sites.

6.6.4. Peroxidase activity and relevance of Prx2 for H_2O_2 defense

In ouranalyses we considered a simplified redox cycle of Prx2. However, a few experiments could improve our estimates and allowa more accurate description of the behavior of the Prx2/Trx cycles.

The rate constant for PSSP formation could be better determined. We estimated this rate constant from the NADPH oxidation assays of (Manta et al., 2009). However, if it was possible to determine the redox state of Prx2 through a spectrometric assay, one could follow the formation and consumption of PSSP and obtain the rate constant for PSSP formation. (Monteiro et al., 2007) used spectrometric assays to determine the redox status of cysteines of the yeast peroxiredoxin 1. Possibly the same method may be done with Prx2 isolated from human erythrocytes to further determine the kinetics of PSSP formation.

Another issue that needs to be further analyzed is what limits the peroxidase activity of Prx2 at high oxidative loads. Our analyses suggest that NADPH (not Trx) concentration, limit Prx2 activity and the maximum rate of H_2O_2 reduction achieved by Prx2. But because the Trx concentration we considered was taken from bovine erythrocytes, this protein also needs to be quantified in human erythrocytes in order to verify if the total Trx concentration may limit the peroxidase activity of Prx2.

Another issue that potentially may affect the peroxidase activity of Prx2 is the kinetics of Trx reduction by TrxR. In our study we considered that TrxR exhibits first-order kinetics with respect to Trx. However, it would be interesting to express the full ping-pong kinetics of TrxR in our models to address how the kinetic parameters of this enzyme relate with oxidative load and NADPH availability. The issue of NADPH availability and how it potentially affects the activity of each enzyme is discussed further below.

In our results we also found that Prx2 has a very high specific activity, comparatively to catalase and GPx1. Because of this, the erythrocyte requires less protein to remain protected against low H_2O_2 than if it was using catalase for instance. However, high oxidative loads limit Prx2 activity, which is when catalase becomes the main defense against H_2O_2. Given that catalases and peroxiredoxins are widely distributed in nature, could the properties of H_2O_2 defense found in the human erythrocyte be shared in other organisms? This will be the case if such organisms possess a peroxidase with very high specific activity and an H_2O_2 dismutase with lower specific activity but that requires less reducing equivalents.

Indeed a few similarities between the main H_2O_2 defense systems found in the human erythrocyte are shared with other organisms. First, studies done in *Saccharomyces cerevisiae* (Munhoz and Netto, 2004), *Escherichia coli* (Seaver and Imlay, 2001) and other bacteria (Cosgrove et al., 2007; Hebrard et al., 2009; LeBlanc et al., 2006) showed that the main defenses of these cells against H_2O_2 complement each other: peroxiredoxins protect the cell against low hydrogen peroxide levels whereas catalases are required to protect the cell against stronger oxidative stress. Second, peroxiredoxins are much more abundant than catalases in *E. coli* (Link et al., 1997; Lopez-Campistrous et al., 2005; Taoka et al., 2004) and *S. cerevisiae* (Ghaemmaghami et al., 2003). Third, in *E. coli* the reactivity of one of the peroxiredoxins with H_2O_2 (Niimura et al., 1995) is much larger than the reactivity of catalases (Hillar et al., 2000)

with the same substrate. Fourth, the specific activity of that peroxiredoxin is more than tenfold higher than the reactivity of catalase with the same substrate[5]. Taken together, these evidences suggest that the principles found in human erythrocytes in terms of redox behavior of its H_2O_2 defenses could be found in other cells. If that is the case, the utilization of peroxiredoxins thus allows cells to minimize the biosynthetic and space costs of H_2O_2 defense, while the utilization of catalases minimizes the cost of H_2O_2 defense in terms of utilization of reducing equivalents.

It could be interesting to address if these features would be observed in *E. coli* and *S. cerevisiae,* explaining why those organisms also possess two types of defenses against H_2O_2. This could be addressed through a similar approach to the one used in this work. A few more issues could also be analyzed: the relevance of each system for H_2O_2 defense; their competition for reducing equivalents when these are scarce; the costs of replacing one of the antioxidants by the other (in terms of consumption of reducing equivalents and concentration of protein required).

6.6.5. Effects of NADPH supply on H_2O_2 defense

It could be very useful to understand the effects of a limited NADPH supply for the contribution of each antioxidant for defense against H_2O_2. Although we expect catalase to not be greatly affected by a low NADPH supply given its low NADPH requirement, NADPH availability may limit the antioxidant activities of Prx2 and GPx1. This would occur when the NADPH supply cannot keep up with the demand for reducing equivalents. The reduction of Prx2 and GSH would then be limited, affecting the contribution of Prx2 and GPx1 for antioxidant protection.

Indeed, in work done after this study we already addressed some of the effects of limited NADPH availability on the activities of Prx2 and GPx1. We already considered full GPx1/GSH/GSR cycles; NADPH consumption by TrxR and GSR; and a saturable NADPH supply by the PPP. We found that the kinetic parameters of TrxR and GSR permit that GSR outcompetes TrxR for NADPH when the demand for reducing equivalents exceeds the supply. This allows the reduction of oxidized glutathione to be privileged over Prx2 regeneration, suggesting that it is more important for the erythrocyte to maintain glutathione in reduced form

---

[5] The peroxiredoxin AHPC has higher specific activity (≈3×10^{-3} mol H_2O_2/s/g, estimated considering k_{cat} = 76 s^{-1} (Baker and Poole, 2003) and MW = 20 762 Da (Kwon et al., 2008)) than the catalase [≈0.1×10^{-3} mol/s/g (Visick and Clarke, 1997)].

than maintaining the peroxidase activity of Prx2. This may be because glutathione reduction enables GPx1-mediated scavenging of organic peroxides and prevents accumulation of oxidized glutathione, a compound toxic for the cell.

Together with the results presented in this report, the work done afterwards shows the complementarity of these antioxidant systems. The utilization of Prx2 allows the cell to keep a low iH_2O_2 and fast response time while minimizing the protein committed to H_2O_2 defense under low oxidative loads. On the other hand, catalase's low NADPH requirements makes its contribution for H_2O_2 defense particularly important under conditions in which NADPH supply limits Prx2 reduction. GPx1 contributes little for H_2O_2 elimination it is important for the elimination of organic peroxides that also accumulate under oxidative stress. Lastly, the kinetic parameters of TrxR and GSR are orchestrated in such way that the GPx1/GSR system has priority over the Prx2/TrxR system in its access to NADPH when NADPH becomes scarce, likely due to GPx1's role in defense against organic peroxides.

6.7. Relevance of the study

Our results bring important insight onto the possible roles of catalase, Prx2 and GPx1 for antioxidant defense in erythrocytes. It was previously thought that catalase was the main defense against H_2O_2 in human erythrocytes. Our results showed that Prx2 is the main defense of the human erythrocyte against H_2O_2 under most physiological conditions.

Peroxiredoxin deficiency and inactivation has been implicated in many diseases such as development of various cancer types (Neumann et al., 2003), anemia (Johnson et al., 2010; Neumann et al., 2003), senescence (Han et al., 2005), Parkinson's disease (Przedborski, 2007), and many other pathologies. Yet, because peroxiredoxins were previously thought to protect only against low H_2O_2 concentrations, the study of those proteins was not an important issue. Our results potentially change this, shedding new light onto the potential role that peroxiredoxins may have for preventing the development of those diseases. By demonstrating that peroxiredoxins are one of the most important proteins in the protection of human erythrocytes from H_2O_2, new studies are required to determine how Prx2 activity is related with the development of those pathologies. Prx2 is a widely distributed protein and development of those

diseases may be associated with the inability to maintain active Prx2 and the H_2O_2-associated progression of those pathologies.

7. Conclusion

Peroxiredoxin 2 is the main defense of human erythrocytes against hydrogen peroxide under most physiological circumstances. It protects this cell upon sustained exposure to low/mild hydrogen peroxide loads. Under strong oxidative conditions its antioxidant activity is impaired and the erythrocyte mainly relies on catalase for the defense against hydrogen peroxide. Even when peroxiredoxin 2 is inactivated, plasma hydrogen peroxide consumption by erythrocytes is limited by membrane permeation.

Due to the much higher specific activity of peroxiredoxin 2, replacement of this protein by catalase or glutathione peroxidase is physiologically not plausible. Also, the very large abundance of peroxiredoxin 2 in the human erythrocyte allows the protection against hydrogen peroxide when the erythrocyte crosses inflammation sites.

Our results have important implications for the study of antioxidant protection and reactive oxygen species-associated diseases in mammalian cells.

8. References

Aebi, H. (1984). Catalase in vitro. Methods Enzymol *105*, 121-126.

Ager, A., and Gordon, J.L. (1984). Differential effects of hydrogen peroxide on indices of endothelial cell function. J Exp Med *159*, 592-603.

Albrecht, V., Roigas, H., Schultze, M., Jacobasch, G., and Rapoport, S. (1971). The influence of pH and methylene blue on the pathways of glucose utilization and lactate formation in erythrocytes of man. Eur J Biochem *20*, 44-50.

Arscott, L.D., Gromer, S., Schirmer, R.H., Becker, K., and Williams, C.H., Jr. (1997). The mechanism of thioredoxin reductase from human placenta is similar to the mechanisms of lipoamide dehydrogenase and glutathione reductase and is distinct from the mechanism of thioredoxin reductase from Escherichia coli. Proc Natl Acad Sci U S A *94*, 3621-3626.

Avissar, N., Whitin, J.C., Allen, P.Z., Wagner, D.D., Liegey, P., and Cohen, H.J. (1989). Plasma selenium-dependent glutathione peroxidase. Cell of origin and secretion. J Biol Chem *264*, 15850-15855.

Awasthi, Y.C., Beutler, E., and Srivastava, S.K. (1975). Purification and properties of human erythrocyte glutathione peroxidase. J Biol Chem *250*, 5144-5149.

Baker, L.M., and Poole, L.B. (2003). Catalytic mechanism of thiol peroxidase from Escherichia coli. Sulfenic acid formation and overoxidation of essential CYS61. J Biol Chem *278*, 9203-9211.

Belousov, V.V., Fradkov, A.F., Lukyanov, K.A., Staroverov, D.B., Shakhbazov, K.S., Terskikh, A.V., and Lukyanov, S. (2006). Genetically encoded fluorescent indicator for intracellular hydrogen peroxide. Nat Methods *3*, 281-286.

Ben-Haim, S., Kupzov, E., Tamir, A., and Israel, O. (2004). Evaluation of 18F-FDG uptake and arterial wall calcifications using 18F-FDG PET/CT. J Nucl Med *45*, 1816-1821.

Bernstein, F.C., Koetzle, T.F., Williams, G.J., Meyer, E.F., Jr., Brice, M.D., Rodgers, J.R., Kennard, O., Shimanouchi, T., and Tasumi, M. (1977). The Protein Data Bank: a computer-based archival file for macromolecular structures. J Mol Biol *112*, 535-542.

Beutler, E. (1977). Glucose-6-phosphate dehydrogenase deficiency and red cell glutathione peroxidase. Blood *49*, 467-469.

Beutler, E. (1984). Red cell metabolism : a manual of biochemical methods, 3rd edn (Orlando, FL, Grune & Stratton).

Biteau, B., Labarre, J., and Toledano, M. (2003). ATP-dependent reduction of cysteine-sulphinic acid by S. cerevisiae sulphiredoxin. Nature *425*, 980-984.

Bonaventura, J., Schroeder, W.A., and Fang, S. (1972). Human erythrocyte catalase: an improved method of isolation and a reevaluation of reported properties. Arch Biochem Biophys *150*, 606-617.

Brin, M., and Yonemoto, R.H. (1958). Stimulation of the glucose oxidative pathway in human erythrocytes by methylene blue. J Biol Chem *230*, 307-317.

Broughton, G.n., Janis, J., and Attinger, C. (2006). Wound healing: an overview. Plast Reconstr Surg *117*, 1e-S-32e-S.

Bunn, H., and Forget, B. (1986). Hemoglobin: molecular, genetic and clinical aspects (WB Saunders Co. Philadelphia).

Bunyan, J., Green, J., Edwin, E.E., and Diplock, A.T. (1960). Studies on vitamin E. 5. Lipid peroxidation in dialuric acid-induced haemolysis of vitamin E-deficient erythrocytes. Biochem J *77*, 47-51.

Cameron, J.R., Skofronick, J.G., and Grant, R.M. (1999). Physics of the Body.

Cha, M., and Kim, I. (1995). Thioredoxin-linked peroxidase from human red blood cell: evidence for the existence of thioredoxin and thioredoxin reductase in human red blood cell. Biochem Biophys Res Commun *217*, 900-907.

Cha, M., Yun, C., and Kim, I. (2000). Interaction of human thiol-specific antioxidant protein 1 with erythrocyte plasma membrane. Biochemistry *39*, 6944-6950.

Chae, H., Chung, S., and Rhee, S. (1994a). Thioredoxin-dependent peroxide reductase from yeast. J Biol Chem *269*, 27670-27678.

Chae, H.Z., Kim, I.H., Kim, K., and Rhee, S.G. (1993). Cloning, sequencing, and mutation of thiol-specific antioxidant gene of Saccharomyces cerevisiae. J Biol Chem *268*, 16815-16821.

Chae, H.Z., Robison, K., Poole, L.B., Church, G., Storz, G., and Rhee, S.G. (1994b). Cloning and sequencing of thiol-specific antioxidant from mammalian brain: alkyl hydroperoxide reductase and thiol-specific antioxidant define a large family of antioxidant enzymes. Proc Natl Acad Sci U S A *91*, 7017-7021.

Chance, B., Greenstein, D.S., and Roughton, F.J. (1952). The mechanism of catalase action. I. Steady-state analysis. Arch Biochem *37*, 301-321.

Chance, B., Sies, H., and Boveris, A. (1979). Hydroperoxide metabolism in mammalian organs. Physiol Rev *59*, 527-605.

Chang, T.S., Jeong, W., Woo, H.A., Lee, S.M., Park, S., and Rhee, S.G. (2004). Characterization of mammalian sulfiredoxin and its reactivation of hyperoxidized peroxiredoxin through reduction of cysteine sulfinic acid in the active site to cysteine. J Biol Chem *279*, 50994-51001.

Cho, C.S., Lee, S., Lee, G.T., Woo, H.A., Choi, E.J., and Rhee, S.G. (2010). Irreversible inactivation of glutathione peroxidase 1 and reversible inactivation of peroxiredoxin II by H2O2 in red blood cells. Antioxid Redox Signal *12*, 1235-1246.

Cohen, G., and Hochstein, P. (1963). Glutathione peroxidase: The primary agent for the elimination of hydrogen peroxide in erythrocytes. Biochemistry *2*, 1420-1428.

Cohen, G., and Hochstein, P. (1964). Generation of Hydrogen Peroxide in Erythrocytes by Hemolytic Agents. Biochemistry *3*, 895-900.

Cohnheim, J. (1877). Thrombose und Embolie: Vorlesung über allgemeine Pathologie. Berlin, Germany: Hirschwald *134*.

Corbett, J.T. (1989). The scopoletin assay for hydrogen peroxide. A review and a better method. J Biochem Biophys Methods *18*, 297-307.

Cosgrove, K., Coutts, G., Jonsson, I.M., Tarkowski, A., Kokai-Kun, J.F., Mond, J.J., and Foster, S.J. (2007). Catalase (KatA) and alkyl hydroperoxide reductase (AhpC) have compensatory roles in peroxide stress resistance and are required for survival, persistence, and nasal colonization in Staphylococcus aureus. J Bacteriol *189*, 1025-1035.

Crow, J.P. (1997). Dichlorodihydrofluorescein and dihydrorhodamine 123 are sensitive indicators of peroxynitrite in vitro: implications for intracellular measurement of reactive nitrogen and oxygen species. Nitric Oxide *1*, 145-157.

Davies, J.M., Lowry, C.V., and Davies, K.J. (1995). Transient adaptation to oxidative stress in yeast. Arch Biochem Biophys *317*, 1-6.

Davies, K.J., and Goldberg, A.L. (1987). Proteins damaged by oxygen radicals are rapidly degraded in extracts of red blood cells. J Biol Chem *262*, 8227-8234.

Dvorak, H.F. (1986). Tumors: wounds that do not heal. Similarities between tumor stroma generation and wound healing. N Engl J Med *315*, 1650-1659.

Evans, E., and Fung, Y. (1972). Improved measurements of the erythrocyte geometry. Microvasc Res *4*, 335-347.

Faggiotto, A., Ross, R., and Harker, L. (1984). Studies of hypercholesterolemia in the nonhuman primate. I. Changes that lead to fatty streak formation. Arteriosclerosis *4*, 323-340.

Flindt, R. (2006). Amazing numbers in biology.

Flohe, L. (1978). Glutathione peroxidase: fact and fiction. Ciba Found Symp, 95-122.

Flohé, L., Loschen, G., Günzler, W., and Eichele, E. (1972). Glutathione peroxidase, V. The kinetic mechanism. Hoppe Seylers Z Physiol Chem *353*, 987-999.

Foppoli, C., Coccia, R., Blarzino, C., and Rosei, M.A. (2000). Formation of homovanillic acid dimer by enzymatic or Fenton system - catalyzed oxidation. Int J Biochem Cell Biol *32*, 657-663.

Fox, J.B., Jr., Nicholas, R.A., Ackerman, S.A., and Swift, C.E. (1974). A multiple wavelength analysis of the reaction between hydrogen peroxide and metmyoglobin. Biochemistry *13*, 5178-5186.

Frei, B., Stocker, R., and Ames, B.N. (1988). Antioxidant defenses and lipid peroxidation in human blood plasma. Proc Natl Acad Sci U S A *85*, 9748-9752.

Gaetani, G., Ferraris, A., Rolfo, M., Mangerini, R., Arena, S., and Kirkman, H. (1996). Predominant role of catalase in the disposal of hydrogen peroxide within human erythrocytes. Blood *87*, 1595-1599.

Gaetani, G.D., Parker, J.C., and Kirkman, H.N. (1974). Intracellular restraint: a new basis for the limitation in response to oxidative stress in human erythrocytes containing low-activity variants of glucose-6-phosphate dehydrogenase. Proc Natl Acad Sci U S A *71*, 3584-3587.

Gaetani, G.F., Galiano, S., Canepa, L., Ferraris, A.M., and Kirkman, H.N. (1989). Catalase and glutathione peroxidase are equally active in detoxification of hydrogen peroxide in human erythrocytes. Blood *73*, 334-339.

Gaetani, G.F., Kirkman, H.N., Mangerini, R., and Ferraris, A.M. (1994). Importance of catalase in the disposal of hydrogen peroxide within human erythrocytes. Blood *84*, 325-330.

Gerber, G., Berger, H., Janig, G.R., and Rapoport, S.M. (1973). Interaction of haemoglobin with ions. Quantitative description of the state of magnesium, adenosine 5'-triphosphate, 2,3-bisphosphoglycerate, and human haemoglobin under simulated intracellular conditions. Eur J Biochem *38*, 563-571.

Gerrity, R.G., Naito, H.K., Richardson, M., and Schwartz, C.J. (1979). Dietary induced atherogenesis in swine. Morphology of the intima in prelesion stages. Am J Pathol *95*, 775-792.

Ghaemmaghami, S., Huh, W., Bower, K., Howson, R., Belle, A., Dephoure, N., O'Shea, E., and Weissman, J. (2003). Global analysis of protein expression in yeast. Nature *425*, 737-741.

Giulivi, C., and Davies, K.J. (1990). A novel antioxidant role for hemoglobin. The comproportionation of ferrylhemoglobin with oxyhemoglobin. J Biol Chem *265*, 19453-19460.

Giulivi, C., Hochstein, P., and Davies, K. (1994). Hydrogen peroxide production by red blood cells. Free Radic Biol Med *16*, 123-129.

Gomes, A., Fernandes, E., and Lima, J.L. (2005). Fluorescence probes used for detection of reactive oxygen species. J Biochem Biophys Methods *65*, 45-80.

Gonzalez-Flecha, B., and Demple, B. (1995). Metabolic sources of hydrogen peroxide in aerobically growing Escherichia coli. J Biol Chem *270*, 13681-13687.

Guidotti, G. (1967). Studies on the chemistry of hemoglobin. I. The reactive sulfhydryl groups. J Biol Chem *242*, 3673-3684.

Gunzler, W.A., Kremers, H., and Flohe, L. (1974). An improved coupled test procedure for glutathione peroxidase (EC 1-11-1-9-) in blood. Z Klin Chem Klin Biochem *12*, 444-448.

Guyton, A.C. (1984). Physiology of the human body (Saunders College Pub.).

Halliwell, B., Clement, M., and Long, L. (2000). Hydrogen peroxide in the human body. FEBS Lett *486*, 10-13.

Han, Y.H., Kim, H.S., Kim, J.M., Kim, S.K., Yu, D.Y., and Moon, E.Y. (2005). Inhibitory role of peroxiredoxin II (Prx II) on cellular senescence. FEBS Lett *579*, 4897-4902.

Harlan, J.M., Levine, J.D., Callahan, K.S., Schwartz, B.R., and Harker, L.A. (1984). Glutathione redox cycle protects cultured endothelial cells against lysis by extracellularly generated hydrogen peroxide. J Clin Invest *73*, 706-713.

Hartz, J., Funakoshi, S., and Deutsch, H. (1973). The levels of superoxide dismutase and catalase in human tissues as determined immunochemically. Clin Chim Acta *46*, 125-132.

Hebrard, M., Viala, J.P., Meresse, S., Barras, F., and Aussel, L. (2009). Redundant hydrogen peroxide scavengers contribute to Salmonella virulence and oxidative stress resistance. J Bacteriol *191*, 4605-4614.

Hillar, A., and Nicholls, P. (1992). A mechanism for NADPH inhibition of catalase compound II formation. FEBS Lett *314*, 179-182.

Hillar, A., Nicholls, P., Switala, J., and Loewen, P.C. (1994). NADPH binding and control of catalase compound II formation: comparison of bovine, yeast, and Escherichia coli enzymes. Biochem J *300 (Pt 2)*, 531-539.

Hillar, A., Peters, B., Pauls, R., Loboda, A., Zhang, H., Mauk, A.G., and Loewen, P.C. (2000). Modulation of the activities of catalase-peroxidase HPI of Escherichia coli by site-directed mutagenesis. Biochemistry *39*, 5868-5875.

Ho, Y., Xiong, Y., Ma, W., Spector, A., and Ho, D. (2004). Mice lacking catalase develop normally but show differential sensitivity to oxidant tissue injury. J Biol Chem *279*, 32804-32812.

Ho, Y.S., Magnenat, J.L., Bronson, R.T., Cao, J., Gargano, M., Sugawara, M., and Funk, C.D. (1997). Mice deficient in cellular glutathione peroxidase develop normally and show no increased sensitivity to hyperoxia. J Biol Chem *272*, 16644-16651.

Hofmann, B., Hecht, H., and Flohé, L. (2002). Peroxiredoxins. Biol Chem *383*, 347-364.

Holmgren, A., and Luthman, M. (1978). Tissue distrubution and subcellular localization of bovine thioredoxin determined by radioimmunoassay. Biochemistry *17*, 4071-4077.

Honig, C.R., Feldstein, M.L., and Frierson, J.L. (1977). Capillary lengths, anastomoses, and estimated capillary transit times in skeletal muscle. Am J Physiol *233*, H122-129.

Ivancich, A., Jouve, H.M., and Gaillard, J. (1996). EPR evidence for a tyrosyl radical intermediate in bovine liver catalase. Journal of the American Chemical Society *118*, 12852-12853.

Ivancich, A., Jouve, H.M., Sartor, B., and Gaillard, J. (1997). EPR investigation of compound I in Proteus mirabilis and bovine liver catalases: formation of porphyrin and tyrosyl radical intermediates. Biochemistry *36*, 9356-9364.

Iyer, G.Y., Islam, M.F., and Quastel, J.H. (1961). Biochemical aspects of phagocytosis. Nature *192*, 535-&.

Jacobson, F.S., Morgan, R.W., Christman, M.F., and Ames, B.N. (1989). An alkyl hydroperoxide reductase from Salmonella typhimurium involved in the defense of DNA against oxidative damage. Purification and properties. J Biol Chem *264*, 1488-1496.

Jang, H., Lee, K., Chi, Y., Jung, B., Park, S., Park, J., Lee, J., Lee, S., Moon, J., Yun, J.*, et al.* (2004). Two enzymes in one; two yeast peroxiredoxins display oxidative stress-dependent switching from a peroxidase to a molecular chaperone function. Cell *117*, 625-635.

Johnson, R., Goyette, G.J., Ravindranath, Y., and Ho, Y. (2000). Red cells from glutathione peroxidase-1-deficient mice have nearly normal defenses against exogenous peroxides. Blood *96*, 1985-1988.

Johnson, R., Goyette, G.J., Ravindranath, Y., and Ho, Y. (2002). Oxidation of glutathione peroxidase-deficient red cells by organic peroxides. Blood *100*, 1515-1516.

Johnson, R., Goyette, G.J., Ravindranath, Y., and Ho, Y. (2005). Hemoglobin autoxidation and regulation of endogenous H2O2 levels in erythrocytes. Free Radic Biol Med *39*, 1407-1417.

Johnson, R., Ho, Y., Yu, D., Kuypers, F., Ravindranath, Y., and Goyette, G. (2010). The effects of disruption of genes for peroxiredoxin-2, glutathione peroxidase-1, and catalase on erythrocyte oxidative metabolism. Free Radic Biol Med *48*, 519-525.

Jones, D.P., Brown, L.A., and Sternberg, P. (1995). Variability in glutathione-dependent detoxication in vivo and its relevance to detoxication of chemical mixtures. Toxicology *105*, 267-274.

Jones, D.P., Mody, V.C., Jr., Carlson, J.L., Lynn, M.J., and Sternberg, P., Jr. (2002). Redox analysis of human plasma allows separation of pro-oxidant events of aging from decline in antioxidant defenses. Free Radic Biol Med *33*, 1290-1300.

Kazura, J.W., Fanning, M.M., Blumer, J.L., and Mahmoud, A.A. (1981). Role of cell-generated hydrogen peroxide in granulocyte-mediated killing of schistosomula of Schistosoma mansoni in vitro. J Clin Invest *67*, 93-102.

Kim, I.H., Kim, K., and Rhee, S.G. (1989). Induction of an antioxidant protein of Saccharomyces cerevisiae by O2, Fe3+, or 2-mercaptoethanol. Proc Natl Acad Sci U S A *86*, 6018-6022.

Kim, K., Kim, I.H., Lee, K.Y., Rhee, S.G., and Stadtman, E.R. (1988). The isolation and purification of a specific "protector" protein which inhibits enzyme inactivation by a thiol/Fe(III)/O2 mixed-function oxidation system. J Biol Chem *263*, 4704-4711.

Kim, K., Rhee, S.G., and Stadtman, E.R. (1985). Nonenzymatic cleavage of proteins by reactive oxygen species generated by dithiothreitol and iron. J Biol Chem *260*, 15394-15397.

King, N.K., and Winfield, M.E. (1963). The mechanism of metmyoglobin oxidation. J Biol Chem *238*, 1520-1528.

Kirkman, H., Rolfo, M., Ferraris, A., and Gaetani, G. (1999). Mechanisms of protection of catalase by NADPH. Kinetics and stoichiometry. J Biol Chem *274*, 13908-13914.

Kirkman, H.N., Gaetani, G.D., Clemons, E.H., and Mareni, C. (1975). Red cell NADP+ and NADPH in glucose-6-phosphate dehydrogenase deficiency. J Clin Invest *55*, 875-878.

Kirkman, H.N., and Gaetani, G.F. (1984). Catalase: a tetrameric enzyme with four tightly bound molecules of NADPH. Proc Natl Acad Sci U S A *81*, 4343-4347.

Kirkman, H.N., and Gaetani, G.F. (1986). Regulation of glucose-6-phosphate dehydrogenase in human erythrocytes. J Biol Chem *261*, 4033-4038.

Kirkman, H.N., Gaetani, G.F., and Clemons, E.H. (1986). NADP-binding proteins causing reduced availability and sigmoid release of NADP+ in human erythrocytes. J Biol Chem *261*, 4039-4045.

Kirkman, H.N., Galiano, S., and Gaetani, G.F. (1987). The function of catalase-bound NADPH. J Biol Chem *262*, 660-666.

Kwon, S., Jung, Y., and Lim, D. (2008). Proteomic analysis of heat-stable proteins in Escherichia coli. BMB Rep *41*, 108-111.

Lacy, F., O'Connor, D.T., and Schmid-Schonbein, G.W. (1998). Plasma hydrogen peroxide production in hypertensives and normotensive subjects at genetic risk of hypertension. J Hypertens *16*, 291-303.

LeBlanc, J.J., Davidson, R.J., and Hoffman, P.S. (2006). Compensatory functions of two alkyl hydroperoxide reductases in the oxidative defense system of Legionella pneumophila. J Bacteriol *188*, 6235-6244.

Lee, T., Kim, S., Yu, S., Kim, S., Park, D., Moon, H., Dho, S., Kwon, K., Kwon, H., Han, Y.*, et al.* (2003). Peroxiredoxin II is essential for sustaining life span of erythrocytes in mice. Blood *101*, 5033-5038.

Lim, Y.S., Cha, M.K., Kim, H.K., and Kim, I.H. (1994a). The thiol-specific antioxidant protein from human brain: gene cloning and analysis of conserved cysteine regions. Gene *140*, 279-284.

Lim, Y.S., Cha, M.K., Yun, C.H., Kim, H.K., Kim, K., and Kim, I.H. (1994b). Purification and characterization of thiol-specific antioxidant protein from human red blood cell: a new type of antioxidant protein. Biochem Biophys Res Commun *199*, 199-206.

Lindner, J.R., Dayton, P.A., Coggins, M.P., Ley, K., Song, J., Ferrara, K., and Kaul, S. (2000). Noninvasive imaging of inflammation by ultrasound detection of phagocytosed microbubbles. Circulation *102*, 531-538.

Lindner, J.R., Song, J., Christiansen, J., Klibanov, A.L., Xu, F., and Ley, K. (2001). Ultrasound assessment of inflammation and renal tissue injury with microbubbles targeted to P-selectin. Circulation *104*, 2107-2112.

Link, A.J., Robison, K., and Church, G.M. (1997). Comparing the predicted and observed properties of proteins encoded in the genome of Escherichia coli K-12. Electrophoresis *18*, 1259-1313.

Little, C., Olinescu, R., Reid, K.G., and O'Brien, P.J. (1970). Properties and regulation of glutathione peroxidase. J Biol Chem *245*, 3632-3636.

Liu, H., Colavitti, R., Rovira, I., and Finkel, T. (2005). Redox-dependent transcriptional regulation. Circ Res *97*, 967-974.

Loew, O. (1900). A New Enzyme of General Occurrence in Organisms. Science *11*, 701-702.

Lopez-Campistrous, A., Semchuk, P., Burke, L., Palmer-Stone, T., Brokx, S.J., Broderick, G., Bottorff, D., Bolch, S., Weiner, J.H., and Ellison, M.J. (2005). Localization, annotation, and comparison of the Escherichia coli K-12 proteome under two states of growth. Mol Cell Proteomics *4*, 1205-1209.

Lotharius, J., and Brundin, P. (2002). Pathogenesis of Parkinson's disease: dopamine, vesicles and alpha-synuclein. Nat Rev Neurosci *3*, 932-942.

Low, F., Hampton, M., Peskin, A., and Winterbourn, C. (2007). Peroxiredoxin 2 functions as a noncatalytic scavenger of low-level hydrogen peroxide in the erythrocyte. Blood *109*, 2611-2617.

Lusis, A. (2000). Atherosclerosis. Nature *407*, 233-241.

Luzzatto, L., and Testa, U. (1978). Human erythrocyte glucose 6-phosphate dehydrogenase: structure and function in normal and mutant subjects. Curr Top Hematol *1*, 1-70.

Maddipati, K.R., Gasparski, C., and Marnett, L.J. (1987). Characterization of the hydroperoxide-reducing activity of human plasma. Arch Biochem Biophys *254*, 9-17.

Maddipati, K.R., and Marnett, L.J. (1987). Characterization of the major hydroperoxide-reducing activity of human plasma. Purification and properties of a selenium-dependent glutathione peroxidase. J Biol Chem *262*, 17398-17403.

Manta, B., Hugo, M., Ortiz, C., Ferrer-Sueta, G., Trujillo, M., and Denicola, A. (2009). The peroxidase and peroxynitrite reductase activity of human erythrocyte peroxiredoxin 2. Arch Biochem Biophys *484*, 146-154.

Marchesi, V.T., and Florey, H.W. (1960). Electron micrographic observations on the emigration of leucocytes. Q J Exp Physiol Cogn Med Sci *45*, 343-348.

Marieb, E., and Hoehn, K. (2007). Human anatomy & physiology (Pearson Education).

Marzocchi, B., Ciccoli, L., Tani, C., Leoncini, S., Rossi, V., Bini, L., Perrone, S., and Buonocore, G. (2005). Hypoxia-induced post-translational changes in red blood cell protein map of newborns. Pediatr Res *58*, 660-665.

Masuoka, N., Sugiyama, H., Ishibashi, N., Wang, D.H., Masuoka, T., Kodama, H., and Nakano, T. (2006). Characterization of acatalasemic erythrocytes treated with low and high dose hydrogen peroxide. Hemolysis and aggregation. J Biol Chem *281*, 21728-21734.

Méplan, C., Crosley, L., Nicol, F., Beckett, G., Howie, A., Hill, K., Horgan, G., Mathers, J., Arthur, J., and Hesketh, J. (2007). Genetic polymorphisms in the human selenoprotein P gene determine the response of selenoprotein markers to selenium supplementation in a gender-specific manner (the SELGEN study). FASEB J *21*, 3063-3074.

Messner, K.R., and Imlay, J.A. (1999). The identification of primary sites of superoxide and hydrogen peroxide formation in the aerobic respiratory chain and sulfite reductase complex of Escherichia coli. J Biol Chem *274*, 10119-10128.

Mills, G.C. (1957). Hemoglobin catabolism. I. Glutathione peroxidase, an erythrocyte enzyme which protects hemoglobin from oxidative breakdown. J Biol Chem *229*, 189-197.

Mills, G.C. (1959). The purification and properties of glutathione peroxidase of erythrocytes. J Biol Chem *234*, 502-506.

Minczykowski, A., Woszczyk, M., Szczepanik, A., Lewandowski, L., and Wysocki, H. (2001). Hydrogen peroxide and superoxide anion production by polymorphonuclear neutrophils in patients with chronic periapical granuloma, before and after surgical treatment. Clin Oral Investig *5*, 6-10.

Misra, H.P., and Fridovich, I. (1972). The generation of superoxide radical during the autoxidation of hemoglobin. J Biol Chem *247*, 6960-6962.

Mitsumoto, A., Takanezawa, Y., Okawa, K., Iwamatsu, A., and Nakagawa, Y. (2001). Variants of peroxiredoxins expression in response to hydroperoxide stress. Free Radic Biol Med *30*, 625-635.

Monteiro, G., Horta, B.B., Pimenta, D.C., Augusto, O., and Netto, L.E. (2007). Reduction of 1-Cys peroxiredoxins by ascorbate changes the thiol-specific antioxidant paradigm, revealing another function of vitamin C. Proc Natl Acad Sci U S A *104*, 4886-4891.

Moon, J., Hah, Y., Kim, W., Jung, B., Jang, H., Lee, J., Kim, S., Lee, Y., Jeon, M., Kim, C.*, et al.* (2005). Oxidative stress-dependent structural and functional switching of a human 2-Cys peroxiredoxin isotype II that enhances HeLa cell resistance to H2O2-induced cell death. J Biol Chem *280*, 28775-28784.

Moore, R., Mankad, M., Shriver, S., Mankad, V., and Plishker, G. (1991). Reconstitution of Ca(2+)-dependent K+ transport in erythrocyte membrane vesicles requires a cytoplasmic protein. J Biol Chem *266*, 18964-18968.

Moore, R., Plishker, G., and Shriver, S. (1990). Purification and measurement of calpromotin, the cytoplasmic protein which activates calcium-dependent potassium transport. Biochem Biophys Res Commun *166*, 146-153.

Moore, R., and Shriver, S. (1994). The cDNA sequence for calpromotin indicates that it plays a significant role in the proliferation and differentiation of hematopoietic-cells. Blood, A *84*, 573.

Mueller, S., Riedel, H., and Stremmel, W. (1997a). Direct evidence for catalase as the predominant H2O2 -removing enzyme in human erythrocytes. Blood *90*, 4973-4978.

Mueller, S., Riedel, H.D., and Stremmel, W. (1997b). Determination of catalase activity at physiological hydrogen peroxide concentrations. Anal Biochem *245*, 55-60.

Munhoz, D.C., and Netto, L.E. (2004). Cytosolic thioredoxin peroxidase I and II are important defenses of yeast against organic hydroperoxide insult: catalases and peroxiredoxins cooperate in the decomposition of H2O2 by yeast. J Biol Chem *279*, 35219-35227.

Nakagawara, A., Nathan, C.F., and Cohn, Z.A. (1981). Hydrogen peroxide metabolism in human monocytes during differentiation in vitro. J Clin Invest *68*, 1243-1252.

Nascimento, H., Belo, L., Fernandes, J., Rocha, S., Quintanilha, A., and Santos-Silva, A. (2010). In vitro studies with 'acatalasemic-like' erythrocytes and hydrogen peroxide: attention to the formation of lysis resistant erythrocytes. Int J Lab Hematol *32*, 127-131.

Neumann, C.A., Krause, D.S., Carman, C.V., Das, S., Dubey, D.P., Abraham, J.L., Bronson, R.T., Fujiwara, Y., Orkin, S.H., and Van Etten, R.A. (2003). Essential role for the peroxiredoxin Prdx1 in erythrocyte antioxidant defence and tumour suppression. Nature *424*, 561-565.

Nicholls, P. (1964). The Formation and Catalytic Role of Catalase Peroxide Compound Ii. Biochim Biophys Acta *81*, 479-495.

Nicholls, P. (1965). Activity of catalase in the red cell. Biochim Biophys Acta *99*, 286-297.

Niethammer, P., Grabher, C., Look, A.T., and Mitchison, T.J. (2009). A tissue-scale gradient of hydrogen peroxide mediates rapid wound detection in zebrafish. Nature *459*, 996-999.

Niimura, Y., Poole, L.B., and Massey, V. (1995). Amphibacillus xylanus NADH oxidase and Salmonella typhimurium alkyl-hydroperoxide reductase flavoprotein components show extremely high scavenging activity for both alkyl hydroperoxide and hydrogen peroxide in the presence of S. typhimurium alkyl-hydroperoxide reductase 22-kDa protein component. J Biol Chem *270*, 25645-25650.

Peskin, A., Low, F., Paton, L., Maghzal, G., Hampton, M., and Winterbourn, C. (2007). The high reactivity of peroxiredoxin 2 with H(2)O(2) is not reflected in its reaction with other oxidants and thiol reagents. J Biol Chem *282*, 11885-11892.

Przedborski, S. (2007). Peroxiredoxin-2 links Cdk5 to neurodegeneration. Nat Med *13*, 907-909.

Raftos, J., Lew, V., and Flatman, P. (1999). Refinement and evaluation of a model of Mg2+ buffering in human red cells. Eur J Biochem *263*, 635-645.

Reiss, M., and Roos, D. (1978). Differences in oxygen metabolism of phagocytosing monocytes and neutrophils. J Clin Invest *61*, 480-488.

Rocha, S., Costa, E., Coimbra, S., Nascimento, H., Catarino, C., Rocha-Pereira, P., Quintanilha, A., Belo, L., and Santos-Silva, A. (2009). Linkage of cytosolic peroxiredoxin 2 to erythrocyte membrane imposed by hydrogen peroxide-induced oxidative stress. Blood Cells Mol Dis *43*, 68-73.

Roche, A.F., Heymsfield, S.B., and Lohman, T.G. (1996). Human body composition (Human Kinetics Publishers).

Rose, N., and Afanasyeva, M. (2003). Autoimmunity: busting the atherosclerotic plaque. Nature medicine *9*, 641.

Roughton, F. (1964). Transport of oxygen and carbon dioxide. Handbook of physiology *1*, 767-825.

Rouhier, N., Gelhaye, E., Sautiere, P.E., Brun, A., Laurent, P., Tagu, D., Gerard, J., de Fay, E., Meyer, Y., and Jacquot, J.P. (2001). Isolation and characterization of a new peroxiredoxin from poplar sieve tubes that uses either glutaredoxin or thioredoxin as a proton donor. Plant Physiol *127*, 1299-1309.

Sarelius, I.H. (1986). Cell flow path influences transit time through striated muscle capillaries. Am J Physiol *250*, H899-907.

Sarsour, E., Kumar, M., Chaudhuri, L., Kalen, A., and Goswami, P. (2009). Redox control of the cell cycle in health and disease. Antioxid Redox Signal *11*, 2985-3011.

Savitz, D., Sidel, V., and Solomon, A. (1964). Osmotic properties of human red cells. J Gen Physiol *48*, 79-94.

Scarpa, M., Momo, F., Viglino, P., Vianello, F., and Rigo, A. (1996). Activated oxygen species in the oxidation of glutathione A kinetic study. Biophysical Chemistry *60*, 53-61.

Scarpa, M., Viglino, P., Contri, D., and Rigo, A. (1984). Generation of superoxide ion in human red blood cell lysates. J Biol Chem *259*, 10657-10659.

Schroder, E., Littlechild, J.A., Lebedev, A.A., Errington, N., Vagin, A.A., and Isupov, M.N. (2000). Crystal structure of decameric 2-Cys peroxiredoxin from human erythrocytes at 1.7 A resolution. Structure *8*, 605-615.

Schwertassek, U., Balmer, Y., Gutscher, M., Weingarten, L., Preuss, M., Engelhard, J., Winkler, M., and Dick, T.P. (2007). Selective redox regulation of cytokine receptor signaling by extracellular thioredoxin-1. EMBO J *26*, 3086-3097.

Scott, M., Lubin, B., Zuo, L., and Kuypers, F. (1991). Erythrocyte defense against hydrogen peroxide: preeminent importance of catalase. J Lab Clin Med *118*, 7-16.

Seaver, L.C., and Imlay, J.A. (2001). Alkyl hydroperoxide reductase is the primary scavenger of endogenous hydrogen peroxide in Escherichia coli. J Bacteriol *183*, 7173-7181.

Shinkarenko, V.S. (1983). An automatic image analysis study of the microcirculation in inflammation. Bulletin of Experimental Biology and Medicine *96*, 1479-1481.

Snyder, L.M., Fortier, N.L., Trainor, J., Jacobs, J., Leb, L., Lubin, B., Chiu, D., Shohet, S., and Mohandas, N. (1985). Effect of hydrogen peroxide exposure on normal human erythrocyte deformability, morphology, surface characteristics, and spectrin-hemoglobin cross-linking. J Clin Invest *76*, 1971-1977.

Springer, T.A. (1994). Traffic signals for lymphocyte recirculation and leukocyte emigration: the multistep paradigm. Cell *76*, 301-314.

Stucker, M., Baier, V., Reuther, T., Hoffmann, K., Kellam, K., and Altmeyer, P. (1996). Capillary blood cell velocity in human skin capillaries located perpendicularly to the skin surface: measured by a new laser Doppler anemometer. Microvasc Res *52*, 188-192.

Svistunenko, D.A., Patel, R.P., Voloshchenko, S.V., and Wilson, M.T. (1997). The globin-based free radical of ferryl hemoglobin is detected in normal human blood. J Biol Chem *272*, 7114-7121.

Szatrowski, T.P., and Nathan, C.F. (1991). Production of large amounts of hydrogen peroxide by human tumor cells. Cancer Res *51*, 794-798.

Takebe, G., Yarimizu, J., Saito, Y., Hayashi, T., Nakamura, H., Yodoi, J., Nagasawa, S., and Takahashi, K. (2002). A comparative study on the hydroperoxide and thiol specificity of the glutathione peroxidase family and selenoprotein P. J Biol Chem *277*, 41254-41258.

Taoka, M., Yamauchi, Y., Shinkawa, T., Kaji, H., Motohashi, W., Nakayama, H., Takahashi, N., and Isobe, T. (2004). Only a small subset of the horizontally transferred chromosomal genes in Escherichia coli are translated into proteins. Mol Cell Proteomics *3*, 780-787.

Thorburn, D., and Kuchel, P. (1987). Glutathione regeneration in density-fractionated human erythrocytes. Biomed Biochim Acta *46*, S248-252.

Thorburn, D.R., and Kuchel, P.W. (1985). Regulation of the human-erythrocyte hexose-monophosphate shunt under conditions of oxidative stress. A study using NMR spectroscopy, a kinetic isotope effect, a reconstituted system and computer simulation. Eur J Biochem *150*, 371-386.

Thornalley, P.J., McLellan, A.C., Lo, T.W.C., Benn, J., and Sönksen, P.H. (1996). Negative association between erythrocyte reduced glutathione concentration and diabetic complications. Clinical science *91*, 575-582.

Tsang, M., and Weatherbee, J. (1981). Thioredoxin, glutaredoxin, and thioredoxin reductase from cultured HeLa cells. Proc Natl Acad Sci U S A *78*, 7478-7482.

Turanov, A., Su, D., and Gladyshev, V. (2006). Characterization of alternative cytosolic forms and cellular targets of mouse mitochondrial thioredoxin reductase. J Biol Chem *281*, 22953-22963.

Urig, S., Lieske, J., Fritz-Wolf, K., Irmler, A., and Becker, K. (2006). Truncated mutants of human thioredoxin reductase 1 do not exhibit glutathione reductase activity. FEBS Lett *580*, 3595-3600.

Varma, S.D., and Devamanoharan, P.S. (1991). Hydrogen peroxide in human blood. Free Radic Res Commun *14*, 125-131.

Visick, J.E., and Clarke, S. (1997). RpoS- and OxyR-independent induction of HPI catalase at stationary phase in Escherichia coli and identification of rpoS mutations in common laboratory strains. J Bacteriol *179*, 4158-4163.

Wagner, T.C., and Scott, M.D. (1994). Single extraction method for the spectrophotometric quantification of oxidized and reduced pyridine nucleotides in erythrocytes. Anal Biochem *222*, 417-426.

Wang, H., and Joseph, J.A. (1999). Quantifying cellular oxidative stress by dichlorofluorescein assay using microplate reader. Free Radic Biol Med *27*, 612-616.

Wasselius, J., Larsson, S., Sundin, A., and Jacobsson, H. (2009). Assessment of inactive, active and mixed atherosclerotic plaques by 18F-FDG-PET; an age group-based correlation with cardiovascular risk factors. Int J Cardiovasc Imaging *25*, 133-140.

Watson, A.D., Leitinger, N., Navab, M., Faull, K.F., Horkko, S., Witztum, J.L., Palinski, W., Schwenke, D., Salomon, R.G., Sha, W*., et al.* (1997). Structural identification by mass spectrometry of oxidized phospholipids in minimally oxidized low density lipoprotein that induce monocyte/endothelial interactions and evidence for their presence in vivo. J Biol Chem *272*, 13597-13607.

Watson, W., and Jones, D. (2003). Oxidation of nuclear thioredoxin during oxidative stress. FEBS Lett *543*, 144-147.

Wever, R., Oudega, B., and Van Gelder, B. (1973). Generation of superoxide radicals during the autoxidation of mammalian oxyhemoglobin. Biochimica et Biophysica Acta (BBA)-Enzymology *302*, 475-478.

Widmaier, E., Raff, H., and Strang, K. (2008). Vander's human physiology (McGraw-Hill Higher Education).

Wilhelm, E., Battino, R., and Wilcock, R.J. (1977). Low-pressure solubility of gases in liquid water. Chemical Reviews *77*, 219-262.

Williams, C.H., Jr. (1995). Mechanism and structure of thioredoxin reductase from Escherichia coli. FASEB J *9*, 1267-1276.

Winterbourn, C. (1985). Free-radical production and oxidative reactions of hemoglobin. Environ Health Perspect *64*, 321-330.

Winterbourn, C., and Stern, A. (1987). Human red cells scavenge extracellular hydrogen peroxide and inhibit formation of hypochlorous acid and hydroxyl radical. J Clin Invest *80*, 1486-1491.

Winterbourn, C.C., Peskin, A.V., and Parsons-Mair, H.N. (2002). Thiol oxidase activity of copper, zinc superoxide dismutase. J Biol Chem *277*, 1906-1911.

Wolfram Research, I. (2008). Mathematica, Version 7.0 edn (Champaign, Illinois, Wolfram Research, Inc.).

Wood, Z., Poole, L., and Karplus, P. (2003a). Peroxiredoxin evolution and the regulation of hydrogen peroxide signaling. Science *300*, 650-653.

Wood, Z., Schröder, E., Robin Harris, J., and Poole, L. (2003b). Structure, mechanism and regulation of peroxiredoxins. Trends Biochem Sci *28*, 32-40.

Worthington, D.J., and Rosemeyer, M.A. (1976). Glutathione reductase from human erythrocytes. Catalytic properties and aggregation. Eur J Biochem *67*, 231-238.

Worthylake, R.A., and Burridge, K. (2001). Leukocyte transendothelial migration: orchestrating the underlying molecular machinery. Curr Opin Cell Biol *13*, 569-577.

Yang, K.S., Kang, S.W., Woo, H.A., Hwang, S.C., Chae, H.Z., Kim, K., and Rhee, S.G. (2002). Inactivation of human peroxiredoxin I during catalysis as the result of the oxidation of the catalytic site cysteine to cysteine-sulfinic acid. J Biol Chem *277*, 38029-38036.

Younkin, S., Oski, F.A., and Barness, L.A. (1971). Mechanism of the hydrogen peroxide hemolysis test and its reversal with phenols. Am J Clin Nutr *24*, 7-13.

Zhou, M., Diwu, Z., Panchuk-Voloshina, N., and Haugland, R.P. (1997). A stable nonfluorescent derivative of resorufin for the fluorometric determination of trace hydrogen peroxide: applications in detecting the activity of phagocyte NADPH oxidase and other oxidases. Anal Biochem *253*, 162-168.

9. Appendix

The following abstracts refer to poster and oral communications of this work.

9.1. Poster presentations

Benfeitas R., Antunes F., Salvador A. (2010). **The role of peroxiredoxin 2 in the protection of human erythrocytes against hydrogen peroxide: a kinetic analysis.**

XVII Congresso Nacional de Bioquímica, Porto, Portugal, 15-17 December.

Peroxiredoxin 2 (Prx2) is a hydrogen peroxide (H_2O_2) reducing protein abundant in human erythrocytes (~0.37 mM). Its high reactivity with H_2O_2 ($k \sim 10^8$ M^{-1} s^{-1}) makes it potentially very relevant for antioxidant protection of these cells. However, erythrocytes' limited capacity for reducing Prx2 to its active form once this protein is oxidized by H_2O_2 raises questions about that relevance in vivo. Seeking to clarify this issue we set up a kinetic model that encompasses the main processes protecting human erythrocytes against H_2O_2. Namely, the glutathione peroxidase (GPx1), catalase and Prx2 systems. We then used the model to examine the dynamic behavior of these processes under various conditions.

Analysis of the relevant concentration and time scales highlights the following. (i) Under basal conditions, assuming a sustained extracellular H_2O_2 (eH_2O_2) concentration <30 nM and <25 nM/s intracellular H_2O_2 (iH_2O_2) production, Prx2 is expected to be fully reduced. Prx2, catalase and GPx1 would then eliminate 99%, 0.6% and 0.1% of the H_2O_2, respectively. (ii) Doses >0.4 mM H_2O_2 entering the erythrocyte over a period of <1 min, or sustained eH_2O_2 concentrations >200 nM fully oxidize Prx2 to its disulfide form. Catalase then becomes the main defense against H_2O_2. (iii) eH_2O_2 consumption by erythrocytes is limited by membrane permeation even when Prx2 is fully oxidized. Thus, although erythrocytes are quite likely the main sink of plasma H_2O_2, Prx2 is dispensable for this role. (iv) Once all Prx2 is oxidized, erythrocytes can regenerate the reduced form in minutes if eH2O2 concentrations and iH_2O_2 production return to basal values. The points above have the following implications. (a) Mere crossing of

inflammation sites is insufficient to cause extensive Prx2 oxidation, as the following reasoning shows. The residence time of a circulating erythrocyte in an inflammation site is determined by the time (~2 s) to cross the capillaries, where these cells are in most intimate contact with the vasculature walls and circulate most slowly. For a dose of 0.4 mM H_2O_2 to enter the erythrocyte in such a short time, the local eH_2O_2 concentration would have to be ~20 μM, sufficient to extensively damage the surrounding endothelial cells. (b) A stepwise increase in Prx2 oxidation through repeated crossing of inflammation sites is very unlikely. This because such crossings are expected to occur many hours in between; time enough for Prx2 to be fully reduced. (c) Short-term eH_2O_2 doses sufficient to fully oxidize Prx2 are only conceivably attained through direct contact of the erythrocytes with activated phagocytes, for instance in immune clearance. (d) However, high enough sustained eH_2O_2 concentrations are conceivable in systemic inflammation. Altogether, our results indicate that Prx2 is the main defense of human erythrocytes against H_2O_2 under most physiological circumstances.

This work was supported by grant PTDC/QUI/70523/2006 from "Fundação para a Ciência e Tecnologia"

Benfeitas R., Antunes F., Salvador A. (2011). **The role of peroxiredoxin 2 in protecting human erythrocytes against hydrogen peroxide: a kinetic analysis.**

XII International Congress on Molecular Systems Biology, Lleida, Spain, 8 – 12 May.

Peroxiredoxin 2 (Prx2) is a hydrogen peroxide (H_2O_2) reducing protein abundant in human erythrocytes (~0.37 mM). Its high reactivity with H_2O_2 ($k \sim 10^8 M^{-1} s^{-1}$) makes it potentially very relevant for antioxidant protection of these cells. However, erythrocytes' limited capacity for reducing Prx2 to its active form once this protein is oxidized by H_2O_2 raises questions about that relevance in vivo. Seeking to clarify this issue we set up a kinetic model that encompasses the main processes protecting human erythrocytes against H_2O_2. Namely, the glutathione peroxidase (GPx1), catalase and Prx2 systems. We then used the model to examine the dynamic behavior of these processes under various conditions.

Analysis of the relevant concentration and time scales highlights the following. (i) Under basal conditions, assuming a sustained extracellular H_2O_2 (eH2O2) concentration <30 nM and <25 nM/s intracellular H_2O_2 (iH_2O_2) production, Prx2 is expected to be fully reduced. Prx2, catalase and GPx1 would then eliminate 99%, 0.6% and 0.1% of the H_2O_2, respectively. (ii) Doses >0.4 mM H_2O_2 entering the erythrocyte over a period of <1 min, or sustained eH_2O_2 concentrations >200 nM fully oxidize Prx2 to its disulfide form. Catalase then becomes the main defense against H_2O_2. (iii) Once all Prx2 is oxidized, erythrocytes can regenerate the reduced form in minutes if eH_2O_2 concentrations and iH_2O_2 production return to basal values. (iv) eH_2O_2 consumption by erythrocytes is limited by membrane permeation even when Prx2 is fully oxidized: under these conditions the log gain of eH_2O_2 consumption by the erythrocyte with respect to changes in the permeability constant is ~0.96, whereas those with respect to changes in catalase and GPx1 concentrations are <0.04 and <0.01, respectively. Thus, although erythrocytes are quite likely the main sink of plasma H_2O_2, Prx2 is dispensable for this role.

The points above have the following implications. (a) Crossing of inflammation sites may plausibly cause substantial but transient Prx2 oxidation, as the following reasoning shows. The residence time of a circulating erythrocyte in an inflammation site is determined by the time (~2 s) to cross the capillaries, where these cells are in most intimate contact with the vasculature walls and circulate most slowly. A dose >0.4 mM H_2O_2 will enter the erythrocyte during this

time if the local eH_2O_2 concentration is >16 μM, which is in the scale of experimentally determined values for inflammatory foci in other organisms. (b) A stepwise increase in Prx2 oxidation through repeated crossing of inflammation sites is very unlikely. This because such crossings are expected to occur many hours in between; time enough for Prx2 to be fully reduced. (c) High enough sustained eH_2O_2 concentrations sufficient to fully oxidize Prx2 are only conceivable in systemic inflammation.

Altogether, our results show that Prx2 is the main defense of these cells against H_2O_2 under most physiological circumstances. However, Prx2 inactivation does not impair the erythrocytes' ability to scavenge eH_2O_2 because the activity of catalase is sufficiently high to eliminate virtually all the incoming H_2O_2.

Work supported by grant PTDC/QUI/70523/2006 from FCT-Portugal.

9.2. Oral communications

Benfeitas R., Antunes F., Salvador A. (2011). **Are the defenses of human erythrocytes against hydrogen peroxide functionally redundant?**

XII International Congress on Molecular Systems Biology, Lleida, Spain, 8 – 12 May.

Human erythrocytes contain three enzymes — peroxiredoxin 2 (Prx2), glutathione peroxidase (GPx1) and catalase — that decompose hydrogen peroxide (H_2O_2). Whereas GPx1 reduces also fatty acid hydroperoxides, and thus has a distinct specificity from Prx2, the specificity of catalase is largely overlapped by Prx2. Further, whereas H_2O_2 reduction via the first two enzymes is stoichiometrically coupled to NADPH consumption, H_2O_2 dismutation via catalase entails minimal NADPH consumption. Why do then erythrocytes rely mainly on Prx2 for protection against H_2O_2? Why is catalase still required despite the extremely large (37000 s^{-1}) pseudo-first-order rate constant of Prx2 for H_2O_2 reduction? And how is access to NADPH prioritized among the Prx2 and the GPx1 redox systems at oxidative loads where that resource becomes limiting?

Using a kinetic model that encompasses these three antioxidant systems we found the following. (1) In order to fully replace Prx2 such that the same H_2O_2 concentration and response time as in normal erythrocytes would be retained ~10 pg catalase (60 pg GPx1) would be required. This amounts to 32% (176%) of the hemoglobin in human erythrocytes. Such a solution could thus impair oxygen transport either by making erythrocytes bigger, and thus less able to cross capillaries, or by reducing the space available for hemoglobin. (2) On the other hand, a mere 0.6% increase in Prx2 concentration would suffice to compensate for the effect of catalase elimination on H_2O_2 concentration and response time at basal oxidative loads. However, as erythrocytes cross inflammatory foci Prx2 can become substantially oxidized, and thus inactive. In such conditions the absence of catalase leads to much higher H2O2 concentrations being transiently attained. (3) The kinetic parameters of thioredoxin reductase and glutathione reductase — enzymes that mediate the transfer of reducing equivalents to the Prx2 and the GPx1 systems, respectively — are orchestrated in such way that the latter enzyme outcompetes the former for NADPH when the demand for reducing equivalents exceeds the supply. This has the effect of privileging the reduction of oxidized glutathione (GSSG) at the cost of delaying Prx2

recovery, consistent with biochemical evidence that GSSG accumulation is deleterious. Under these circumstances, catalase activity becomes very important to avoid strong H_2O_2 accumulation and further glutathione oxidation.

Altogether, our results illuminate the functional complementarily among apparently overlapping erythrocyte defenses against H_2O_2. Namely, although Prx2 is the main defense at low to moderate H_2O_2 concentrations, at the high H_2O_2 concentrations that may be attained in inflammation sites catalase becomes the main defense. Further, the kinetic parameters of the Prx2 and the GPx1 system are orchestrated in such way as to prioritize GSSG reduction over Prx2 reduction.

Work supported by grant PTDC/QUI/70523/2006 from FCT-Portugal.